PHYSICAL REVIEW B VOLUME 9, NUMBER 10 15 MAY 1974

Quantum resonances in the valence bands of germanium. I. Theoretical considerations

K. Suzuki* and J. C. Hensel
Bell Laboratories, Murray Hill, New Jersey 07974

(Received 17 July 1973)

The structure of the Γ_{25}^{+} degenerate valence band of Ge has been investigated by a comprehensive study of the complex "quantum" resonance spectra from electric-dipole transitions in the system of anomalously spaced low-lying Landau levels produced by an applied magnetic field. This paper, the first of a series of four, is devoted to the development of a systematic theoretical spectroscopy to serve as a framework for the analysis of our experiments which will be discussed in succeeding papers. Using group-theoretical techniques, following Luttinger, we construct a generalized effective-mass Hamiltonian for holes, including the effects of elastic strain, in the full six-dimensional space of Γ_{25}^{+} to encompass the spin-orbit-split-off band. The formulation in the extended space sheds considerable light on two important consequences of spin-orbit coupling, the anisotropy of the hole g factor (the Luttinger q term) and a new effect, the spin-dependent contribution to the valence-band deformation potentials. From the Hamiltonian for Γ_{25}^{+} we project, making the split appropriate to large spin-orbit interaction, the Hamiltonian belonging to the subspace of the band edge Γ_{8}^{+}. We examine the nature of its eigenstates and develop a systematic scheme based on group theory for classifying the magnetic eigenstates, in terms of which selection rules for quantum transitions can be expressed in unusually clear and compact form. A formalism is presented for generating complete, "synthesized" quantum-resonance spectra starting with the eigenvalues and eigenfunctions of the effective-mass Hamiltonian. A further projection, representing the decoupling of the Γ_{8}^{+} band by large uniaxial stress, is expanded to second order to evaluate the corrections to the hole effective masses and g factors at finite stress. Finally, we consider the interaction between the projected spaces of the stress-decoupled band-edge states and the spin-orbit-split-off states which contributes two important shifts to the quantum-resonance effective masses: the second-order magnetic interaction and the interaction from the cross terms of strain and magnetic field.

I. INTRODUCTION

In a uniform magnetic field $\vec{H}$ the continuum of states in the energy bands of a solid coalesce into discrete quantum states called Landau states. Cyclotron-resonance absorption of electrons and holes may be viewed as induced electric-dipole transitions between these discrete Landau states. The present work constitutes a study of the spectroscopy of *quantum*-resonance transitions for holes in the valence bands of germanium.

Seldom in practice is this quantum aspect of cyclotron resonance manifest in a significant way.[1] Usually Landau levels form a "ladder" with equally spaced "rungs" so allowed transitions take place at a single energy $\hbar\omega_c$ defined by a *classical* cyclotron angular frequency $\omega_c = eH/m^*c$, m^* being the effective mass of the charge carrier. In this case cyclotron resonance may be satisfactorily interpreted from a dynamical standpoint in terms of the classical motion of the carrier on an energy surface of the semiconductor (or Fermi surface, in the case of a metal) without recourse to quantum mechanics.

An important exception to this elementary interpretation occurs for cyclotron resonance in *degenerate* bands such as typically found at the valence band edge in many cubic semiconductors such as Ge and Si. In their treatment of this problem by effective-mass theory Luttinger and Kohn[2,3] predicted the remarkable result that the levels near the bottom of the Landau ladders would have characteristically irregular spacings compared to the higher levels which, in accordance with the correspondence principle, tend toward "classical" uniformity. "Quantum" deviations in cyclotron resonances arising from these anomalous levels would be expected to appear at low temperatures and high magnetic fields. Experimental investigation of these quantum effects is important because first, it would verify the theory and in particular the validity of the effective-mass approach and second, a detailed study could, in principle, provide a most comprehensive picture of the valence-band structure.

The first experiments under quantum conditions ($\hbar\omega_c \gtrsim k\Theta$, where Θ denotes the temperature) were done in Ge by Fletcher, Yager, and Merritt.[4] They observed complex quantum spectra consisting of a multiplicity of hole resonances which replaced the usual two classical hole resonances, the "light"- and "heavy"-hole lines, measured earlier by Dresselhaus, Kip, and Kittel[5] and Dexter, Zeiger, and Lax.[6] Subsequent quantum experiments by others[7,8] in Ge at greater resolution have extended the original measurements and revealed additional structure.

Unfortunately, the initial impetus of these early achievements has not been sustained. While there is essentially no question that the observed spectra are indeed the quantum effects predicted by Luttinger and Kohn,[2,3] attempts[7-9] at their detailed interpretation in terms of theory have so far been disappointing. The difficulties as well as their reasons are now in retrospect quite clear. First, experimental identifications of the lines in the spectra have proved all but impossible to make. Second, the alternative of reproducing the line positions by brute-force numerical computation has not been particularly fruitful either partly for the reason that known values of the five band parameters γ_1, γ_2, γ_3, κ, and q which appear in the effective-mass Hamiltonian proved to be insufficiently precise. (In fact, no measurements whatsoever had been made of κ and q, the two parameters which describe the hole g factor.) Inasmuch as the identifications of lines and the determination of band parameters hinge sensitively upon each other, one has little confidence that, without either being firmly established, a trial-and-error "search" program would necessarily converge to a unique solution. Third, the least obvious but most serious pitfall has been the neglect, with few exceptions,[10,11] of the effects of k_H, the wave vector along $\vec{H}$. It is now clear from our experiments that k_H effects have a more profound influence on the character of the spectra than has been suspected heretofore and cannot be neglected even as a first approximation. The further complexity introduced by the k_H problem essentially precludes trial-and-error methods altogether.

Reviewing these difficulties, one would not be optimistic that cyclotron-resonance experiments could lead us to our objectives of testing the theory and measuring the band structure of Ge unless some new approach to the problem is found. One expedient, exploited previously in the classical study of the valence bands of Si,[12] is uniaxial stress which removes the degeneracy of the valence bands. It will be seen that uniaxial stress can also be the key[13,14] to untangling the intricacies of the quantum spectra in Ge.

The complete work[15] has been divided into four papers. This, the first paper, deals with theoretical topics needed for the subsequent analysis of cyclotron-resonance experiments in Ge given in the three remaining papers of this series[16-18] (hereafter, respectively, referred to as Papers II, III, and IV). In Paper II, cyclotron-resonance experiments in uniaxially stressed Ge are analyzed with two goals in mind: first, identification of the principal quantum lines and, second, determination from these lines precision values of the three effective-mass parameters γ_1, γ_2, and γ_3. In Paper III we describe "combined" resonance experiments (also using uniaxial stress) which yield the first measurements of the parameters κ and q. The strain experiments in Papers II and III also directly measure valence-band uniaxial deformation potentials. Using the band parameters thus obtained we analyze in Paper IV the experimental spectra in unstressed Ge.[18] The intensities of all quantum transitions are calculated and integrated over k_H to generate "synthesized" quantum spectra which we fit to the experimental spectra. The over-all agreement of these various experiments with theory and, in particular, the excellent, detailed agreement of the theoretical and experimental spectra at zero stress in regard to line positions, intensities, and line shapes represent perhaps the most extensive and rigorous experimental verification yet made of the Luttinger-Kohn effective-mass theory.

In this paper we set up a theoretical framework, based on the effective-mass theory, for the quantum-resonance spectroscopy of the Landau states belonging to the Γ_{25}^{+} valence band[19] edge of Ge. Our approach to the problem is reminiscent of that originally taken by Luttinger[3]; however, for the analysis of our experiments it is necessary that the scope of his theory be substantially extended in the following respects: First, we must include in the most general way possible the effects of a uniaxial stress. Second, because a uniaxial stress can give rise to significant interactions between the spin-orbit–split-off band Γ_7^{+} and the Γ_8^{+} band edge, it is necessary to encompass both by taking the entire Γ_{25}^{+} valence-band manifold into consideration. (This effect, although more complicated for the quantum case, is similar to that discussed by Hasegawa[20] for classical reasonances in Si.) Third, we must forego the customary practice of setting $k_H = 0$; for, as it turns out, an interpretation of the quantum spectrum (at least for Ge) is not possible if this assumption is made. Fourth, we do not restrict ourselves to the case of $\vec{H}$ along a particular crystallographic axis, but rather attempt to formulate the problem in such a way that solutions to the Hamiltonian, quantum numbers, selection rules, etc., can be expressed in a natural way for an arbitrary direction of $\vec{H}$.

In Sec. II we begin by constructing on symmetry grounds the full 6×6 effective-mass Hamiltonian for Γ_{25}^{+} including spin-orbit, magnetic, and strain interactions. The parameters appearing in the Hamiltonian are expressed by $\vec{k}\cdot\vec{\pi}$ perturbation theory. When spin-orbit and/or strain interactions are strong enough to split the states of the Γ_{25}^{+} band to a significant degree, it is convenient to decouple the full 6×6 Hamiltonian into Hamiltonians appropriate to the smaller subspaces of the split states. We develop a formal decoupling technique employing projection operators to do this. One important aspect included in Sec. II is a detailed treatment of spin-dependent terms in the Hamiltonian; we find these can give substantial contributions, first, in the form of the parameter q, which describes the anisotropy of the hole g factor, and second, as spin-dependent deformation potentials.

Section III is devoted to a brief discussion of the microwave power absorption due to the cyclotron resonance of holes. An expression, the "spectral function," is given for the absorption line shape which can be used to generate spectra for direct comparison with experimental recorder traces.

In the remaining three sections we consider, in sucession, projected subspaces from the six-dimensional space of Γ_{25}^{+} given in Sec. II. Section IV describes the split appropriate for large spin-orbit interaction. We discuss the nature of the eigenstates of the 4×4 projected effective-mass Hamiltonian for Γ_8^{+} and develop a scheme for their classification according to quantum numbers based on symmetry properties of the Hamiltonian. Using these quantum numbers we express the selection rules for quantum-resonance (electric dipole) transitions. Allowed transitions are categorized according to the type of symmetry-breaking interaction present in the Hamiltonian.

In Sec. V we project from Γ_8^{+} the two two-dimensional subspaces which decouple when a uniaxial stress is applied. The various kinds of resonance phenomena which can occur in these subspaces are discussed; namely, cyclotron resonance, harmonic resonance, combined resonance, and spin resonance. Expressions are given for effective masses and g factors including first-order corrections which derive from the second-order projection expansion.

As a final step we consider in Sec. VI the second-order projection generated by the 2×4 "cross space" in the Γ_{25}^{+} Hamiltonian which connects Γ_8^{+} and Γ_7^{+}. This projection is responsible for characteristic linear strain-induced shifts of certain cyclotron-resonance lines in Γ_8^{+}.

We conclude the main body of the paper with a brief discussion of the effects of higher-order strain and magnetic interactions which originate from bands external to the manifold of Γ_{25}^{+}.

In the Appendixes we (i) analyze from a group-theoretical standpoint several "exactly" soluble cases due to Luttinger,[3] (ii) outline a useful formalism for classifying free-electron Landau states, and (iii) list systematically the interactions representing some higher-order strain effects.

Numerical calculations and comparisons with experiment will be presented in the appropriate experimental papers (II–IV).

II. EFFECTIVE-MASS HAMILTONIAN

A. Phenomenological Hamiltonians

The valence band edge of germanium is constructed of triply degenerate Bloch orbitals ϵ_1, ϵ_2, ϵ_3 (transforming like yz, zx, xy) which belong to the symmetry Γ_{25}^{+} of the cubic group[19] O_h and are derived from the symmetric combinations (bonding) of predominantly $4p$ and $3d$ atomic functions centered at each of the two interpenetrating fcc lattices. Inclusion of the two independent spin functions generates a set of six independent spin orbitals, which span the six-dimensional space in which we work throughout this paper.

We consider three distinct interactions within this manifold, namely, the spin-orbit, the magnetic, and the strain interactions. In the effective-mass approximation each of these interactions can be represented by a 6×6 matrix phenomenological or "spin" Hamiltonian which, according to Luttinger,[3] can be constructed solely on the basis of symmetry. In the following we generalize Luttinger's argument to allow for an arbitrarily strong spin-orbit interaction. We utilize the angular-momentum matrices $\vec{I}$ for $I=1$ and the Pauli matrices $\vec{\sigma}$ to represent the orbital and spin angular momentum, respectively, associated with the basis Bloch states. These satisfy the fundamental commutation relations

$$\begin{aligned} &\vec{I}\times\vec{I}=i\vec{I}\ , \\ &\tfrac{1}{2}\vec{\sigma}\times\tfrac{1}{2}\vec{\sigma}=\tfrac{1}{2}i\vec{\sigma}\ , \\ &\sigma_\mu\sigma_\nu+\sigma_\nu\sigma_\mu=2\delta_{\mu\nu}\ . \end{aligned} \tag{1}$$

Each of the vector components as well as their products can be classified according to the irreducible representations of the cubic group. Because of the finite magnitude of $\vec{I}$ and $\vec{\sigma}$, no powers higher than second in $\vec{I}$ and first in $\vec{\sigma}$ are independent of the lower (see caption of Table II), and therefore, the total number of independent matrices is finite, specifically 36, which is the number of independent elements of a 6×6 matrix. The 36 independent matrices are listed in the third column of Table I. The coordinates x, y, z are taken to be the cubic axes.

The lowest-order effective-mass Hamiltonians can be constructed below from the condition that they be invariant under the cubic operations.

(i) *Spin-orbit interaction.* The only invariant which depends on both spin and orbit is $\vec{I}\cdot\vec{\sigma}$, thus

$$\mathcal{H}_{so}=\tfrac{1}{3}\Lambda(\vec{I}\cdot\vec{\sigma})\ , \tag{2}$$

where Λ is a constant, the spin-orbit splitting.

(ii) *Magnetic interaction.* The magnetic effect can be described in the effective-mass theory by a vector $\vec{k}$ which satisfies the commutation relation

$$\vec{k}\times\vec{k}=e\vec{H}/i\hbar c\ , \tag{3}$$

TABLE I. A tabulation of the 36 independent matrices constructed from $\vec{I}$ and $\vec{\sigma}$ classified according to the cubic group O_h representations. The remaining members of the multidimensional representations Γ_{12}^+, Γ_{15}^+, and Γ_{25}^+ can be obtained by cyclic permutation. In column 2 an additional classification is made according to the representations $D^{(l)}$ of the full rotation group $R^+(3)$ for which the given set of operators form a partial basis. [Each set, while complete in O_h, does not necessarily span the entire space of $D^{(l)}$.] The classification by $D^{(l)}$ has merit in that, first, no matrix constructed from $\vec{I}$ and $\vec{\sigma}$ and transforming according to $D^{(l)}$ with $l>3$ is independent of those with lower l and, second, all projections of the $(\vec{I}, \vec{\sigma})$ matrices on the $J=\frac{3}{2}$, $J=\frac{1}{2}$, and "cross"-spaces are zero if $l>3$, $l>1$, and $l>2$, respectively (i.e., $D^{(l)}$ is invariant upon projection in O_h). In the last column we list the projected operators on the $M_J=\pm\frac{1}{2}$ subspace of $J=\frac{3}{2}$ for the symmetry D_{4h} appropriate for $T \parallel [001]$. As we pass from O_h to D_{4h} the basis operators of the multidimensional representations split as dictated by the compatibility relations (all representations have a + superscript):

$$\begin{array}{llllll} O_h: & \Gamma_1 & \Gamma_2 & \Gamma_{12} & \Gamma_{15} & \Gamma_{25} \\ D_{4h}: & \Gamma_1 & \Gamma_3 & \Gamma_1+\Gamma_3 & \Gamma_2+\Gamma_5 & \Gamma_4+\Gamma_5 \,. \end{array}$$

Except for the representation Γ_{12}^+, which has but two linearly independent basis operators explicitly given, the correspondence of the projected operators in the last column with the permutations of the basis operators in column 3 is self-evident.

Representation[a] O_h	$R^+(3)$	Basis operators	Projection on $J=\frac{3}{2}$	Projection on $J=\frac{1}{2}$	Cross-space[b] $(J=\frac{3}{2})\times(J=\frac{1}{2})$	Projection on $(J, M_J)=(\frac{3}{2}, \pm\frac{1}{2})$ for D_{4h}
Γ_1^+	$D^{(0)}$	1	1	1	0	$1\ (\Gamma_1)$
	$D^{(0)}$	$\vec{I}\cdot\vec{\sigma}$	1	-2	0	$1\ (\Gamma_1)$
Γ_2^+	$D^{(3)}$	$\{I_yI_z\}\sigma_x+\text{c.p.}$	$J_xJ_yJ_z+J_zJ_yJ_x$	0	0	$0\ (\Gamma_3)$
Γ_{12}^+	$D^{(2)}$	$I_x^2-I_y^2$	$\frac{1}{3}(J_x^2-J_y^2)$	0	$I_x^2-I_y^2$	$\begin{cases} I_z^2-\frac{1}{3}I^2 \rightarrow -\frac{1}{3}\ (\Gamma_1) \\ I_x^2-I_y^2 \rightarrow 0\ (\Gamma_3) \end{cases}$
	$D^{(2)}$	$I_x\sigma_x-I_y\sigma_y$	$\frac{2}{3}(J_x^2-J_y^2)$	0	$-(I_x^2-I_y^2)$	$\begin{cases} I_z\sigma_z-\frac{1}{3}\vec{I}\cdot\vec{\sigma} \rightarrow -\frac{2}{3}\ (\Gamma_1) \\ I_x\sigma_x-I_y\sigma_y \rightarrow 0\ (\Gamma_3) \end{cases}$
	$D^{(2)}$	$\{I_x(I_y\sigma_z-I_z\sigma_y)\}-\{I_y(I_z\sigma_x-I_x\sigma_z)\}$	0	0	$-\frac{3}{2}i(I_x^2-I_y^2)$	$0\ (\Gamma_1+\Gamma_3)$
Γ_{15}^+	$D^{(1)}$	I_x	$\frac{2}{3}J_x$	$\frac{4}{3}J_x$	I_x	$\begin{cases} \frac{1}{3}\sigma_z\ (\Gamma_2) \\ \frac{2}{3}\sigma_x,\ \frac{2}{3}\sigma_y\ (\Gamma_5) \end{cases}$
	$D^{(1)}$	σ_x	$\frac{2}{3}J_x$	$-\frac{2}{3}J_x$	$-2I_x$	$\begin{cases} \frac{1}{3}\sigma_z\ (\Gamma_2) \\ \frac{2}{3}\sigma_x,\ \frac{2}{3}\sigma_y\ (\Gamma_5) \end{cases}$
	$D^{(1)}$	$I_y\sigma_z-I_z\sigma_y$	0	0	$3iI_x$	$0\ (\Gamma_2+\Gamma_5)$
	$D^{(1)}$	$(I_x^2-\frac{1}{3}I^2)\sigma_x+\{I_xI_y\}\sigma_y+\{I_zI_x\}\sigma_z$	$\frac{2}{9}J_x$	$-\frac{20}{9}J_x$	$\frac{5}{6}I_x$	$\begin{cases} \frac{1}{9}\sigma_z\ (\Gamma_2) \\ \frac{2}{9}\sigma_x,\ \frac{2}{9}\sigma_y\ (\Gamma_5) \end{cases}$
	$D^{(3)}$	$(I_x^2-\frac{1}{3}I^2)\sigma_x-\frac{2}{3}(\{I_xI_y\}\sigma_y+\{I_zI_x\}\sigma_z)$	$\frac{10}{9}J_x^3-\frac{41}{18}J_x$	0	0	$\begin{cases} -\sigma_z\ (\Gamma_2) \\ \frac{1}{2}\sigma_x,\ \frac{1}{2}\sigma_y\ (\Gamma_5) \end{cases}$
Γ_{25}^+	$D^{(2)}$	$\{I_yI_z\}$	$\frac{1}{3}\{J_yJ_z\}$	0	$\{I_yI_z\}$	$0\ (\Gamma_4+\Gamma_5)$
	$D^{(2)}$	$I_y\sigma_z+I_z\sigma_y$	$\frac{4}{3}\{J_yJ_z\}$	0	$-2\{I_yI_z\}$	$0\ (\Gamma_4+\Gamma_5)$
	$D^{(2)}$	$(I_y^2-I_z^2)\sigma_x-(\{I_xI_y\}\sigma_y-\{I_zI_x\}\sigma_z)$	0	0	$3i\{I_yI_z\}$	$0\ (\Gamma_4+\Gamma_5)$
	$D^{(3)}$	$(I_y^2-I_z^2)\sigma_x+2(\{I_xI_y\}\sigma_y-\{I_zI_x\}\sigma_z)$	$2\{(J_y^2-J_z^2)J_x\}$	0	0	$\begin{cases} 0\ (\Gamma_4) \\ \frac{3}{2}\sigma_x,\ -\frac{3}{2}\sigma_y\ (\Gamma_5) \end{cases}$

[a] The notation of DKK (Ref. 5) is used for the cubic group representations.

[b] The form of the operator defines the 4×2 rectangular matrix in (J, M_J) representation which connects the subspaces $J=\frac{3}{2}$ (Γ_8) and $J=\frac{1}{2}$ (Γ_7).

where $\vec{H}$ is an external magnetic field. The lowest powers of $\vec{k}$ are decomposed according to irreducible representations as

$$\begin{aligned} &\Gamma_1^+: \ 1,\ k^2\,, \\ &\Gamma_{15}^-: \ k_x,\ k_y,\ k_z\,, \\ &\Gamma_{15}^+: \ k_xk_y-k_yk_x=eH_z/i\hbar c,\ \text{etc.}\,, \\ &\Gamma_{12}^+: \ k_x^2-k_y^2,\ k_y^2-k_z^2\,, \\ &\Gamma_{25}^+: \ k_xk_y+k_yk_x,\ \text{etc.} \end{aligned} \tag{4}$$

With the help of Table I we write the following cubic invariant which includes powers of $\vec{k}$ not higher than the second:

$$\begin{aligned} \mathcal{H}_k = \frac{\hbar^2}{2m}\Big(& [A_1+B_1(\vec{I}\cdot\vec{\sigma})]k^2 \\ & +[A_2(I_x^2-\tfrac{1}{3}I^2)+B_2(I_x\sigma_x-\tfrac{1}{3}\vec{I}\cdot\vec{\sigma})]k_x^2+\text{c.p.} \\ & +[A_3(I_xI_y+I_yI_x)+B_3(I_x\sigma_y+I_y\sigma_x)]\{k_xk_y\}+\text{c.p.}\Big) \\ & +\frac{e\hbar}{mc}[A_4I_x+B_4\sigma_x+B_4'(I_x^2-\tfrac{1}{3}I^2)\sigma_x \end{aligned}$$

$$+B_4''(\{I_xI_y\}\sigma_y+\{I_xI_z\}\sigma_z)]H_x+\text{c.p.}\ , \tag{5}$$

where the factors $\hbar^2/2m$ and $e\hbar/mc$ are inserted to make the A's and the B's dimensionless. The curly bracket is used throughout to denote the symmetric product

$$\{AB\}=\tfrac{1}{2}(AB+BA)\ , \tag{6}$$

and c.p. implies addition of cyclically permuted terms. Inclusion in Eq. (5) of the spin-dependent terms, as we shall see later, is essential in obtaining a nonvanishing q term in the projected Hamiltonian.

(iii) *Strain interaction.* A uniform strain is represented by a strain tensor[21] $\epsilon_{\mu\nu}=\frac{1}{2}(\partial u_\mu/\partial x_\nu+\partial u_\nu/\partial x_\mu)$ (symmetric in μ and ν) whose components decompose in cubic symmetry as follows:

$$\begin{aligned}&\Gamma_1^+:\ \epsilon_{xx}+\epsilon_{yy}+\epsilon_{zz}\ ,\\&\Gamma_{15}^+:\ \epsilon_{xx}-\epsilon_{yy},\ \epsilon_{yy}-\epsilon_{zz}\ ,\\&\Gamma_{25}^+:\ \epsilon_{xy},\ \epsilon_{yz},\ \epsilon_{zx}\ .\end{aligned} \tag{7}$$

The cubic invariant linear in strain gives the following strain Hamiltonian:

$$\begin{aligned}\mathcal{H}_e=&[D_1+E_1(\vec{\mathrm{I}}\cdot\vec{\sigma})](\epsilon_{xx}+\epsilon_{yy}+\epsilon_{zz})\\&+[D_2(I_x^2-\tfrac{1}{3}I^2)+E_2(I_x\sigma_x-\tfrac{1}{3}\vec{\mathrm{I}}\cdot\vec{\sigma})]\epsilon_{xx}+\text{c.p.}\\&+[D_3(I_xI_y+I_yI_x)+E_3(I_x\sigma_y+I_y\sigma_x)]\epsilon_{xy}+\text{c.p.}\end{aligned} \tag{8}$$

Form (8) can be obtained from the magnetic Hamiltonian (5) by replacing $k_\mu k_\nu$ with $\epsilon_{\mu\nu}$ and dropping all antisymmetric terms which appeared by virtue of the noncommutivity (3).

B. Perturbation theory

In Sec. II A we introduced a number of phenomenological parameters through the process of constructing Hamiltonians from symmetry properties alone. These parameters, on the other hand, can be evaluated by working in the perturbation theory on the Bloch states at the center of the Brillouin zone. The perturbations which give rise to the three interactions are

$$\text{spin-orbit:}\quad \mathcal{H}_{so}=\vec{\sigma}\cdot\vec{\mathrm{h}}\ , \tag{9}$$

$$\text{magnetic:}\quad \mathcal{H}_k=\frac{\hbar^2k^2}{2m}+\frac{\hbar}{m}\vec{\mathrm{k}}\cdot\vec{\pi}+g_s\frac{e\hbar}{4mc}\vec{\sigma}\cdot\vec{\mathrm{H}}\ , \tag{10}$$

$$\text{strain:}\quad \mathcal{H}_e=(\mathfrak{D}_{\mu\nu}+\mathfrak{D}_{\mu\nu\lambda}\sigma_\lambda)\epsilon_{\mu\nu}\ , \tag{11}$$

where g_s is the free-electron g value ($g_s=2.0023$) and

$$\vec{\pi}=\vec{\mathrm{p}}+\frac{\hbar}{4mc^2}\vec{\sigma}\times\nabla V\ , \tag{12}$$

$$\vec{\mathrm{h}}=\frac{\hbar}{4m^2c^2}\nabla V\times\vec{\mathrm{p}}\ , \tag{13}$$

V being the periodic crystal potential. $\mathfrak{D}_{\mu\nu}$ and $\mathfrak{D}_{\mu\nu\lambda}$ are the spin-independent and spin-dependent deformation operators which will be discussed later.

The relationship between the "spin" Hamiltonians (2), (5), and (8) and the perturbation Hamiltonians (9)–(11) is established in the following way. First, taking the matrix element of Eq. (9) and comparing it with Eq. (2) we have

$$\Lambda=3i\langle\epsilon_1|h_z|\epsilon_2\rangle\ . \tag{14}$$

Next, we work to the second order in the perturbation (10), separate the symmetric and antisymmetric products of $\vec{\mathrm{k}}$ using Eq. (3), and obtain the matrix element

$$\begin{aligned}&\frac{\hbar^2}{2m}k^2\delta_{ij}+\frac{\hbar^2}{2m^2}\sum_l\frac{\langle i|\pi_\mu|l\rangle\langle l|\pi_\nu|j\rangle+\langle i|\pi_\nu|l\rangle\langle l|\pi_\mu|j\rangle}{E_0-E_l}\{k_\mu k_\nu\}\\&\qquad+\frac{e\hbar}{4mc}\left(g_s\sigma_\lambda+e_{\lambda\mu\nu}\sum_l\frac{\langle i|\pi_\mu|l\rangle\langle l|\pi_\nu|j\rangle-\langle i|\pi_\nu|l\rangle\langle l|\pi_\mu|j\rangle}{im(E_0-E_l)}\right)H_\lambda\ ,\end{aligned} \tag{15}$$

where $e_{\lambda\mu\nu}$ is the antisymmetric unit tensor. In Eq. (15) i,j refer to the degenerate states (ϵ_1, ϵ_2, ϵ_3) of the valence-band-edge manifold with energy E_0; and l refers to a state outside it. Comparison of terms of same symmetry in Eqs. (5) and (15) leads to the following result. First, replacing $\vec{\pi}$ by $\vec{\mathrm{p}}$ in Eq. (15) we obtain spin-independent coefficients which are

$$\begin{aligned}A_1&=1+\tfrac{1}{3}(F+2G+2H_1+2H_2)\ ,\\A_2&=-F-2G+H_1+H_2\ ,\\A_3&=-F+G-H_1+H_2\ ,\end{aligned} \tag{16}$$

$$A_4=\tfrac{1}{4}(F-G-H_1+H_2)\ ,$$

where

$$\begin{aligned}F&=\frac{2}{m}\sum_{\Gamma_2^-}\frac{|\langle\epsilon_1|p_x|\beta,l\rangle|^2}{E_0-E_l}\ ,\\G&=\frac{2}{m}\sum_{\Gamma_{12}^-}\frac{|\langle\epsilon_1|p_x|\gamma_1,l\rangle|^2}{E_0-E_l}\ ,\\H_1&=\frac{2}{m}\sum_{\Gamma_{15}^-}\frac{|\langle\epsilon_1|p_y|\delta_3,l\rangle|^2}{E_0-E_l}\ ,\\H_2&=\frac{2}{m}\sum_{\Gamma_{25}^-}\frac{|\langle\epsilon_1|p_y|\epsilon_3,l\rangle|^2}{E_0-E_l}\ .\end{aligned} \tag{17}$$

are the constants originally defined by Dresselhaus, Kip, and Kittel (DKK).[5] (We have made them dimensionless.) In Fig. 1 we indicate the approximate positions[22] of the energy levels in Ge at $\vec{k}=0$ to locate the states that perturb the valence band edge.

It is worth noting that the position and orthogonalized-plane-wave (OPW) nature of the levels in Fig. 1 provide a clue to the relative magnitudes of F, G, H_1, and H_2. In Ge the largest are H_1 and F which derive from the nearby states Γ_{15}^- and Γ_2^-, respectively, both predominantly of [111] plane-wave character which gives a strong overlap with the valence-band state Γ_{25}^+ similarly composed. Rather smaller is G which derives from the more remote Γ_{12}^- state whose character, predominantly [200] plane waves, differs from the Γ_{25}^+ state. Considerably smaller yet H_2 derives from Γ_{25}^- states, the lowest of which (not shown in Fig. 1) has [220] plane-wave character and lies far, ~ 25–30 eV (free-electron estimate), above Γ_{25}^+. Thus the relative magnitudes are expected to fall in the order $|F|, |H_1| > |G| \gg |H_2|$.

Next, retaining the second term in Eq. (12) and picking up only terms first order in spin-orbit interaction we obtain, by comparison with Eq. (5), the spin-dependent coefficients

$$\begin{aligned}
B_2 &= B_3 = -\tfrac{3}{2}B_1 = 2\sum_l \frac{p_y^{1l}V_x^{l2} - p_x^{1l}V_y^{l2}}{i(E_0-E_l)} \\
&= -\frac{1}{2mc^2}\langle\epsilon_1|(\vec{r}\times\nabla V)_z|\epsilon_2\rangle , \\
B_4 &= \tfrac{1}{4}g_s + \frac{2}{3}\sum_l \frac{p_x^{1l}V_x^{l1} + 2p_y^{1l}V_y^{l1}}{i(E_0-E_l)} \\
&= \tfrac{1}{4}g_s + \frac{1}{6mc^2}\langle\epsilon_1|\vec{r}\cdot\nabla V|\epsilon_1\rangle , \\
B_4' &= \sum_l \frac{p_x^{1l}V_x^{l1} - p_y^{1l}V_y^{l1}}{i(E_0-E_l)} = \frac{1}{4mc^2}\langle\epsilon_1|x\frac{\partial V}{\partial x} - y\frac{\partial V}{\partial y}|\epsilon_1\rangle , \\
B_4'' &= \sum_l \frac{p_y^{1l}V_x^{l2} + p_x^{1l}V_y^{l2}}{i(E_0-E_l)} \\
&= \frac{1}{4mc^2}\langle\epsilon_1|y\frac{\partial V}{\partial x} + x\frac{\partial V}{\partial y}|\epsilon_2\rangle ,
\end{aligned} \tag{18}$$

where

$$\begin{aligned}
p_x^{1l} &= \langle\epsilon_1|p_x|l\rangle , \\
V_x^{l1} &= \langle l|\frac{\hbar}{4m^2c^2}\frac{\partial V}{\partial x}|\epsilon_1\rangle .
\end{aligned} \tag{19}$$

As the spin-orbit contribution is usually much smaller than the purely orbital one, we neglect second-order spin-orbit terms entirely.

The deformation-potential constants appearing in Eq. (8) can be obtained in a similar way by taking the intraband matrix elements of the deformation operators which are "even" under inversion. The spin-independent deformation operator, discussed in detail by Whitfield[23] and Pikus and Bir,[24] has the form

$$\mathfrak{D}_{\mu\nu} = -(1/m)p_\mu p_\nu + V_{\mu\nu} , \tag{20}$$

where $V_{\mu\nu}$ represents the derivative of crystal potential V with respect to strain $\epsilon_{\mu\nu}$. The spin-dependent deformation operator derives from the change in spin-orbit interaction under strain. It is given by

$$\begin{aligned}
\mathfrak{D}_{\mu\nu\lambda} &= (-\delta_{\mu\nu}\delta_{\lambda\alpha} + \tfrac{1}{2}\delta_{\mu\lambda}\delta_{\nu\alpha} + \tfrac{1}{2}\delta_{\nu\lambda}\delta_{\mu\alpha})h_\alpha \\
&\quad + h_{\mu\nu\lambda} + \sum_l \frac{\mathfrak{D}_{\mu\nu}|l\rangle\langle l|h_\lambda + h_\lambda|l\rangle\langle l|\mathfrak{D}_{\mu\nu}}{E_0-E_l} ,
\end{aligned} \tag{21}$$

where the vector $\vec{h}$ is defined by Eq. (13) and

$$\vec{h}_{\mu\nu} = (\hbar/4m^2c^2)\nabla V_{\mu\nu}\times\vec{p} . \tag{22}$$

The first and second terms in Eq. (21) come from the first-order strain perturbation, while the last term is contributed from the second-order perturbation arising from the strain and spin-orbit interactions through the intermediate states Γ_{12}^+, Γ_{15}^+, and Γ_{25}^+ (see Fig. 1). Comparison of Eqs. (8) and (11) gives the following deformation potential constants:

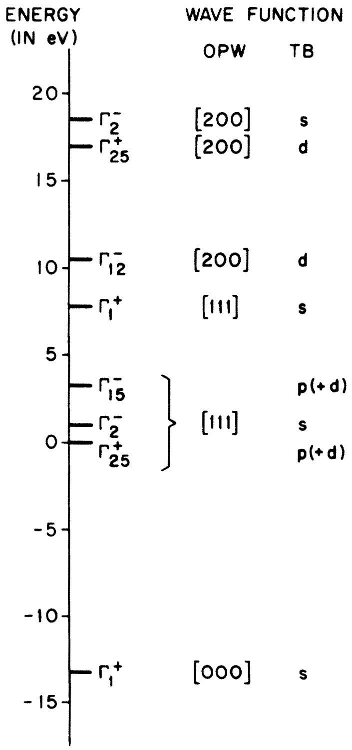

FIG. 1. Approximate positions of energy levels in Ge at $\vec{k}=0$ (see Ref. 22). The character of each wave function may be inferred roughly from the parent OPW or tight-binding (TB) states from where it derives. Spin-orbit interaction is not included.

$$\begin{aligned} D_1 &= \tfrac{1}{3}\langle \epsilon_1 | \mathfrak{D}_{xx} + 2\mathfrak{D}_{yy} | \epsilon_1 \rangle \ , \\ D_2 &= -\langle \epsilon_1 | \mathfrak{D}_{xx} - \mathfrak{D}_{yy} | \epsilon_1 \rangle \ , \\ D_3 &= -2\langle \epsilon_1 | \mathfrak{D}_{xy} | \epsilon_2 \rangle \ , \end{aligned} \tag{23}$$

and

$$\begin{aligned} E_1 &= \tfrac{1}{3} i\langle \epsilon_2 | \mathfrak{D}_{xxx} + 2\mathfrak{D}_{yyx} | \epsilon_3 \rangle \ , \\ E_2 &= i\langle \epsilon_2 | \mathfrak{D}_{xxx} - \mathfrak{D}_{yyx} | \epsilon_3 \rangle \ , \\ E_3 &= 2i\langle \epsilon_2 | \mathfrak{D}_{xyy} | \epsilon_3 \rangle \ . \end{aligned} \tag{24}$$

C. Projection

Although the Hamiltonians presented in Sec. II B are complete, it is often inconvenient to work in the full six-dimensional space of Γ_{25}^{+}. Under certain conditions it suffices to work entirely in a particular subspace or to treat the effect of complementary subspaces by perturbation theory. We point out first the relative magnitudes of the energies involved in a typical experiment:

$$\textit{energy gap} \gg \textit{spin-orbit energy} \gg \textit{magnetic, strain and thermal energies}. \tag{25}$$

This suggests that we diagonalize the spin-orbit Hamiltonian $\mathcal{H}_{so}$ first. Defining the total angular momentum by $\vec{J} = \vec{I} + \frac{1}{2}\vec{\sigma}$, we see

$$\mathcal{H}_{so} = \tfrac{1}{3}\Lambda(J^2 - I^2 - \tfrac{1}{4}\sigma^2) = \begin{cases} \tfrac{1}{3}\Lambda & \text{for } J = \tfrac{3}{2} \\ -\tfrac{2}{3}\Lambda & \text{for } J = \tfrac{1}{2} \ . \end{cases} \tag{26}$$

Thus, $\mathcal{H}_{so}$ splits the six-dimensional space into a four-dimensional $J = \frac{3}{2}$ subspace (Γ_8^{+}) and a two-dimensional $J = \frac{1}{2}$ subspace (Γ_7^{+}). Now, we project the magnetic and strain Hamiltonians onto each of the spin-orbit-split subspaces with the aid of the projection operators P and Q in the following manner:

$$\begin{aligned} \mathcal{H}_{3/2} &= \tfrac{1}{3}\Lambda + P(\mathcal{H}_k + \mathcal{H}_e)P + P(\mathcal{H}_k + \mathcal{H}_e) \\ &\quad \times Q(1/\Lambda)Q(\mathcal{H}_k + \mathcal{H}_e)P + \cdots \ , \end{aligned} \tag{27}$$

$$\begin{aligned} \mathcal{H}_{1/2} &= -\tfrac{2}{3}\Lambda + Q(\mathcal{H}_k + \mathcal{H}_e)Q - Q(\mathcal{H}_k + \mathcal{H}_e) \\ &\quad \times P(1/\Lambda)P(\mathcal{H}_k + \mathcal{H}_e)Q + \cdots \ . \end{aligned} \tag{28}$$

The general formulas for projection $\vec{I}$, $\vec{\sigma} \to \vec{J}$ ($J = \frac{3}{2}$ or $J = \frac{1}{2}$) are given in Table II in reducible tensor forms. In cubic symmetry the projected Hamiltonians (27) and (28) can be expressed as cubic invariants using the angular-momentum matrices $\vec{J}$ similar to the way discussed in Sec. II A. The fourth and fifth columns of Table I show the projection on the subspaces $J = \frac{3}{2}$ and $J = \frac{1}{2}$ of each independent matrix reduced for cubic symmetry. The first-order projections [the second terms in Eqs. (27) and (28)] are particularly simple and have the following forms:

$J = \frac{3}{2}$:

$$\begin{aligned} P\mathcal{H}_k P = -(\hbar^2/m)\{&\gamma_1 \tfrac{1}{2}k^2 - \gamma_2[(J_x^2 - \tfrac{1}{3}J^2)k_x^2 + \text{c.p.}] \\ &- 2\gamma_3[\{J_x J_y\}\{k_x k_y\} + \text{c.p.}]\} \end{aligned}$$

TABLE II. General expressions in (reducible) tensor form which enumerate all possible projections of operators containing $\vec{I}$ and $\vec{\sigma}$ onto the subspaces of $\Gamma_8(J = \frac{3}{2})$, $\Gamma_7(J = \frac{1}{2})$, and the rectangular cross space $\Gamma_8 \times \Gamma_7$. Any higher power of $\vec{\sigma}$ and $\vec{I}$ can be reduced to lower powers by the use of Eq. (1) and the formula

$$\{I_\lambda, \{I_\mu I_\nu\}\} = \tfrac{1}{2}\delta_{\mu\nu} I_\lambda + \tfrac{1}{4}(\delta_{\mu\lambda} I_\nu + \delta_{\nu\lambda} I_\mu) \ .$$

For $J = \frac{3}{2}$ there exist only 16 ($= 4^2$) independent matrices (powers not higher than third in the components of $\vec{J}$). Any higher powers can be reduced by repeated use of the commutation relaxation $\vec{J} \times \vec{J} = i\vec{J}$ and the formula

$$\begin{aligned} \{\{J_\kappa J_\lambda\}, \{J_\mu J_\nu\}\} = \tfrac{5}{4}(\delta_{\kappa\lambda}\{J_\mu J_\nu\} + \delta_{\mu\nu}\{J_\kappa J_\lambda\}) \\ - \tfrac{33}{16}\delta_{\kappa\lambda}\delta_{\mu\nu} + \tfrac{3}{4}(\delta_{\kappa\mu}\delta_{\lambda\nu} + \delta_{\kappa\nu}\delta_{\lambda\mu}) \ . \end{aligned}$$

Operator	Projection[a] on Γ_8 ($J = \frac{3}{2}$)	Projection on Γ_7 ($J = \frac{1}{2}$)	Cross space[b] $\Gamma_8 \times \Gamma_7$
I_μ	$\frac{2}{3}J_\mu$	$\frac{4}{3}J_\mu$	I_μ
σ_μ	$\frac{2}{3}J_\mu$	$-\frac{2}{3}J_\mu$	$-2I_\mu$
$\{I_\mu I_\nu\}$	$\frac{1}{3}\{J_\mu J_\nu\} + \frac{1}{4}\delta_{\mu\nu}$	$\frac{2}{3}\delta_{\mu\nu}$	$\{I_\mu I_\nu\}$
$I_\mu \sigma_\nu$	$\frac{2}{3}\{J_\mu J_\nu\} - \frac{1}{2}\delta_{\mu\nu}$	$-\frac{2}{3}\delta_{\mu\nu}$	$-\{I_\mu I_\nu\} + \frac{3}{2}[I_\mu, I_\nu] + \frac{2}{3}\delta_{\mu\nu}$
$\{I_\mu I_\nu\}\sigma_\lambda$	$\frac{2}{3}\{J_\mu J_\nu J_\lambda\} - \frac{1}{18}\delta_{\mu\nu} J_\lambda$ $- \frac{7}{18}(\sigma_{\mu\lambda} J_\nu + \delta_{\nu\lambda} J_\mu)$	$-\frac{2}{3}(\delta_{\mu\lambda} J_\nu + \delta_{\nu\lambda} J_\mu)$	$-\frac{3}{2}\delta_{\mu\nu} I_\lambda + \frac{1}{4}(\delta_{\mu\lambda} I_\nu + \delta_{\nu\lambda} I_\mu)$ $- \frac{1}{2}\{I_\mu, [I_\nu, I_\lambda]\} - \frac{1}{2}\{I_\nu, [I_\mu, I_\lambda]\}$

[a] The "triple" symmetric product $\{J_\mu J_\nu J_\lambda\}$ is defined by $\{J_\mu J_\nu J_\lambda\} = (3!)^{-1}\sum_P J_{P(\mu)} J_{P(\nu)} J_{P(\lambda)}$, where P is a permutation of μ, ν, λ.

[b] The form of the operator defines the 4×2 rectangular matrix in (J, M_J) representation which connects the subspaces Γ_8 ($J = \frac{3}{2}$) and Γ_7 ($J = \frac{1}{2}$).

$$-(e\hbar/mc)(\kappa J_x + qJ_x^3)H_x + \mathrm{c.p.}\,, \qquad (29)$$

$$P\mathcal{H}_e P = D_d(\epsilon_{xx} + \mathrm{c.p.}) + \tfrac{2}{3}D_u[(J_x^2 - \tfrac{1}{3}J^2)\epsilon_{xx} + \mathrm{c.p.}] + \tfrac{2}{3}D_u'(2\{J_x J_y\}\epsilon_{xy} + \mathrm{c.p.})\,, \qquad (30)$$

with

$$\gamma_1 = -A_1 - B_1\,,$$
$$\gamma_2 = \tfrac{1}{6}A_2 + \tfrac{1}{3}B_2\,,$$
$$\gamma_3 = \tfrac{1}{6}A_3 + \tfrac{1}{3}B_3\,, \qquad (31)$$
$$\kappa = -\tfrac{2}{3}A_4 - \tfrac{2}{3}B_4 + \tfrac{23}{18}B_4' - \tfrac{3}{2}B_4''\,,$$
$$q = -\tfrac{2}{3}B_4' + \tfrac{2}{3}B_4''\,,$$
$$D_d = D_1 + E_1\,,$$
$$D_u = \tfrac{1}{2}D_2 + E_2\,, \qquad (32)$$
$$D_u' = \tfrac{1}{2}D_3 + E_3\,;$$

$J = \frac{1}{2}$:

$$Q\mathcal{H}_k Q = -(\hbar^2/2m)\gamma_1' k^2 - g'(e\hbar/2mc)\vec{\mathrm{J}}\cdot\vec{\mathrm{H}}\,, \qquad (33)$$

$$Q\mathcal{H}_e Q = D_d'(\epsilon_{xx} + \mathrm{c.p.})\,, \qquad (34)$$

with

$$\gamma_1' = -A_1 + 2B_1\,,$$
$$g' = -\tfrac{8}{3}A_4 + \tfrac{4}{3}B_4 + \tfrac{16}{9}B_4' + \tfrac{8}{3}B_4''\,, \qquad (35)$$
$$D_d' = D_1 - 2E_1\,. \qquad (36)$$

The effective-mass parameters (31) and the deformation potential constants (32) associated with $J = \frac{3}{2}$ bands conform with the definitions of Luttinger[3] and those of Kleiner and Roth,[25] respectively.[26]

Another useful projection is applicable in the $J = \frac{3}{2}$ manifold when, in addition to (25), the condition

strain energy $\gg$ *magnetic and thermal energies* (37)

is satisfied. Anisotropic strain generally splits the $J = \frac{3}{2}$ quartet into two doublets; and then we can project $\mathcal{H}_k$ further onto one of the strain-split subspaces. The projection scheme is shown in Fig. 2 for three particularly simple directions of uniaxial strain. This will be discussed further in Sec. V.

D. Spin-dependent contributions

It is clear from the discussion of Sec. II B that all the coefficients of those terms in the "spin" Hamiltonians (5) and (8) which depend on both orbit and spin vanish in the absence of spin-orbit interaction. Such terms have traditionally been neglected on the grounds that the spin-orbit interaction is much smaller than the purely orbital effect. Even with large spin-orbit interaction their existence is hardly evident if only the first-order projections are considered, because spin-independent and spin-dependent terms such as $I_x^2 - \frac{1}{3}I^2$ and

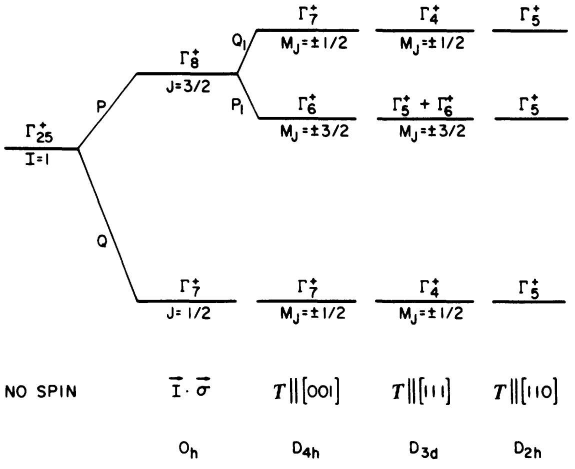

FIG. 2. Splitting of the Γ_{25}^+ valence band edge in Ge resulting from the spin-orbit interaction $\vec{\mathrm{I}}\cdot\vec{\sigma}$ followed by a uniaxial compressive stress T applied along each of the principal crystallographic directions. The projection operators associated with each splitting are shown.

$I_x\sigma_x - \frac{1}{3}\vec{\mathrm{I}}\cdot\vec{\sigma}$ both give the same form, $J_x^2 - \frac{1}{3}J^2$ (or zero), on projection on the $J = \frac{3}{2}$ (or $J = \frac{1}{2}$) subspace and cannot be distinguished from one another. The only exception in which spin-dependent effects are isolated and, therefore, recognizable in the $J = \frac{3}{2}$ subspace is the q term in Eq. (29) which is seen by Eq. (31) to arise exclusively from spin-dependent sources. In prior work the q term has (incorrectly) been neglected in Ge, where the spin-orbit interaction is moderately weak; but for reasons which will become evident we have found it necessary to reexamine its origin and estimate its magnitude more carefully. In fact, we find that the whole subject of spin-dependent effects warrants closer attention overall.

By the analysis in the previous sections, q is seen to be comprised of the components B_4' and B_4'' which, in turn, can be evaluated using the second-order perturbation formulas (18). On the basis of these formulas Kohn (in an unpublished work) concluded that q in Ge is extremely small, i.e., $q \lesssim 10^{-3}$, thus justifying its neglect in the Hamiltonian (29). The smallness of this result is due primarily to the fact that the relevant second-order expressions (18) always contain matrix elements of the *derivative* of the crystal potential which is slowly varying outside the atomic cores. We have uncovered additional and more important contributions previously overlooked which come from a formally higher order[27] of perturbation, namely, from the cross product of the spin-orbit and magnetic interactions. The most important terms then are those involving the diagonal matrix element of spin-orbit interaction, namely,

$$\frac{\hbar^2}{m^2}\sum_{l}\frac{\langle i|p_\mu|l\rangle\langle l|\mathcal{H}_{so}|l\rangle\langle l|p_\nu|j\rangle}{(E_0-E_l)^2}k_\mu k_\nu\;, \tag{38}$$

where, now, $\vec{\pi}$ has been replaced by $\vec{p}$. This formula clearly shows that among the four representations connected by $\vec{p}$ with Γ_{25}^{+}, only two, Γ_{15}^{-} and Γ_{25}^{-}, with nonzero spin-orbit splitting can contribute. We thus redefine the B constants previously given in Eq. (18) by dropping the negligible second-order terms and replacing them by third-order perturbation terms h_1 and h_2 as follows:

$$\begin{aligned} &B_1=-\tfrac{1}{9}(h_1-h_2),\quad B_2=-\tfrac{1}{3}(h_1-h_2),\\ &B_3=\tfrac{1}{3}(h_1+h_2),\quad B_4=\tfrac{1}{4}g_s+\tfrac{1}{18}(h_1-h_2)\;,\\ &B_4'=-\tfrac{1}{6}(h_1-h_2),\quad B_4''=\tfrac{1}{6}(h_1+h_2)\;, \end{aligned} \tag{39}$$

where

$$h_1=\frac{2}{m}\sum_{\Gamma_{15}^{-}}\frac{|\epsilon_1|p_y|\delta_{3,l}\rangle|^2\Delta_{15,l}}{(E_0-E_l)^2}\;, \tag{40}$$

$$h_2=\frac{2}{m}\sum_{\Gamma_{25}^{-}}\frac{|\langle\epsilon_1|p_y|\epsilon_{3,l}\rangle|^2\Delta_{25,l}}{(E_0-E_l)^2}\;. \tag{41}$$

In the above,

$$\begin{aligned} &\Delta_{15,l}=3i\langle\delta_{1,l}\,|h_z|\,\delta_{2,l}\rangle\;,\\ &\Delta_{25,l}=3i\langle\epsilon_{1,l}\,|h_z|\,\epsilon_{2,l}\rangle \end{aligned} \tag{42}$$

are the spin-orbit splittings of the lth Γ_{15}^{-} and Γ_{25}^{-} bands, respectively. For the same reasons that H_2 is very small we should expect h_2 to be quite negligible. On the other hand, h_1 can be roughly estimated on the assumption that both H_1 and h_1 are predominantly contributed by a single Γ_{15}^{-} band, which is located ~ 3 eV above Γ_{25}^{+} and, for which $\Delta_{15}\sim 0.2$ eV.[28] Since $H_1\sim -5.3$[17] this gives

$$h_1\sim H_1\,\frac{\Delta_{15}}{(E_0-E_l)}\sim 0.3\;, \tag{43}$$

and we obtain

$$q=\tfrac{2}{9}h_1\sim 0.06\;. \tag{44}$$

This constant is small compared, say, to κ ($\kappa\sim 3.4$); but it can be detected in precision experiments (see Paper III). In materials with larger spin-orbit interaction, we would expect the magnitude of q to be correspondingly larger.[29]

Besides accounting for the q term in its entirety, the spin contributions, h_1 and h_2, also appear as small "corrections" in the definitions of the effective-mass parameters γ_1, γ_2, γ_3, and κ in Eq. (31). This fact must be taken into account (in Paper III) in evaluating the DKK band parameters F, G, H_1, and H_2 from experimental measurements of γ_1, γ_2, γ_3, and κ.

Another interesting contribution of the spin-dependent terms appears in the strain Hamiltonian. In this case, since no equivalent to the q term exists, the spin-dependent part cannot be distinguished from the spin-independent one in the first-order projection. However, two methods can be suggested to detect its contribution. First, the most straightforward way, in principle, would be to measure the change of spin-orbit splitting of the $J=\frac{3}{2}$ and $J=\frac{1}{2}$ bands as a function of a hydrostatic pressure.[30] This directly measures E_1. Second, one could look for uniaxial stress effects which derive from the second-order projection [the third term in Eqs. (27) and (28)]. Here the pertinent deformation potential is $\frac{1}{2}(D_2-E_2)$ or $\frac{1}{2}(D_3-E_3)$ instead of $\frac{1}{2}(D_2+2E_2)$ or $\frac{1}{2}(D_3+2E_3)$ as given by Eq. (32) for the $J=\frac{3}{2}$ projection. Comparison of measurements of uniaxial deformation potentials made inside and outside of the $J=\frac{3}{2}$ manifold would directly resolve the spin-dependent components E_2 and E_3 from the spin-independent components D_2 and D_3. (See Sec. VI.) Such an analysis is carried out in Paper II.

It is not a simple matter to estimate the spin-dependent deformation potentials E_1, E_2, and E_3 from the formal expressions (24). Only the first term of the spin-dependent deformation operator $\mathfrak{D}_{\mu\nu\lambda}$ in Eq. (21) can be readily evaluated. It simply represents the change of spin-orbit interaction by the scaling effect under strain and gives the spherical contribution

$$E_1=-\tfrac{2}{9}\Lambda,\quad E_2=E_3=\tfrac{1}{3}\Lambda\;. \tag{45}$$

This result by itself is equivalent to making the "deformable-ion" approximation.

Serious difficulties are encountered in attempts to evaluate the second term $h_{\mu\nu\lambda}$ in Eq. (21), since it involves the derivative of the change in the potential, $V_{\mu\nu}$, under strain. Thus far we have not found a realistic yet tractable model on which to base such a calculation.

The third (second-order) term in Eq. (21) is probably unimportant in Ge since the lowest relevant states (Γ_{12}^{+}, Γ_{15}^{+}, and Γ_{25}^{+}) are at least $E_l-E_0\sim 10$ eV above the valence band.

III. SPECTRAL FUNCTION

In this section we derive the absorption line-shape function or "spectral" function which describes the electric-dipole power absorption spectrum arising from quantum resonances in a crystal which lies in a microwave electric field $\vec{\mathcal{E}}$ having fixed frequency and specific polarization. This function maps the shape of the experimental recorder traces one observes when the "dc" magnetic field $\vec{H}$ is swept over the resonance regions. We shall not go into the subject of line broadening in a general way; rather our goal is to develop the spectral function in a form suitable for computation of "synthesized" cyclotron resonance spectra starting with the solutions of the effective-mass equation.

In the past it has been customary to analyze cyclotron-resonance spectra in terms of line positions and intensities calculated for $k_H = 0$ with an appropriate collision-time line broadening chosen to approximate the line shapes. A few attempts[8,9,11] have been made to relax the $k_H = 0$ assumption and incorporate by perturbation methods (near $k_H = 0$) the inhomogeneous broadening due to the dependence of the transition energy on k_H. However, this approach is too restrictive for our present needs; we shall see in succeeding papers that it is unlikely that the quantum cyclotron-resonance spectra in the degenerate valence bands of Ge could be unravelled in such a simple way. Serious complications arise in reality due to the fact that not only are the observed spectra composed of a superposition of numerous quantum resonances each k_H broadened, but also transitions can take place in regions of k_H space away from $k_H = 0$ (noncentral transitions). Where k_H mixing of two or more transitions is appreciable it becomes difficult to trace the transitions as continuous functions of k_H. It is necessary, therefore, to establish a more powerful method of spectral analysis which automatically copes with such complex situations.

In addition, some confusion has existed in previous work in regard to the dependence of the line-shape function on magnetic field. This would be unimportant if our attention were confined to localized structure (or a single line), but for the case of the hole transitions in Ge the spectrum can span a range of effective mass of more than a factor of 10. When the magnetic field must be scanned over such a range (we assume that the microwave frequency is kept fixed) it is imperative that the dependence of the intensity on the magnetic field be properly taken into account to ensure a quantitative and unambiguous fit to the observed spectra.

The development of the spectral function initiated from the analysis of the resonance spectra in Paper IV for unstressed or "cubic" Ge where the k_H broadening is most pronounced. However, the formalism is applicable for stressed crystals and has been employed in a few instances in Paper II where detailed analysis of line shapes is required.

A harmonic electric field of frequency $\omega (> 0)$ is described by

$$\vec{A} = (ic/\omega)\vec{\mathcal{E}} e^{i\omega t} , \tag{46}$$

and gives rise to an interaction with electron

$$\mathcal{H}' = (e/c)\vec{A} \cdot \vec{v} = (ie/\omega)\vec{\mathcal{E}} \cdot \vec{v} e^{i\omega t} , \tag{47}$$

where $\vec{v}$ is the electron velocity defined by

$$\vec{v} = \frac{1}{\hbar}\frac{\partial \mathcal{H}_k}{\partial \vec{k}} . \tag{48}$$

The power absorption per electron from the microwave electric field is expressed as a sum

$$\sum_{(s,t)} (E_s - E_t)(f_t - f_s) w_{st} \tag{49}$$

over all pairs of states (s, t) with statistical occupation probability f and energy E. In Eq. (49) w_{st} is the transition probability[31] per unit time deriving from the interaction Hamiltonian (47) (plus its Hermitian conjugate) and is given as usual by

$$\begin{aligned} w_{st} = (2\pi/\hbar)(e^2/4\omega^2)[& |\langle s|\vec{\mathcal{E}} \cdot \vec{v}|t\rangle|^2 \delta(E_s - E_t + \hbar\omega) \\ & + |\langle t|\vec{\mathcal{E}} \cdot \vec{v}|s\rangle|^2 \delta(E_s - E_t - \hbar\omega)] , \end{aligned} \tag{50}$$

which, on substitution into Eq. (49) gives the power absorption

$$\frac{\pi e^2}{2\omega} \sum_{\substack{(s,t) \\ E_s > E_t}} (f_t - f_s) |\langle t|\vec{\mathcal{E}} \cdot \vec{v}|s\rangle|^2 \delta(E_s - E_t - \hbar\omega) . \tag{51}$$

The power absorption (51) depends on the temperature through the distribution function f and on magnetic field via level energies and matrix elements. As the magnetic field is swept in a typical experiment the entire level structure scales continuously and linearly with the field. It is therefore convenient to separate the linear field dependence from the "intrinsic" level structure by introducing the following dimensionless quantities.

(i) *Dimensionless magnetic field.* We can represent the magnetic field in the dimensionless form,

$$\eta = eH/mc\omega . \tag{52}$$

In this section it is convenient to let η and H range formally from $-\infty$ to $+\infty$ in order to encompass both states of circular polarization.

(ii) *Dimensionless hole energy.* Conventionally the hole energy is also expressed in a dimensionless form

$$\epsilon = -Emc/\hbar e|H| . \tag{53}$$

The sense of this quantity is *positive* with *increasing* hole excitation. In the present work it is appropriate to assume that ϵ is independent of H just as in the case of a simple band at $k_H = 0$. However, for cases in which the bands are appreciably nonparabolic, E is nonlinear in H, and we cannot make this idealization.

(iii) *Dimensionless momentum and matrix element.* The summation on the indices (s, t) in Eq. (51) extends over all pairs of magnetic states. In particular, the solutions of the effective-mass equation possess a definite momentum k_H which is conserved in an electric dipole transition (see Sec. IV). Therefore, the total line shape, expressed by Eq. (51), consists of a superposition of transitions occurring at each value of k_H. If we separate the k_H summation from the rest, we can replace it by an integral, having first introduced the quasicontinuous dimensionless parameter

$$\zeta = (e|H|/\hbar c)^{-1/2} k_H \; . \tag{54}$$

Next, we introduce a dimensionless matrix element $F_{ts}(\zeta)$ according to[32]

$$\langle t, k_H | \vec{\mathcal{E}} \cdot \vec{v} | s, k_H \rangle = (|\vec{\mathcal{E}}|/m)(e\hbar|H|/c)^{1/2} F_{ts}(\zeta) \; , \tag{55}$$

with

$$F_{ts}(\zeta) = \langle t, \zeta | \vec{e} \cdot \vec{u} | s, \zeta \rangle \; , \tag{56}$$

where now s and t represent all quantum numbers other than k_H, $\vec{u}$ is the dimensionless velocity

$$\vec{u} = (c/e|H|\hbar)^{1/2} m\vec{v} \; , \tag{57}$$

and $\vec{e}$ is the polarization vector of the microwave electric field.[33] The dimensionless matrix element $F_{ts}(\zeta)$ is independent of magnetic field under the same circumstances that ϵ is.

We assume the magnetic field is swept slowly enough so the holes are distributed according to Boltzmann statistics corresponding to the instantaneous magnetic field. Also we assume that the number of carriers generated by photoexcitation remains constant. Under these conditions, the power absorption P per hole at magnetic field η is given by

$$P = (e^2 |\vec{\mathcal{E}}|^2 \pi / 2m\omega) W(\eta) \; , \tag{58}$$

with

$$W(\eta) = \frac{1}{Z(\eta)} \eta^2 (1 - e^{-\gamma}) \int_0^\infty d\zeta \times \sum_{\substack{s,t \\ \eta_{ts} > 0}} [\, |F_{ts}(\zeta)|^2 \delta(\eta - \eta_{ts}) + |F_{st}(\zeta)|^2 \delta(\eta + \eta_{ts})] e^{-|\eta| \gamma \epsilon_s(\zeta)} \; , \tag{59}$$

where $Z(\eta)$ is the partition function

$$Z(\eta) = \int_0^\infty d\zeta \sum_s e^{-|\eta|\gamma\epsilon_s(\zeta)} \; , \tag{60}$$

and

$$\gamma = \hbar\omega / k\Theta \; , \tag{61}$$

$$\eta_{ts} = (\epsilon_t - \epsilon_s)^{-1} \; . \tag{62}$$

The summation on s and t extends over all eigenstates with a fixed ζ. We call Eq. (59) the spectral function, since it completely determines the shape of absorption from $H = 0$ to ∞ ($\eta = 0$ to ∞) or $H = -\infty$ to 0, whichever the case may be. In Paper IV we shall see that the dependence of $\epsilon_s(\zeta)$ on ζ is often far from parabolic which rules out a simple evaluation of the integral (59) as attempted previously[8]; instead, for meaningful results, we must resort to numerical procedures.

To clear up the confusion noted earlier in regard to the magnetic field dependence of the spectral function we briefly trace the origins of the important factors comprising the coefficient in Eq. (59). Two factors favor the intensity of transitions at high effective mass (i.e., high η); they are η^2 in the numerator and $Z(\eta)$ in the denominator. In the former, one power of η comes from the matrix element squared, and one power originates from the density of states (i.e., from the transformation of the argument of the δ functions to dimensionless form). Although the partition function $Z(\eta)$ depends upon the details of the level structure and is not a simple function of η (and γ) it, nevertheless, always decreases monotonically with η, very rapidly when γ is large. All other factorable quantities containing $\vec{H}$ appear in both numerator and denominator (partition function) and, hence, cancel. Failure to recognize this cancellation has led to erroneous results in earlier work.[34]

The factors in Eq. (59) responsible for the structure of the spectrum are the matrix element F_{ts} and the density of states representated by the δ function. The former (which must be calculated at each value of ζ) gives the selection rules and relative intensities. It will be discussed in more detail in Sec. IV. In practice one usually takes into account the effects of collision broadening by replacing the δ function by a smoother line-shape function $g(\eta - \eta_{ts})$ suitably normalized:

$$\int_{-\infty}^{\infty} g(\eta - \eta_{ts}) d\eta = 1 \; . \tag{63}$$

We employ in our calculations the Lorentzian function

$$g(\eta - \eta_{ts}) = \frac{\eta_{ts}}{\omega\tau\pi} \frac{1}{(\eta - \eta_{ts})^2 + (\eta_{ts}/\omega\tau)^2} \; , \tag{64}$$

where τ is the collision time.

Equations (59) and (64) form the basis of line-shape analyses in Papers II–IV.

IV. SOLUTION OF EFFECTIVE-MASS EQUATION AND SELECTION RULES

In this section we examine the nature of the eigenstates of the "spin" Hamiltonian given in Sec. II and of the quantum-resonance transition matrix elements, which connect these eigenstates, given in Sec. III. Because of the complexity of the valence bands of Ge, explicit solutions to the Hamiltonian can only be obtained by numerical methods for the general case (mentioned briefly at the end of this section). Nevertheless, without actually solving the effective-mass equation we can gain considerable insight into the nature of these solutions through the elucidation of their symmetry properties—a basis on which we shall establish schemes for classification of energy levels and selection rules for cyclotron-resonance transitions. In this discussion the following conditions will be assumed:

(i) We confine our consideration to the $J = \frac{3}{2}$ (Γ_8)

band, i.e., the first-order projections (29) and (30) are used as Hamiltonians. [Modifications which occur when we lift this restriction will be discussed in Sec. VI. It should be pointed out that conclusions based on symmetry are not affected by expanding the manifold to include the $J=\frac{1}{2}$ (Γ_7) band.]

(ii) The external strain is assumed to be of uniaxial nature and applied along one of the three simplest directions, [001], [111], and [110]. We briefly remark on stress directions having symmetry lower than these at the end of this section.

(iii) We assume that the static magnetic field lies along the stress axis $(T \parallel \vec{H})$. This highest symmetry case is the one of greatest interest to us. (Other cases will be discussed in Sec. V under more restrictive conditions.)

We begin by defining our coordinate systems. Consistent with the condition (iii) we set up a right-handed coordinate system (x_1, x_2, x_3) with x_3 along the magnetic field (and directed in the same sense). We define the dimensionless momentum along the field by

$$\zeta = (\hbar c/eH)^{1/2} k_H = (\hbar c/eH)^{1/2} k_3 , \tag{65}$$

and, following Luttinger, introduce the harmonic-oscillator creation and annihilation operators by

$$\begin{aligned} a^\dagger &= (\hbar c/2eH)^{1/2}(k_1 + ik_2) , \\ a &= (\hbar c/2eH)^{1/2}(k_1 - ik_2) , \end{aligned} \tag{66}$$

which, from Eq. (3), satisfy the commutation relation

$$\begin{aligned} &[a, a^\dagger] = 1 , \\ &[a, \zeta] = [a^\dagger, \zeta] = 0 . \end{aligned} \tag{67}$$

Similarly, in the same coordinate system we define the raising and lowering angular-momentum operators for $J=\frac{3}{2}$ as follows:

$$J_\pm = (J_1 \pm i J_2)/\sqrt{2} , \tag{68}$$

which obey the commutation relations

$$[J_\pm, J_3] = \mp J_\pm, \quad [J_+, J_-] = J_3 . \tag{69}$$

A. Axial and nonaxial parts

Frequently it is convenient to split the magnetic Hamiltonian (29) into a "spherical" or isotropic part

$$-\frac{\hbar^2}{m}\left[(\tfrac{1}{2}\gamma_1 + \tfrac{5}{4}\gamma_2)k^2 - \gamma_2(\vec{J}\cdot\vec{k})^2 + \frac{e}{\hbar c}(\kappa + \tfrac{1}{2}\gamma_2)(\vec{J}\cdot\vec{H})\right] \tag{70}$$

and a nonspherical part

$$-\frac{\hbar^2}{m}\left[(\gamma_2 - \gamma_3)(2\{J_x J_y\}\{k_x k_y\} + \text{c.p.}) + q\,\frac{e}{\hbar c}(J_x^3 H_x + \text{c.p.})\right] \tag{71}$$

because the spherical part can be diagonalized exactly and the remaining antisotropic parts (71), if they are sufficiently small (i.e., $\gamma_3 - \gamma_2$, $q \ll \gamma_1$, γ_2 and κ), can be treated by perturbation theory. For discussions of symmetry, however, it is preferable to make a different split into axial and nonaxial parts consistent with the axial symmetry established by the stress and magnetic field.

Before doing this let us also rewrite the strain Hamiltonian (30) in spherical and nonspherical parts. We express Eq. (30) (omitting the dilatational part) in terms of the magnitude T of the uniaxial stress ($T>0$ for tension and $T<0$ for compression) and its direction cosines (τ_x, τ_y, τ_z) referred to the cubic crystal axes:

$$\begin{aligned} \mathcal{H}_e = {} & \epsilon_u[(J_x^2 - \tfrac{1}{3}J^2)\tau_x^2 + \text{c.p.}] \\ & + \epsilon_u'[2\{J_x J_y\}\tau_x\tau_y + \text{c.p.}] . \end{aligned}$$

This separates straightforwardly into an isotropic part

$$\epsilon_u[(\vec{J}\cdot\vec{\tau})^2 - \tfrac{5}{4}] \tag{72}$$

and an anisotropic part

$$-(\epsilon_u - \epsilon_u')[2\{J_x J_y\}\tau_x\tau_y + \text{c.p.}] , \tag{73}$$

where

$$\epsilon_u = \tfrac{2}{3}(s_{11} - s_{12})D_u T, \quad \epsilon_u' = \tfrac{1}{3}s_{44}D_u' T , \tag{74}$$

and s_{11}, s_{12}, and s_{44} are the cubic elastic compliance constants.

We now rearrange both magnetic and strain Hamiltonians, (70)–(73), into axial and nonaxial parts. The Hamiltonians (70) and (72) always have axial symmetry about $\vec{H}$ (and T); whereas (71) and (73) split further into an axial and nonaxial part in a way depending upon the direction of $\vec{H}$ with respect to the crystallographic axes. At this point we introduce the variables (65) and (66) and following the usual practice we denote the transformed spin Hamiltonian by D and the axial and nonaxial parts by D^{a} and D^{na}, respectively, so that

$$D = D^{\text{a}} + D^{\text{na}} . \tag{75}$$

Below we list the explicit forms[35] for D^{a} and D^{na} for $\vec{H}$ and T $(T \parallel \vec{H})$ along each of the principal crystallographic directions [001], [111], and [110]. (All energies are measured in units of $-\hbar eH/mc$.) In each case the Hamiltonian is expressed in coordinates (x_1, x_2, x_3) given in Table III which embody the symmetry of the stressed system (this table also lists for each case the components of the strain tensor $\epsilon_{\mu\nu}$):

$T \parallel \vec{H} \parallel [001]$:

$$\begin{aligned} D^{\text{a}} = {} & \gamma_1 S + \gamma_2 S_0 - 2\gamma_3 S_1 - \tfrac{1}{2}(\gamma_2 + \gamma_3) S_2 \\ & + \kappa J_3 + q J_3^3 - x_u(J_3^2 - \tfrac{5}{4}) , \end{aligned} \tag{76}$$

$$D^{\text{na}} = \tfrac{1}{2}(\gamma_2 - \gamma_3)(J_+^2 a^{\dagger 2} + J_-^2 a^2) ; \tag{77}$$

TABLE III. The strain tensor components $\epsilon_{\mu\nu}$ referred to the cubic axes for a uniaxial stress T oriented along each of the principal crystallographic directions. Also listed for each symmetry are the transformations $(x, y, z) \rightarrow (x_1, x_2, x_3)$ of the cubic axes to the coordinate systems $(x_3 \parallel T)$ employed in the text.

$T \parallel [001]$	$T \parallel [111]$	$T \parallel [110]$
$\epsilon_{xx} = \epsilon_{yy} = s_{12} T$	$\epsilon_{xx} = \epsilon_{yy} = \epsilon_{zz} = \frac{1}{3}(s_{11} + 2s_{12}) T$	$\epsilon_{xx} = \epsilon_{yy} = \frac{1}{2}(s_{11} + s_{12}) T$
$\epsilon_{zz} = s_{11} T$	$\epsilon_{xy} = \epsilon_{yz} = \epsilon_{zx} = \frac{1}{6} s_{44} T$	$\epsilon_{zz} = s_{12} T$
$\epsilon_{xy} = \epsilon_{yz} = \epsilon_{zx} = 0$		$\epsilon_{xy} = \frac{1}{4} s_{44} T$
		$\epsilon_{yz} = \epsilon_{zx} = 0$
$x_1 = x$	$x_1 = (1/\sqrt{6})(x + y - 2z)$	$x_1 = (1/\sqrt{2})(x - y)$
$x_2 = y$	$x_2 = (1/\sqrt{2})(-x + y)$	$x_2 = -z$
$x_3 = z$	$x_3 = (1/\sqrt{3})(x + y + z)$	$x_3 = (1/\sqrt{2})(x + y)$

$T \parallel \vec{\mathrm{H}} \parallel [111]$:

$$D^{\mathrm{a}} = \gamma_1 S + \gamma_3 S_0 - \tfrac{2}{3}(2\gamma_2 + \gamma_3) S_1 - \tfrac{1}{3}(\gamma_2 + 2\gamma_3) S_2 + \kappa J_3 + q\left(\tfrac{41}{12} - \tfrac{2}{3} J_3^2\right) J_3 - x_u'\left(J_3^2 - \tfrac{5}{4}\right) , \tag{78}$$

$$D^{\mathrm{na}} = \tfrac{2}{3}(\gamma_2 - \gamma_3)\left(\{J_+ J_3\} a^{\dagger 2} + \{J_- J_3\} a^2 + J_+^2 a^\dagger \zeta + J_-^2 a \zeta\right) - \tfrac{1}{3} q \left(J_+^3 + J_-^3\right) ; \tag{79}$$

$T \parallel \vec{\mathrm{H}} \parallel [110]$:

$$\begin{aligned} D^{\mathrm{a}} = {} & \gamma_1 S + \tfrac{1}{4}(\gamma_2 + 3\gamma_3) S_0 - (\gamma_2 + \gamma_3) S_1 - \tfrac{1}{8}(3\gamma_2 + 5\gamma_3) S_2 \\ & + \kappa J_3 + q\left(\tfrac{41}{16} - \tfrac{1}{4} J_3^2\right) J_3 - \tfrac{1}{4}(x_u + 3x_u')\left(J_3^2 - \tfrac{5}{4}\right) , \end{aligned} \tag{80}$$

$$\begin{aligned} D^{\mathrm{na}} = {} & (\gamma_2 - \gamma_3)\left[-\tfrac{3}{8}\left(J_+^2 a^{\dagger 2} + J_-^2 a^2\right) + \tfrac{1}{4}\left(J_+^2 + J_-^2\right) \right. \\ & \times \left(a^\dagger a + \tfrac{1}{2} - \zeta^2\right) - \tfrac{3}{8}\left(J_3^2 - \tfrac{5}{4}\right)\left(a^{\dagger 2} + a^2\right) \\ & \left. - \left(\{J_+ J_3\} a^\dagger \zeta + \{J_- J_3\} a \zeta\right) \right] \\ & + \tfrac{3}{4} q \left(J_+ J_3 J_+ + J_- J_3 J_-\right) - \tfrac{1}{4}(x_u - x_u')\left(J_+^2 + J_-^2\right) . \end{aligned} \tag{81}$$

In the above,

$$\begin{aligned} S &= a^\dagger a + \tfrac{1}{2} + \tfrac{1}{2}\zeta^2 , \\ S_0 &= \left(J_3^2 - \tfrac{5}{4}\right)\left(a^\dagger a + \tfrac{1}{2} - \zeta^2\right) , \\ S_1 &= \{J_+ J_3\} \zeta a + \{J_- J_3\} \zeta a^\dagger , \\ S_2 &= J_+^2 a^2 + J_-^2 a^{\dagger 2} . \end{aligned} \tag{82}$$

are all axially symmetric operators and

$$\begin{aligned} x_u &= \epsilon_u / (\hbar e H / mc) , \\ x_u' &= \epsilon_u' / (\hbar e H / mc) \end{aligned} \tag{83}$$

are dimensionless strain-splitting constants.

The Hamiltonians (76)–(81) thus recast are now in a form more appropriate for the analysis of Sec. IV B.

It is clear from Eqs. (71) and (72) that the nonaxial part for any direction is proportional to either $\gamma_2 - \gamma_3$, $x_u - x_u'$, or q. The nonaxial contribution due to $\gamma_2 - \gamma_3$ is often referred to as the "warping" as this term is responsible for the warped or fluted shape of the constant-energy surfaces of the valence bands.

B. Classification of eigenstates

A systematic spectroscopy for cyclotron resonance in complex bands requires a scheme to classify the magnetic eigenstates. This scheme should satisfy the following criteria:

(i) Each eigenstate should be labeled by making maximum use of quantum numbers based on symmetry (and having thus a simple physical interpretation); and the status of each quantum number (whether it be "good" or "bad") should reflect the condition of the corresponding symmetry.

(ii) The selection rules for transitions should be expressible in terms of the quantum numbers, and the violation of selection rules should follow as a natural consequence of the loss of one or more symmetries.

(iii) The scheme should be universal in the sense that it should be applicable for an arbitrary orientation of $\vec{\mathrm{H}}$; and, accordingly, it should be possible to match corresponding eigenstates as $\vec{\mathrm{H}}$ is rotated from one crystal axis to another.

In the past a number of methods for labeling Landau levels have been used all of which fail on one or more of the above counts usually because the symmetries of the problem have not been thoroughly understood nor fully exploited. In this section we outline a new and more satisfactory scheme for spectroscopic notation based on the transformation properties of the Hamiltonians (76)–(81) which we shall employ in succeeding papers to label states and identify quantum transitions.

It is known that the operators (66) with the commutation relation (67) generate a series of harmonic oscillator states which are equally spaced in energy. In a three-dimensional problem each of these levels (Landau levels) is enormously degenerate due to a remaining degree of freedom which does not appear in the Hamiltonian. For the purpose of distinguishing each state, we define another set of canonical variables by

$$\begin{aligned} b^\dagger &= (\hbar c / 2eH)^{1/2}(k_1 - ik_2) + i(eH/2\hbar c)^{1/2}(x_1 - ix_2) , \\ b &= (\hbar c / 2eH)^{1/2}(k_1 + ik_2) - i(eH/2\hbar c)^{1/2}(x_1 + ix_2) , \end{aligned} \tag{84}$$

with the commutation relations

$$\begin{aligned} [b, b^\dagger] &= 1 , \\ [a, b] &= [a^\dagger, b^\dagger] = [a^\dagger, b] = [a, b^\dagger] = 0 , \\ [b, \zeta] &= [b^\dagger, \zeta] = 0 . \end{aligned} \tag{85}$$

The physical significance of the variables $b^\dagger$ and b is fully discussed in Appendix B. By virtue of the commutation relations (67) and (85) we can define the basis oscillator states by the following conditions:

$$\begin{aligned} a^\dagger a \,|n_a, n_b, \zeta\rangle &= n_a \,|n_a, n_b, \zeta\rangle , \\ b^\dagger b \,|n_a, n_b, \zeta\rangle &= n_b \,|n_a, n_b, \zeta\rangle , \end{aligned}$$

$$\begin{aligned}
\frac{1}{i}\frac{\partial}{\partial x_3}|n_a,n_b,\zeta\rangle &= (eH/\hbar c)^{1/2}\zeta\,|n_a,n_b,\zeta\rangle\ ,\\
a^\dagger|n_a,n_b,\zeta\rangle &= (n_a+1)^{1/2}|n_a+1,n_b,\zeta\rangle\ ,\\
a|n_a,n_b,\zeta\rangle &= (n_a)^{1/2}|n_a-1,n_b,\zeta\rangle\ ,\\
b^\dagger|n_a,n_b,\zeta\rangle &= (n_b+1)^{1/2}|n_a,n_b+1,\zeta\rangle\ ,\\
b|n_a,n_b,\zeta\rangle &= (n_b)^{1/2}|n_a,n_b-1,\zeta\rangle\ ,\\
&(n_a,n_b=0,1,2,\ldots)\ .
\end{aligned} \tag{86}$$

The states are mutually orthogonal with respect to n_a, n_b, and ζ and are assumed to be correctly normalized over the crystal volume.

A convenient way of classifying eigenstates is to use the symmetry operations which leave the system invariant. To do this we will need to split the Hamiltonian (75) further into a part D_1 that depends on ζ and a part D_0 that does not:

$$\begin{aligned}
&D=D_0^{\mathrm{a}}+D_1^{\mathrm{a}}+D_0^{\mathrm{na}}+D_1^{\mathrm{na}}\ ,\\
&D_0=D_0^{\mathrm{a}}+D_0^{\mathrm{na}},\quad D_1=D_1^{\mathrm{a}}+D_1^{\mathrm{na}}\ ,\\
&D^{\mathrm{a}}=D_0^{\mathrm{a}}+D_1^{\mathrm{a}},\quad D^{\mathrm{na}}=D_0^{\mathrm{na}}+D_1^{\mathrm{na}}\ .
\end{aligned} \tag{87}$$

The *full* Hamiltonian D possesses the following two kinds of symmetry properties.

(i) From Eqs. (67) and (85),

$$[\zeta, D]=0\ , \tag{88}$$

$$[b^\dagger b, D]=0\ , \tag{89}$$

and hence ζ and $n_b=b^\dagger b$ are always good quantum numbers.

(ii) The nonaxial part D^{na} given by Eqs. (77), (79), and (81) has a fourfold, threefold and twofold rotational symmetry reflecting the crystallographic symmetry of the axes. Group theoretically, the operator C_ν which rotates the entire system through $2\pi/\nu$ about the $\vec{\mathrm{H}}$, T-axis has the properties

$$\begin{aligned}
&C_\nu a^\dagger C_\nu^{-1}=e^{-2\pi i/\nu}a^\dagger\ ,\quad C_\nu a C_\nu^{-1}=e^{2\pi i/\nu}a\ ,\\
&C_\nu J_\pm C_\nu^{-1}=e^{\mp 2\pi i/\nu}J_\pm\ ,\quad C_\nu J_3 C_\nu^{-1}=J_3\ ,
\end{aligned} \tag{90}$$

and, thus, commutes with D,

$$[C_\nu, D]=0 \tag{91}$$

as can be verified directly from the Hamiltonians (76)–(81) with $\nu=4$, 3, and 2 for $T\parallel\vec{\mathrm{H}}\parallel[001]$, [111], and [110], respectively. The operator C_ν generates a cyclic double group of order 2ν, in which $(C_\nu)^\nu$ has the representation -1, and, consequently, the one-dimensional representation of C_ν has to be one of the νth roots of -1, namely, $e^{-(2K-3)\pi i/\nu}$ $(K=0,\ldots,\nu-1)$. The quantum number K, therefore, can be assigned to those states whose total wave function $|K\rangle$ transforms as

$$C_\nu|K\rangle=e^{-(2K-3)\pi i/\nu}|K\rangle\quad(K=0,\ldots,\nu-1)\ . \tag{92}$$

We have additional symmetry properties applicable to portions of the Hamiltonian.

(iii) Axial part, D^{a}: From (67), (69), and (82), we can define an operator

$$N=J_3+a^\dagger a+\tfrac{3}{2} \tag{93}$$

which commutes with the axial part D^{a} of the full Hamiltonian

$$[N, D^{\mathrm{a}}]=0\ . \tag{94}$$

This is simply an expression of the conservation of the $\vec{\mathrm{H}}$ component, $J_3+a^\dagger a-b^\dagger b$, of the total (Bloch state plus oscillator state) angular momentum. [We have dropped $b^\dagger b$ which also commutes with D^{a} (see Sec. IV C), and have added $\frac{3}{2}$ to simplify numbering.] The eigenvalues of the operator N are clearly

$$N=M_J+n_a+\tfrac{3}{2}\ .$$

The quantum number N assumes the values 0, 1, 2, ..., since M_J ranges from $-\frac{3}{2}$ to $+\frac{3}{2}$ and n_a takes on the values 0, 1, 2, ...

(iv) $k_H=0$ part, D_0: At $\zeta=0$, we can utilize the parity operator π. This is a 180° rotation about $\vec{\mathrm{H}}$ in $\vec{\mathrm{k}}$ space, so that

$$\begin{aligned}
&\pi a^\dagger\pi^{-1}=-a^\dagger\ ,\\
&\pi a\pi^{-1}=-a\ ,\\
&\pi\vec{\mathrm{J}}\pi^{-1}=\vec{\mathrm{J}}\ .
\end{aligned} \tag{95}$$

Since the spin Hamiltonian D_0 contains only products of even powers of a and $a^\dagger$, it follows that

$$[\pi, D_0]=0\ . \tag{96}$$

The eigenstates of D_0, therefore, can be classified according to the eigenvalues of π, which are ±1.

Summarizing, from Eqs. (88), (89), (91), (94), and (96) we list following quantum numbers which can be assigned to each "spin" Hamiltonian:

$$\begin{aligned}
D_0^{\mathrm{a}}&:\ \zeta, n_b, K, N, \pi\ ,\\
D^{\mathrm{a}}&:\ \zeta, n_b, K, N\ ,\\
D_0&:\ \zeta, n_b, K, \pi\ ,\\
D&:\ \zeta, n_b, K\ .
\end{aligned} \tag{97}$$

The application of these quantum numbers will be illustrated in the experimental papers (Papers II–IV). Some of the lower-symmetry quantum numbers can become redundant when the system takes on a higher symmetry. In the case of axial symmetry, for example, a state with quantum numbers N, n_b transforms under a rotation through θ about $\vec{\mathrm{H}}$ as

$$\begin{aligned}
C_\theta|N,n_b\rangle&=\exp[-i(J_3+a^\dagger a-b^\dagger b)\theta\,|N,n_b\rangle\\
&=\exp[-i(N-n_b-\tfrac{3}{2})\theta]\,|N,n_b\rangle\ ,
\end{aligned}$$

since the Bloch and oscillator states have the angular momenta J_3 and $a^\dagger a-b^\dagger b$, respectively, satisfying the condition (93). In particular for $\theta = 2\pi/\nu$

$$C_\nu |N, n_b\rangle = \exp\{-[2(N - n_b) - 3]\pi i/\nu\} |N, n_b\rangle ,$$

which, by comparison with (92), leads to

$$N - n_b \equiv K \; (\mathrm{mod}\, \nu) ,$$

or, for $n_b = 0$,

$$N \equiv K \; (\mathrm{mod}\, \nu) .$$

This might give the impression that K is redundant and, hence, unnecessary. However, its role becomes significant as soon as we deviate from axial symmetry, particularly in cases of strong nonaxial mixing, where N can no longer be defined while K can. Furthermore, we have a useful property that energy levels with different K cross while those with same K repel, as they approach one another in a diagram in which the levels are plotted as functions of either ζ or strain magnitude.

The quantum numbers we have given in (97) while fairly complete are not quite sufficient to uniquely label each state. In the extreme case where the nonaxial terms are very large, a simple identification of states becomes impossible since all states of the same K are strongly mixed and, hence, indistinguishable except by a rank ordering according to their energy. However, if the nonaxial terms are weak so that a one-to-one correspondence with the states of the axial Hamiltonian is not lost, then the additional quantum numbers N and π of D_0^a can still be considered "approximate" quantum numbers and used to classify states. Also, in practice the harmonic-oscillator quantum number n_a sometimes serves as an additional label. Its merit lies in the fact that it becomes a good quantum number in the high stress limit (see Sec. V) where the eigenstates are approximated by a single harmonic oscillator. This point is further discussed in Papers II and III.

C. Selection rules

The selection rules[36] for cyclotron-resonance (electric-dipole) transitions between Landau states can be expressed very compactly in terms of the quantum number scheme in (97). The transition probability is calculated from the matrix element in Eq. (51), which can be rewritten as

$$\langle t | \vec{\mathcal{E}} \cdot \vec{\mathrm{v}} | s\rangle = (|\vec{\mathcal{E}}|/m)(eH\hbar/c)^{1/2} \times \langle t | e_+ u_- + e_- u_+ + e_3 u_3 | s\rangle , \tag{98}$$

where

$$u_3 = -\frac{\partial D}{\partial \zeta} ,$$
$$u_+ = \frac{1}{\sqrt{2}}(u_1 + i u_2) = -\frac{\partial D}{\partial a} , \tag{99}$$
$$u_- = \frac{1}{\sqrt{2}}(u_1 - i u_2) = -\frac{\partial D}{\partial a^\dagger}$$

are the dimensionless velocity components and

$$e_3 \text{ and } e_\pm = (e_1 \pm i e_2)/\sqrt{2} \tag{100}$$

are the components of the polarization vector. Here e_+ and e_-, taken individually, would correspond, respectively, to a left-hand and a right-hand circularly polarized electric field.

The existence or nonexistence of the matrix elements (98) imply certain selection rules for electric-dipole transitions, each corresponding to a symmetry property described in Sec. IV B.

(i) From Eqs. (67), (85), and (99), we note that ζ and $b^\dagger b$ commute with $\vec{\mathrm{u}}$,

$$[\zeta, \vec{\mathrm{u}}] = 0 , \tag{101}$$
$$[b^\dagger b, \vec{\mathrm{u}}] = 0 , \tag{102}$$

which leads to the trivial selection rules

$$\Delta\zeta = 0 \quad \text{for all polarizations,} \tag{103}$$
$$\Delta n_b = 0 \quad \text{for all polarizations.} \tag{104}$$

The quantum number n_b associated with $b^\dagger b$ is now seen to be totally superfluous, i.e., a "dummy," because it neither affects the energy nor is changed in any physical transitions. The system with one value of n_b is simply a replica of that with another n_b. In the line-shape formula (59), the summation on the initial state s should include all values of n_b, but the same summations appearing in both the numerator and denominator $[Z(\eta)]$ cancel. We therefore assume throughout that $n_b = b^\dagger b = 0$

(ii) As regards the rotational symmetry about the $\vec{\mathrm{H}}$, T axis, the velocity operators satisfy

$$C_\nu u_3 C_\nu^{-1} = u_3 ,$$
$$C_\nu u_\pm C_\nu^{-1} = e^{\mp 2\pi i/\nu} u_\pm , \tag{105}$$

which can be readily verified from the structure of the Hamiltonians (76)–(81) for $\nu = 4$, 3, 2 corresponding to the three principal crystallographic directions. In other words u_3, u_+, and u_- belong to the one-dimensional representations $D^{(K)}$ of the rotation group about the ν-fold direction where, respectively, $K = 0$ and $+1$ and $\nu - 1$ ($\equiv -1$).

It is worth noting at this point that the relationships (105) can be derived in an alternative and more elegant fashion (and one which affords a convenient way to calculate matrix elements) by expressing the matrix element of $u_\pm$ between eigenstates of D in terms of the creation and annihilation operators, $a^\dagger$, a. From Eqs. (67) and (99) we have

$$[a, D] = [a, a^\dagger] \frac{\partial D}{\partial a^\dagger} = -u_- ;$$

so that by taking the matrix element of u_- between the two eigenstates of D with energies ϵ_s and ϵ_t, we obtain[37]

$$\langle t|a|s\rangle(\epsilon_s-\epsilon_t)=-\langle t|u_-|s\rangle\ ,$$
$$\langle t|u_-|s\rangle=\frac{1}{\eta_{ts}}\langle t|a|s\rangle\ , \tag{106}$$

where η_{ts} is defined by Eq. (62). Similarly, we have

$$\langle t|u_+|s\rangle=-\frac{1}{\eta_{ts}}\langle t|a^\dagger|s\rangle\ . \tag{107}$$

With the aid of (106) and (107), the symmetry properties (105) follow immediately from Eq. (90).

With (98) and (105), the following selection rules are readily established for $\Delta K\equiv K_t-K_s$:

$$\begin{aligned}\Delta K&=0 \quad \text{for polarization } e_3\ ,\\ \Delta K&=1 \quad \text{for polarization } e_-\ ,\\ \Delta K&=-1 \quad \text{for polarization } e_+\ .\end{aligned} \tag{108}$$

It is important to note that implicit in the statement (108) is the understanding that $\Delta K=\pm(\nu-1)$ is equivalent to $\Delta K=\mp1$ owing to the congruence (modulo ν) property of the quantum number K. (Thus, for example, a $K=3\to K=0$ transition for e_- polarization is allowed in fourfold symmetry.)

(iii) and (iv) In general, Eqs. (103), (104), and (108) are the only "universal" selection rules that can be derived rigorously from the symmetry of the system. There are, however, several additional "approximate" selection rules corresponding to each constituent Hamiltonian appearing in (87):

$$D=D_0^{\mathrm{a}}+D_1^{\mathrm{a}}+D_0^{\mathrm{na}}+D_1^{\mathrm{na}}\ .$$

D_0^{a}, which is usually assumed to be the dominant term in the Hamiltonian, has the highest symmetry and, correspondingly, gives rise to the most restrictive selection rules (classified as type M_0) involving the quantum numbers N and π. The selection rules on N and π follow automatically from their definitions in Sec. IV A if we once again note that $u_\pm$ and u_3 are $\Delta N=\pm1$ and 0 operators, respectively [see Eq. (105) *et seq.*] and have negative parity. The addition of each of the symmetry-breaking Hamiltonians, D_1^{a}, D_0^{na}, and D_1^{na}, introduces transitions—which we classify M_1, M_2, and M_3, respectively—with a matrix element proportional to the added Hamiltonian.

The selection rules for circularly polarized $e_\pm$ and longitudinal e_3 electric fields are summarized in Table IV; this classification immediately indicates which transitions are allowed under different conditions and roughly gives their order-of-magnitude intensity. The M_0 transitions are always present (subject to their selection rules) and presumed to be the strongest. The M_1-type transitions are possible only through the longitudinal momentum k_H; hence they are referred to as noncentral or *k_H transitions*. The M_2-type transitions stem from the warping of the band; they are sometimes called *harmonic transitions*. The M_3 transitions, which are *k_H-harmonic transitions*, require the participation of both k_H and warping and are generally the weakest type.

In addition to application of the selection rules in Table IV in a strict sense, one can sometimes further characterize transitions if it is possible to maintain a one-to-one correspondence between the eigenstates of D and those of D_0^{a} such that N and π are, roughly speaking, "good" quantum numbers. If this is true, then the omitted entries in Table IV would read $\Delta N=$ any integer but ∓1 (consistent with the ΔK selection rule) or $\Delta\pi=$ no, specifying the symmetry-broken transitions not allowed by the higher symmetry selection rules of type M_0.

As remarked earlier, it is not always possible to identify states with the quantum numbers of D_0^{a}. It becomes particularly difficult to do so when two interacting levels are close in energy, in which case the only valid selection rules are (108). In many cases, however, the above classification is possible and can be used to considerable advantage.

D. Polarization characteristics

A look at the spectral function (59) shows that the conditions under which a transition $s\to t$ can give rise to an absorption are, first, that the matrix element F_{ts} exist and, second, that $\eta_{ts}=(\epsilon_t$

TABLE IV. Classification of selection rules for quantum resonance transitions in degenerate bands. (These selection rules are in addition to $\Delta\zeta=0$ and $\Delta n_b=0$ which always apply.) Where entries are omitted either N or π is not a "good" quantum number; and, strictly speaking, a selection rule is not defined (see text).

		Selection rules					
			$e_\pm$			e_3	
Type	Relative matrix element	ΔK	ΔN	$\Delta\pi$	ΔK	ΔN	$\Delta\pi$
M_0	$\gamma_1,\ \gamma_2,\ \gamma_3$	∓1	∓1	yes	0	0	yes
M_1	$\gamma_2\zeta,\ \gamma_3\zeta$	∓1	∓1		0	0	
M_2	$\gamma_2-\gamma_3$	∓1		yes	0		yes
M_3	$(\gamma_2-\gamma_3)\zeta$	∓1			0		

$-\epsilon_s)^{-1}$ be positive. (Note again that $|F_{ts}|^2$ is not necessarily equal to $|F_{st}|^2$.) The combination of both conditions results in the well-known polarization rules for cyclotron resonances in simple bands. Let us consider, for example, a hole in a spherical band having an effective mass of $1/\gamma$ ($\gamma > 0$) for which the Hamiltonian, eigenvalues, and transition matrix element are

$$\begin{aligned} D &= \gamma(a^\dagger a + \tfrac{1}{2} + \tfrac{1}{2}\zeta^2) \ , \\ \epsilon_{N,\zeta} &= \gamma(N + \tfrac{1}{2} + \tfrac{1}{2}\zeta^2) \ , \\ F_{N_s,N_t} &= -\gamma[e_+(N_s)^{1/2}\delta_{N_t,N_s-1} \\ &\quad + e_-(N_s+1)^{1/2}\delta_{N_t,N_s+1} + e_3\delta_{N_t,N_s}] \ , \\ \eta_{N_t,N_s} &= \frac{1}{\gamma(N_t - N_s)} \ . \end{aligned} \tag{109}$$

We see that resonance absorption can occur only for the transition $N \rightarrow N+1$ in the e_- polarization. (Resonance occurs at $\eta = 1/\gamma$.) For electrons ($\gamma < 0$) absorption occurs only for the opposite sense of polarization e_+. Absorption either for holes or electrons is forbidden for longitudinal polarization e_3.

These simple polarization rules must be modified when we consider quantum transitions in complex bands. The energy criterion $\epsilon_t - \epsilon_s > 0$ is again a necessary condition for absorption. However, the kinds of transitions which can take place is only restricted, in general, by the selection rules (108). Thus, there can exist transitions of both types $\Delta K = +1$ and -1—active in opposite senses of polarization e_- and e_+, respectively—which satisfy the energy criterion. While spectra taken with either sense of polarization will contain resonance lines, their appearance may be quite different. In fact, for $\vec{H} \parallel [001]$ and $\vec{H} \parallel [111]$ one set of allowed transitions ($\Delta K = -1$) will be active only for e_+ whereas the other set ($\Delta K = +1$) will be active for e_-. The two spectra will be mutually exclusive; there will be no lines common to both. However, for $\vec{H} \parallel [110]$ the selection rules for e_+ and e_- are identical (recall that for $\nu = 2$, $\Delta K = +1$ and -1 are equivalent) so allowed transitions will be active for both polarizations e_+ and e_-, although their intensities will not necessarily be the same.

In contrast to the case for simple bands, it is possible for absorption resonances to appear in the longitudinal polarization $\vec{\mathcal{E}} \parallel \vec{H}$ owing to allowed transitions obeying the selection rule $\Delta K = 0$.

The selection rules in Table IV become somewhat less restrictive when the electric fields are linearly polarized (the more common experimental situation). A linearly polarized electric field in the x_1x_2 plane (perpendicular to $\vec{H}$) and directed at an angle δ from the x_1 axis can be represented by two counter-rotating circular-polarization components

$$e_+ = 2^{-1/2}e^{i\delta}, \quad e_- = 2^{-1/2}e^{-i\delta}, \quad e_3 = 0 \ .$$

Since both circular components are present in equal intensity we cannot distinguish between + and − in the selection rules in Table IV. Both kinds of transition will be excited by a linearly polarized field.

An anisotropy in the transition intensity can exist for linearly polarized fields when $\vec{H}$ lies along an axis of low symmetry, i.e., $\vec{H} \parallel [110]$ ($\nu = 2$). To see this we write the matrix element squared as

$$2|F_{ts}|^2 = (u_+)^2_{ts} + (u_-)^2_{ts} + 2(u_+)_{ts}(u_-)_{ts}\cos 2\delta \ . \tag{110}$$

(We take the matrix elements of $u_\pm$ to be real.) For $\vec{H} \parallel [001]$ and $\vec{H} \parallel [111]$ ($\nu = 4$ and 3, respectively) the selection rules (108) do not permit $(u_+)_{ts}$ and $(u_-)_{ts}$ to exist simultaneously. Therefore, the last term in Eq. (110) must vanish and the intensity is independent of the angle δ. However, when $\vec{H} \parallel [110]$ ($\nu = 2$) every allowed transition is active in both polarizations e_+ and e_-; so the last term in Eq. (110) is, in general, nonvanishing causing an anisotropy when the electric field is rotated in the (110) plane. {A marked difference is observed in the relative intensity of absorption peaks between spectra obtained ($\vec{H} \parallel [110]$) with $\vec{\mathcal{E}} \parallel [1\bar{1}0]$ ($\delta = 0$) and $\vec{\mathcal{E}} \parallel [00\bar{1}]$ ($\delta = \frac{1}{2}\pi$) although the peak positions remain the same. See Paper IV.}

E. Solution of the effective-mass equation

Since there are at most only four independent wave functions corresponding to each value of N, the axial Hamiltonian can be solved exactly by diagonalizing it within this four-dimensional space. The nonaxial part, on the other hand, breaks the N selection rule and introduces a coupling which extends into a space of infinite dimensions. The general way of tackling this problem is to expand the wave function in harmonic oscillators

$$\psi_{n_b,\zeta} = \sum_{n_a=0}^{\infty} \sum_{M_J=-3/2}^{3/2} a_{n_a}(M_J) u_{n_a,n_b,\zeta} |M_J\rangle \tag{111}$$

and solve the secular equation in $a_{n_a}(M_J)$ generated by the effective-mass equation, $\mathcal{H}\psi_{n_b,\zeta} = E\psi_{n_b,\zeta}$.[38] The secular matrix splits into ν submatrices, each submatrix corresponding to a definite value of the quantum number K. At $\zeta = 0$, each submatrix further splits into two according to $\pi = \pm 1$. In general no further decoupling occurs, and we still have to diagonalize an infinite matrix. In a numerical calculation, the matrix is truncated at a size which can be handled from a practical standpoint and yet is large enough to give the desired states accurately. More details of actual calculations will be given in the experimental papers (Papers II–IV).

Luttinger discovered two analytically soluble cases, the "spherical" case ($\gamma_3 = \gamma_2$, $q = 0$) and the trigonal case, $\vec{H}\parallel[111]$ ($k_H=0$), for which the infinite secular matrix breaks up into finite tractable blocks. For the latter case the reasons underlying the decoupling have heretofore been quite obscure. A discussion in Appendix A explores the symmetries of these cases and sheds considerable light on the origins of the decoupling phenomena.

F. Axes of lower symmetry

Directions of $\vec{H}\parallel T$ other than [001], [111], and [110] (and their equivalents) correspond to $\nu=1$ in the scheme discussed in this section. Among the quantum numbers listed in Eq. (97), K is always zero and the corresponding K selection rules (108) become completely nonrestrictive and trivial. We then only have the rigorous selection rules (103) and (104), and approximate selection rules derived from D_0^{a}, D_1^{a}, and D_0^{na}. The secular equation for the Landau eigenstates enjoys generally no splitting, except the one for $k_H=0$.

V. HIGH-STRESS LIMIT

When the external stress is so large that the strain energy greatly exceeds the magnetic energy, it is more heuristic to diagonalize the strain and magnetic energies stepwise rather than to directly diagonalize their combination. A uniaxial stress splits the fourfold Bloch states with $J=\frac{3}{2}$ (Γ_8) into a pair of doublets, a twofold degeneracy still remaining due to Kramers' theorem. If this splitting were infinite, magnetic levels would be formed within each pair of the strain-split Bloch bands. The Landau level structure within such a doublet is much simpler than that in the original quartet and enables us to understand the resonance spectrum at high stresses. We discuss in this section the behavior of the spectra in the high-stress regime, starting from the limit mentioned above. Mathematically the procedure consists in expanding the Hamiltonian in the inverse powers of strain splitting and projecting it onto one of the strain-split subspaces.

Let us start with the strain Hamiltonian (30) (omitting the dilatational part), which for a uniaxial stress in the direction (τ_x, τ_y, τ_z) can be written as the sum of (72) and (73). This can be easily diagonalized to give the strain energies $\pm\epsilon$, where

$$\epsilon=\epsilon_u[1+3(\beta^2-1)(\tau_x^2\tau_y^2+\tau_y^2\tau_z^2+\tau_z^2\tau_x^2)]^{1/2} \tag{112}$$

expressed in terms of β, the splitting anisotropy parameter defined by

$$\beta=\frac{\epsilon_u'}{\epsilon_u}=\frac{D_u' s_{44}/2}{D_u(s_{11}-s_{12})}\ . \tag{113}$$

To see the nature of the strain splitting, we calculate the commutator between the strain Hamiltonian and the component of the angular momentum along the stress $\vec{J}\cdot\vec{\tau}=\tau_x J_x+\tau_y J_y+\tau_z J_z$ and obtain from Eqs. (73) and (113),

$$[\mathcal{H}_e, \vec{J}\cdot\vec{\tau}]=2i\epsilon_u(\beta-1)[(\tau_x^2-\tau_y^2)\tau_z\{J_xJ_y\}+\text{c.p.}]\ . \tag{114}$$

From this we see that for $\beta\neq 1$ the commutator vanishes only when T lies along two special directions: (i) $T\parallel[111]$ (or its equivalents), i.e. $\tau_x^2=\tau_y^2=\tau_z^2$; and (ii) $T\parallel[001]$ (or its equivalents), i.e., $\tau_x=\tau_y=0$. For these cases we say that the strain splitting is "uniaxial," i.e., the strain-split states can be chosen to have a definite eigenvalue M_J of the projected angular momentum $\vec{J}\cdot\vec{\tau}$. We thus can write (assuming $\beta>0$)

$$\begin{aligned} P\mathcal{H}_eP&=-\epsilon\quad M_J=\pm\tfrac{1}{2}\ ,\\ &=+\epsilon,\quad M_J=\pm\tfrac{3}{2} \end{aligned} \tag{115}$$

for $T\parallel[001]$ and $T\parallel[111]$, where ϵ generically denotes ϵ_u and ϵ_u', respectively. For $\beta=1$, $\mathcal{H}_e$ commutes with $\vec{J}\cdot\vec{\tau}$ in any direction, and the splitting given by Eq. (112) does not depend on the direction in which stress is applied. This remarkable case is referred to as "isotropic quantization."[39] With $\beta\neq 1$ it is not generally possible to specify strain-split states by the quantum number M_J. But, if the strain anisotropy is small, i.e., β is close to unity, then for any direction of T the fourfold band edge splits into two Kramers doublets whose wave functions are predominantly composed of pure states, either $\pm\frac{3}{2}$ or $\pm\frac{1}{2}$, of $\vec{J}\cdot\vec{\tau}$. (In Ge β has been determined[40] to be $\beta\approx+0.7$ or not too far from unity.) It is therefore reasonable that we continue to label the strain-split states according to M_J and consider Eq. (115) to hold for an arbitrary direction of uniaxial stress.

We now project the Hamiltonian (27) further onto each of the subspaces, $M_J=\pm\frac{3}{2}$ and $M_J=\pm\frac{1}{2}$, using the projection operators P_1 and Q_1. The leading terms in the projections are

$$\begin{aligned} \mathcal{H}_{\pm 3/2}&=\tfrac{1}{3}\Lambda+\epsilon+P_1P\mathcal{H}_kPP_1+P_1P\mathcal{H}_kPQ_1(1/2\epsilon)Q_1P\mathcal{H}_kPP_1\\ &\quad+P_1P(\mathcal{H}_k+\mathcal{H}_e)Q(1/\Lambda)Q(\mathcal{H}_k+\mathcal{H}_e)PP_1+\cdots\ , \end{aligned} \tag{116}$$

$$\begin{aligned} \mathcal{H}_{\pm 1/2}&=\tfrac{1}{3}\Lambda-\epsilon+Q_1P\mathcal{H}_kPQ_1-Q_1P\mathcal{H}_kPP_1(1/2\epsilon)P_1P\mathcal{H}_kPQ_1\\ &\quad+Q_1P(\mathcal{H}_k+\mathcal{H}_e)Q(1/\Lambda)Q(\mathcal{H}_k+\mathcal{H}_e)PQ_1+\cdots\ . \end{aligned} \tag{117}$$

The projected Hamiltonians (116) and (117) are no longer invariant under the cubic group O_h; instead they are invariant under an appropriate subgroup of O_h representing the symmetry of the stressed system, which is D_{4h}, D_{3d}, or D_{2h} corresponding, respectively, to $T\parallel[001]$, [111], or [110].

The projected Hamiltonian (117) is next evaluated for each of these three principal cases. We restrict our attention to the $M_J=\pm\frac{1}{2}$ bands as only these bands in Ge are thermally populated ($\epsilon<0$) and amenable to resonance studies at liquid-He temperatures with large, *compressional* ($T<0$) stresses[41] (the most typical experimental situation). The development for the $M_J=\pm\frac{3}{2}$ case, in principle, would proceed along identical lines. Our coordinate system ($x_1x_2x_3$) with x_3 along T is the same one used in Sec. IV. We first dispatch several preliminary details.

The projection process is simplified if we choose the phase of the wave functions judiciously so that for $T\parallel[001]$ the projection of $\vec{J}$ is

$$\begin{aligned} Q_1J_3Q_1&=\begin{pmatrix}\frac{1}{2}&0\\0&-\frac{1}{2}\end{pmatrix}\equiv\tfrac{1}{2}\sigma_3\ ,\\ Q_1J_1Q_1&=\begin{pmatrix}0&1\\1&0\end{pmatrix}\equiv\sigma_1\ ,\\ Q_1J_2Q_1&=\begin{pmatrix}0&-i\\i&0\end{pmatrix}\equiv\sigma_2\ . \end{aligned}\tag{118}$$

The matrices σ_1, σ_2, σ_3 (the Pauli matrices), and the 2×2 unit matrix are linearly independent and serve as a basis on which to express any 2×2 matrix. In D_{4h}, J_1 and J_2 belong to Γ_5 as do σ_1 and σ_2. J_3 and σ_3 belong to Γ_2, and 1 belongs to Γ_1. By using the compatibility relation, we can establish the correspondence of all the independent J matrices to σ matrices. This is given in the final column of Table I. The projection of the fourth term on the right-hand side of Eq. (117) is readily obtained through the algebraic relation

$$(Q_1\mathcal{H}P_1)(P_1\mathcal{H}Q_1)=Q_1\mathcal{H}^2Q_1-(Q_1\mathcal{H}Q_1)^2\ ,\tag{119}$$

where $\mathcal{H}$ is any J matrix. Consideration of the fifth term requires a full 6×6 matrix and will be discussed in Sec. VI. The projection for $T\parallel[111]$ is obtained in a similar way. The case with $T\parallel[110]$ is somewhat more complicated because it involves the unitary transformation that diagonalized the strain Hamiltonian. In this case $\vec{J}$ is projected as

$$\begin{aligned} Q_1J_3Q_1&=\tfrac{1}{2}(-1+\eta_1+3\eta_2)\sigma_3\ ,\\ Q_1J_1Q_1&=\tfrac{1}{4}(2+\eta_1+3\eta_2)\sigma_1\ ,\\ Q_1J_2Q_1&=\tfrac{1}{4}(2+\eta_1+3\eta_2)\sigma_2\ , \end{aligned}\tag{120}$$

where[42]

$$\begin{aligned} \eta_1&=(1+3\beta^2)^{-1/2}\equiv\cos\eta\ ,\\ \eta_2&=\beta(1+3\beta^2)^{-1/2}\equiv(1/\sqrt{3})\sin\eta\ . \end{aligned}\tag{121}$$

Summarizing the results, for each of the three principal directions of stress, we can write the first order projection on the $M_J=\pm\frac{1}{2}$ subspace [the third term in Eq. (117)] in the form

$$\begin{aligned} &-\frac{\hbar^2}{2}\left(\frac{k_1^2}{m_1}+\frac{k_2^2}{m_2}+\frac{k_3^2}{m_3}\right)\\ &-\frac{e\hbar}{4mc}\,(g_1H_1\sigma_1+g_2H_2\sigma_2+g_3H_3\sigma_3)\ . \end{aligned}\tag{122}$$

This clearly describes an ellipsoidal energy surface with an anisotropic g tensor. The effective masses m_1, m_2, m_3 and the g factors g_1, g_2, g_3, depend on the direction of stress and are given in Table V.

The second-order projections on $M_J=\pm\frac{1}{2}$ [the fourth term in Eq. (117)] are

TABLE V. Strain splitting energies, effective masses, and g factors of the (J, M_J) = ($\frac{3}{2}$, $\pm\frac{1}{2}$) band for the three principal directions of stress. For $T\parallel[110]$, the axes 1 and 2 are chosen along $[1\bar{1}0]$ and $[00\bar{1}]$, respectively. The anisotropy parameters β, η_1, and η_2 are defined by Eqs. (113) and (121) in the text.

T	[001]	[111]	[110]
ϵ	ϵ_u	$\epsilon_u'=\beta\epsilon_u$	$\frac{1}{2}\epsilon_u(1+3\beta^2)^{1/2}$
m/m_1	$\gamma_1-\gamma_2$	$\gamma_1-\gamma_3$	$\gamma_1+\eta_1\gamma_2-3\eta_2\gamma_3$
m/m_2	$\gamma_1-\gamma_2$	$\gamma_1-\gamma_3$	$\gamma_1-2\eta_1\gamma_2$
m/m_3	$\gamma_1+2\gamma_2$	$\gamma_1+2\gamma_3$	$\gamma_1+\eta_1\gamma_2+3\eta_2\gamma_3$
g_1	$4\kappa+10q$	$4\kappa+7q$	$(2+\eta_1+3\eta_2)\kappa+\frac{1}{2}(7+17\eta_1-9\eta_2)q$
g_2	$4\kappa+10q$	$4\kappa+7q$	$(2+\eta_1+3\eta_2)\kappa+\frac{1}{2}(13+14\eta_1)q$
g_3	$2\kappa+\frac{1}{2}q$	$2\kappa+\frac{13}{2}q$	$(-2+2\eta_1+6\eta_2)\kappa+\frac{1}{2}(-7+13\eta_1+21\eta_2)q$

$T\parallel[001]$:

$$\begin{aligned} -\frac{1}{2\epsilon_u}\frac{3\hbar^4}{m^2}\Big\{&\tfrac{1}{4}\gamma_2^2(k_1^2-k_2^2)^2+\gamma_3^2(\{k_1k_2\}^2+\{k_2k_3\}^2+\{k_3k_1\}^2)+\left(\frac{e}{\hbar c}\right)\Big[\gamma_3^2(k_1^2H_1\sigma_1+k_2^2H_2\sigma_2-k_3^2H_3\sigma_3)\\ &+\gamma_2\gamma_3(k_2^2H_1\sigma_1+k_1^2H_2\sigma_2)+(\gamma_2-\gamma_3-\kappa)\gamma_3(H_2\sigma_1+H_1\sigma_2)\{k_1k_2\}-(\gamma_2+\gamma_3)\gamma_3(\{k_1k_3\}\sigma_1+\{k_2k_3\}\sigma_2)H_3\\ &+\gamma_2\gamma_3(k_1^2+k_2^2)H_3\sigma_3+(\gamma_3-\kappa)\gamma_3(\{k_1k_3\}H_1+\{k_2k_3\}H_2)\sigma_3-\tfrac{1}{2}\kappa\gamma_2(k_1^2-k_2^2)(H_1\sigma_1-H_2\sigma_2)\Big]+\left(\frac{e}{\hbar c}\right)^2\frac{\kappa^2}{4}(H_1^2+H_2^2)\Big\}\ . \end{aligned}\tag{123}$$

$T\parallel[111]$:

$$\begin{aligned} -\frac{1}{2\epsilon_u'}\frac{\hbar^4}{m^2}\Big\{&(\gamma_2^2+2\gamma_3^2)\{k_+^2,k_-^2\}+2(2\gamma_2^2+\gamma_3^2)\{\{k_3k_+\}\{k_3k_-\}\}-2(\gamma_2^2-\gamma_3^2)[\{k_+^2,\{k_+k_3\}\}+\{k_-^2,\{k_-k_3\}\}]\\ &+\left(\frac{e}{\hbar c}\right)\Big[(2\gamma_2^2+\gamma_3^2)\{(k_+H_-+k_-H_+-k_3H_3)k_3\}\sigma_3+2(\gamma_2^2+2\gamma_3^2)\{k_+k_-\}H_3\sigma_3+2(\gamma_2^2-\gamma_3^2)(k_+^2H_++k_-^2H_-)\sigma_3 \end{aligned}$$

$$-6\gamma_2\gamma_3[\{(k_-\sigma_+ + k_+\sigma_-)k_3\}H_3 - \{k_-k_+\}(H_-\sigma_+ + H_+\sigma_-)] - \kappa(2\gamma_2+\gamma_3)\{(H_+k_- + H_-k_+)k_3\}\sigma_3 - \kappa(\gamma_2+2\gamma_3)(k_-^2H_+\sigma_+ + k_+^2H_-\sigma_-)$$
$$+\kappa(\gamma_2-\gamma_3)(k_+^2H_+ + k_-^2H_-)\sigma_3 + 2\kappa(\gamma_2-\gamma_3)\{(k_+H_+\sigma_+ + k_-H_-\sigma_-)k_3\}\Big] + \left(\frac{e}{\hbar c}\right)^2\frac{3}{4}\kappa^2 2H_+H_-\Big\}\ , \qquad (124)$$

where the ± components of a vector $\vec{A}$ are everywhere defined by $A_\pm = 2^{-1/2}(A_1 \pm iA_2)$. For $T \parallel [110]$ the expression for the second-order projection is rather lengthy and is not included here. In the above forms (123) and (124), the contributions from the q term in the magnetic Hamiltonian (29) have been neglected. We note that the second-order projections are of order k^4/ϵ, thus representing the lowest-order energy *corrections* to the strain-independent levels of the $(T=\infty)$ Hamiltonian (122) which appear as we depart from the limit $T\to\infty$.

If an external magnetic field is now applied having direction cosines $(\beta_1, \beta_2, \beta_3)$ with respect to the principal axes of the ellipsoid, we can diagonalize the first-order projection (122) by using appropriate creation and annihilation operators, $a^\dagger$ and a, similar to those defined in Eq. (66) and satisfying the commutation relation (67). (We now have to quantize along $\vec{H}$ which in general lies in a different direction from "3", the stress axis.) The longitudinal momentum k_H is again a constant of motion and represented by its dimensionless form (54). The energy corrections—proportional to H^2 (corresponding to k^4) and inversely proportional to the strain splitting—which come from the second-order projection, are evaluated by taking the expectation value of the latter with respect to the first-order eigenstates of (122). It is usually convenient first to rewrite the second-order projection in terms of $a^\dagger$, a, and ζ. When expressed in this way, contributions to the expectation value can arise only from the diagonal terms like $a^{\dagger 2}a^2 + a^2a^{\dagger 2}$ and $(a^\dagger a + aa^\dagger)\zeta^2$. Thus the total energy up to second order and measured in units of $-\hbar eH/mc$ is given in the form[43]

$$\epsilon(n,\pm,\zeta) = x + \left(\frac{m}{m_0^*}\right)(n+\tfrac{1}{2}) + \tfrac{1}{2}\left(\frac{m}{m_H}\right)\zeta^2 \pm \tfrac{1}{4}g$$
$$+\frac{1}{2x}\{A(n^2+n) + B(2n+1)\zeta^2$$
$$+C \pm [D(2n+1) + E\zeta^2]\}\ , \qquad (125)$$

where $x = \epsilon/(\hbar eH/mc)$, and

$$\frac{1}{m_0^*} = \left(\frac{\beta_1^2}{m_2m_3} + \frac{\beta_2^2}{m_3m_1} + \frac{\beta_3^2}{m_1m_2}\right)^{1/2}\ ,$$
$$\frac{1}{m_H} = \frac{\beta_1^2}{m_1} + \frac{\beta_2^2}{m_2} + \frac{\beta_3^2}{m_3}\ , \qquad (126)$$
$$g = (g_1^2\beta_1^2 + g_2^2\beta_2^2 + g_3^2\beta_3^2)^{1/2}\ .$$

The meaning of the pair of high-stress quantum numbers $(n,\pm)$ will become apparent in the suceeding discussion. The coefficients A, B, etc., in Eq. (125) are complicated functions of the band parameters γ_1, γ_2, γ_3, and κ whose form generally depends strongly on the direction of $\vec{H}$ with respect to T. We discuss below the two cases of greatest experimental interest, namely, those for which the magnetic field lies either parallel or perpendicular to the stress. In the high-stress case, the dependence on the longitudinal momentum k_H does not play as important a role as it does in the absence of stress, since the k_H dependence under high stress is determined mainly by the ellipsoidal projection. It is usually possible, therefore, to assume that $k_H = 0$.

A. $\vec{H} \parallel T$

In the geometry $\vec{H} \parallel T$ the transitions induced by microwave fields in the strain-split valence bands may be classified into four major categories. In the first are the "conventional" cyclotron resonances analogous to those found in simple bands, while the remaining three categories represent additional kinds of resonances originating from various terms in the second-order projection. Each category is distinguished by characteristic selection rules which operate for the Landau and Bloch quantum numbers $(n, M_J = \pm\frac{1}{2})$, respectively. (For the case $T \parallel [110]$ and $\beta \neq 1$, $M_J = \pm\frac{1}{2}$ is to be understood in the sense mentioned earlier.)

Expressions for the coefficients A, B, C, D, and E appearing in Eq. (125) are given in Table VI for the geometry $\vec{H} \parallel T$.

1. *Cyclotron resonance:* $\Delta n = \pm 1$, $\Delta M_J = 0$

At very large stresses ordinary cyclotron resonances obeying the selection rule $\Delta n = 1$ occur at fields corresponding to the classical "tube" mass of the energy ellipsoid (122). For $T \parallel [001]$ and $T \parallel [111]$ the first-order projection (122) has axial symmetry about $T(m_1 = m_2,\ g_1 = g_2)$ and the only allowed transitions are in the hole-sense polarization (e_- and $\Delta n = +1$). For $T \parallel [110]$ the lack of axial symmetry allows the $\Delta n = +1$ transitions to appear weakly in the electron sense of polarization as well (i.e., e_+ and $\Delta n = +1$). The second-order energy contributions to the Landau levels, the last four terms of Eq. (125), represent quantum shifts which depend on n and $M_J = \pm\frac{1}{2}$. These energy shifts can be large enough at intermediate stresses to split the classical resonance line into (n, M_J) components. As $T\to\infty$ these second-order effects $(\propto 1/\epsilon)$ become vanishingly small and the fine

TABLE VI. Second-order correction coefficients in the $\epsilon(n,\pm,\zeta)$ [Eq. (125)] at the high-stress limit for the $\vec{H} \parallel T$ configuration. For $T \parallel [001]$ and [111] the coefficients are exact to second order. For $T \parallel [110]$ the exact coefficients are rather clumsy in form; for simplicity we quote here only their "first-order expansions" based on the assumptions: $(\gamma_3-\gamma_2)/\gamma_2$, q, $\beta-1 \ll 1$. It should be noted that in the spherical case, $\gamma_3=\gamma_2$, one obtains $A=B=C=D=-E=3\gamma_2^2$ for every direction.

T	[001]	[111]	[110]
A	$\frac{3}{2}(\gamma_2^2+\gamma_3^2)$	$\gamma_2^2+2\gamma_3^2$	$\frac{3}{4}\gamma_2(5\gamma_3-\gamma_2)$
B	$3\gamma_3^2$	$2\gamma_2^2+\gamma_3^2$	$3\gamma_2\gamma_3$
C	$\frac{3}{2}(\gamma_2^2+\gamma_3^2)$	$\gamma_2^2+2\gamma_3^2$	$\frac{3}{4}\gamma_2(5\gamma_3-\gamma_2)$
D	$3\gamma_2\gamma_3$	$\gamma_2^2+2\gamma_3^2$	$\frac{3}{4}\gamma_2(5\gamma_3-\gamma_2)$
E	$-3\gamma_3^2$	$-(2\gamma_2^2+\gamma_3^2)$	$-3\gamma_2\gamma_3$

structure collapses into an inhomogeneously broadened "classical" resonance.

2. *Harmonic resonances:* $\Delta n > 1$, $\Delta M_J = 0$

Matrix elements of the second-order projections [e.g., (123)] connect states not connected by the first-order projection (122) giving rise in the spectrum to a series of "harmonic" transitions $\Delta n > 1$ ($\Delta M_J = 0$) in addition to the ordinary cyclotron resonances. The exact nature of the Δn selection rule depends upon the degree of rotational symmetry (ν) about the $\vec{H}$, T axis. Since the existence of the harmonic transitions requires an admixture from the strain-split partner $M_J = \pm\frac{3}{2}$ (in addition to "warping") the intensity of the harmonic resonances vanishes at large stress as $1/\epsilon^2$.

3. *Spin resonance:* $\Delta n = 0$, $\Delta M_J = \pm 1$

Also connected by matrix elements of the second-order projection are different Bloch states having the same Landau quantum number. This transition represents an electric-dipole-induced spin resonance excited in the polarization $\vec{\mathcal{E}} \perp \vec{H}$. The fact that the effective inverse "spin" mass for this transition, $\frac{1}{2}g_3/m$, is a simple combination of κ and q suggests doing spin resonance experiments to determine these constants directly. Unfortunately, it would be difficult to resolve the spin transitions from the much stronger cyclotron quantum resonances which also appear in this same geometry, $\vec{\mathcal{E}} \perp \vec{H}$. A further drawback is the fact that the spin transition requires k_H participation, i.e., it vanishes at $k_H = 0$.

4. *Combined resonance:* $\Delta n = \pm 1$, $\Delta M_J = \mp 1$

The final possibility is a simultaneous change of both Bloch and Landau quantum numbers, that is, a cyclotron resonance with a spin flip. This resonance is termed a "combined" resonance. Since

TABLE VII. Classification of transitions within the $M_J = \pm\frac{1}{2}$ bands at the high-stress limit for the configuration $\vec{H} \parallel T$. The symmetry index $\nu = 2, 3, 4$ for $T \parallel [110]$, [111], and [001], respectively. The components m_1, m_2, m_3 and g_1, g_2, and g_3 are given in Table V. The coefficients A and D are listed in Table VI.

Type of resonance transition	Polarization	Initial and final states	Inverse effective mass	Second-order corrections to inverse effective masses	Lowest order dimensionless matrix element F_{ts}	
					$T \parallel [001]$	$T \parallel [111]$
Cyclotron	e_-	$(n,\ \pm) \rightarrow (n+1,\ \pm)$	$(m_1m_2)^{-1/2}$	$\frac{1}{mx}[A(n+1) \pm D]$	$(\gamma_1-\gamma_2)(n+1)^{1/2}$	$(\gamma_1-\gamma_3)(n+1)^{1/2}$
Harmonic	e_+	$(n,\ \pm) \rightarrow (n+\nu-1,\ \pm)$	$(\nu-1)(m_1m_2)^{-1/2}$	$\frac{\nu-1}{2mx}[A(2n+\nu) \pm 2D]$	$\frac{1}{2x}3(\gamma_2^2-\gamma_3^2)[(n+1)(n+2)(n+3)]^{1/2}$	$-\frac{1}{2x'}6(\gamma_2^2-\gamma_3^2)\zeta[(n+1)(n+2)]^{1/2}$
Spin	e_-	$(n,\ -) \rightarrow (n,\ +)$	$\frac{1}{2}g_3/m$	$\frac{1}{mx}D(2n+1)$	$-\frac{1}{2x}3\sqrt{2}\ (\gamma_2+\gamma_3)\gamma_3\zeta$	$-\frac{1}{2x'}6\sqrt{2}\ \gamma_2\gamma_3\zeta$
Combined	e_3	$(n,\ +) \rightarrow (n+1,\ -)$	$(m_1m_2)^{-1/2}-\frac{1}{2}g_3/m$	$\frac{1}{mx}(A-2D)(n+1)$	$-\frac{1}{2x}3\sqrt{2}\ (\gamma_2+\gamma_3)\gamma_3(n+1)^{1/2}$	$-\frac{1}{2x'}6\sqrt{2}\ \gamma_2\gamma_3(n+1)^{1/2}$

the combined resonance, unlike the spin resonance, is active in the longitudinal polarization $\vec{\mathcal{E}} \parallel \vec{H}$, it should enable us to make a direct determination of the g factor (g_3) and, in turn, the parameters κ and q, which can only be measured with great difficulty otherwise.

Table VII summarizes the types of transitions which occur for $\vec{H} \parallel T$ and lists expressions for their effective masses. The transition matrix elements are also included for the cases $T \parallel [001]$ and $T \parallel [111]$.

B. $\vec{H} \perp T$

In the configuration $\vec{H} \perp T$, as for the prior case, the first-order projection (122) only gives rise to cyclotron resonances, $\Delta n = \pm 1$, of the ordinary kind. However, the second-order projection introduces additional types of resonances (even more numerous than before because of the lower symmetry of the geometry $\vec{H} \perp T$) of a rather complicated nature. Most are of little interest to us, and we shall not consider them further. One second-order effect of importance is the shift of the ordinary cyclotron-resonance transitions from their stress-independent ($T \to \infty$ limit) positions given by the first-order projection (122). The energy levels (including second-order corrections) are again described by Eq. (125) [the label $\pm$ of the Bloch states now has a slightly different meaning from before (see Paper II)], so that the effective mass for a cyclotron transition $(n, \pm) \to (n+1, \pm)$ is given by

$$\frac{m}{m^*} = \frac{m}{m_0^*} + \frac{1}{2x}\left[2A(n+1) \pm 2D\right] \qquad (127)$$

at $\zeta = 0$. The constants A and D are given in Table VIII for important cases.

VI. INTERACTION WITH SPLIT-OFF BAND

In Sec. II we constructed "spin" Hamiltonians for the full sixfold degenerate band edge Γ_{25}^+ which in turn we projected onto either of the spin-orbit-split subspaces Γ_8^+ ($J = \frac{3}{2}$) and Γ_7^+ ($J = \frac{1}{2}$). Thus far we have not taken into account the higher-order "couplings" which exist between these projected spaces nor higher-order interactions with bands external to both. Such effects (neglected in the usual effective-mass approximation) can produce marked line shifts for quantum resonances. Because the spin-orbit splitting is often considerably smaller than other energy gaps we here shall assume the dominant higher-order contributions to come exclusively from the interaction between spin-orbit partners and ignore the other bands altogether. We consider, then, in this section the perturbation of the Landau levels of Γ_8^+, derived in Secs. IV and V, by the spin-orbit–split-off band Γ_7^+.

The lowest-order perturbations from Γ_7^+ are given by the third term in the projection (27), which contains three types of products $\mathcal{H}_e^2$, $\{\mathcal{H}_k \mathcal{H}_e\}$, and $\mathcal{H}_k^2$. The explicit forms for these products can be obtained straightforwardly by multiplying the two off-diagonal rectangular matrices connecting the subspaces $J = \frac{3}{2}$ and $J = \frac{1}{2}$ (consult column 6 of Table I). An alternative and more general derivation which follows the spirit of Sec. II A, is to construct higher-order cubic invariants from k_μ, $\epsilon_{\mu\nu}$, and J_μ ($J = \frac{3}{2}$) and determine the coefficient of individual terms by comparing their matrix elements with corresponding ones obtained by direct multiplication of the rectangular matrices. The resulting three Hamiltonians $\mathcal{H}_{ee}$, $\mathcal{H}_{ke}$, and $\mathcal{H}_{kk}$ representing, respectively, the three types of products above, are thus expressed like the first-order projections in Sec. II as invariant linear combinations of the 16 independent J matrices listed in column 4 of Table I. From the product $\{\mathcal{H}_k \mathcal{H}_e\}$ we obtain

$$\begin{aligned}
\mathcal{H}_{ke} &= \frac{1}{\Lambda}\left[(P\mathcal{H}_e Q)(Q\mathcal{H}_k P) + (P\mathcal{H}_k Q)(Q\mathcal{H}_e P)\right] \\
&= -\frac{1}{\Lambda}\frac{\hbar^2}{m}\Bigl\{-4D_w'\,\Gamma_3(\epsilon_{xy}\{k_x k_y\} + \text{c.p.}) - 2D_w\Gamma_2(\epsilon_{xx}k_x^2 + \text{c.p.} - \tfrac{1}{3}\epsilon_{\lambda\lambda}k^2) \\
&\qquad - \left[4D_w'\,\Gamma_3\epsilon_{yz}\{k_y k_z\} - \tfrac{4}{3}D_w\Gamma_2(\epsilon_{xx}k_x^2 + \epsilon_{yy}k_z^2 + \epsilon_{zz}k_y^2)\right](J_x^2 - \tfrac{1}{3}J^2) + \text{c.p.} \\
&\qquad + \left[4D_w'\,\Gamma_3(\epsilon_{yz}\{k_z k_x\} + \epsilon_{zx}\{k_y k_z\}) + \tfrac{4}{3}D_w\Gamma_3(\epsilon_{xx} + \epsilon_{yy} - 2\epsilon_{zz})\{k_x k_y\} + \tfrac{4}{3}D_w'\,\Gamma_2\epsilon_{xy}(k_x^2 + k_y^2 - 2k_z^2)\right]\{J_x J_y\} + \text{c.p.}\Bigr\} \\
&\qquad - \frac{1}{\Lambda}\frac{e\hbar}{mc}K\Bigl\{\tfrac{4}{3}D_w'\,(\epsilon_{xy}H_z + \text{c.p.})(J_x J_y J_z + J_z J_y J_x) + \left[\tfrac{3}{2}D_w(\epsilon_{yy} + \epsilon_{zz} - 2\epsilon_{xx})H_x + \tfrac{7}{3}D_w'\,(\epsilon_{xy}H_y + \epsilon_{zx}H_z)\right]J_x + \text{c.p.} \\
&\qquad - \left[\tfrac{2}{3}D_w(\epsilon_{yy} + \epsilon_{zz} - 2\epsilon_{xx})H_x + \tfrac{4}{3}D_w'\,(\epsilon_{xy}H_y + \epsilon_{zx}H_z)\right]J_x^3 + \text{c.p.} \\
&\qquad + \left[\tfrac{2}{3}D_w(\epsilon_{yy} - \epsilon_{zz})H_x + \tfrac{4}{3}D_w'\,(\epsilon_{xy}H_y - \epsilon_{zx}H_z)\right]V_x + \text{c.p.}\Bigr\},
\end{aligned} \qquad (128)$$

where

$$D_w = \tfrac{1}{2}(D_2 - E_2), \quad D_w' = \tfrac{1}{2}(D_3 - E_3), \quad \Gamma_2 = \tfrac{1}{6}(A_2 - B_2), \quad \Gamma_3 = \tfrac{1}{6}(A_3 - B_3), \quad K = -\tfrac{2}{3}(A_4 - 2B_4 + \tfrac{1}{3}B_4' + \tfrac{1}{2}B_4''), \qquad (129)$$

and

$$V_x=\{(J_y^2-J_z^2)J_x\} \ . \tag{130}$$

The product $\mathcal{H}_e^2$ can be obtained from the expression for $\mathcal{H}_{ke}$, Eq. (128), by dividing the latter by 2 and replacing the k terms, $(\hbar^2/m)\Gamma_2 k_x^2$, $(\hbar^2/m)\Gamma_3\{k_x k_y\}$, and H_x, with the strain terms $\frac{2}{3}D_w\epsilon_{xx}$, $\frac{2}{3}D'_w\epsilon_{xy}$, and 0, respectively (plus cyclic permutations). The result is

$$\begin{aligned}\mathcal{H}_{ee}=&\frac{1}{\Lambda}(P\mathcal{H}_e Q)(Q\mathcal{H}_e P)\\ =&-\frac{1}{\Lambda}\Big\{-\tfrac{4}{3}D_w'^2(\epsilon_{xy}^2+\text{c.p.})-\tfrac{2}{3}D_w^2[\epsilon_{xx}^2+\text{c.p.}-\tfrac{1}{3}(\epsilon_{\lambda\lambda})^2]\\ &-\Big[\tfrac{4}{3}D_w'^2\epsilon_{yz}^2-\tfrac{4}{9}D_w^2(\epsilon_{xx}^2+2\epsilon_{yy}\epsilon_{zz})\Big](J_x^2-\tfrac{1}{3}J^2)+\text{c.p.}\\ &+2\Big[\tfrac{4}{3}D_w'^2\epsilon_{yz}\epsilon_{zx}+\tfrac{4}{9}D_w D_w'(\epsilon_{xx}+\epsilon_{yy}-2\epsilon_{zz})\epsilon_{xy}\Big]\{J_x J_y\}+\text{c.p.}\Big\} \ .\end{aligned} \tag{131}$$

Finally the product $\mathcal{H}_k^2$ can also be obtained essentially by inspection from $\mathcal{H}_{ke}$ by dividing the first half by 2, and making the "inverse" substitution of $\frac{3}{2}(\hbar^2/m)\Gamma_2 k_x^2$ and $\frac{3}{2}(\hbar^2/m)\Gamma_3\{k_x k_y\}$ for $D_w\epsilon_{xx}$ and $D'_w\epsilon_{xy}$, respectively (plus adding a term which comes from the product $\vec{\mathrm{H}}$ times $\vec{\mathrm{H}}$). The result is

$$\begin{aligned}\mathcal{H}_{kk}=&\frac{1}{\Lambda}(P\mathcal{H}_k Q)(Q\mathcal{H}_k P)\\ =&-\frac{1}{\Lambda}\left(\frac{\hbar^2}{m}\right)^2\Big\{-3\Gamma_3^2(\{k_x k_y\}^2+\text{c.p.})-\tfrac{3}{2}\Gamma_2^2(k_x^4+\text{c.p.}-\tfrac{1}{3}k^4)\\ &-\Big[3\Gamma_3^2\{k_y k_z\}^2-\Gamma_2^2(k_x^4+2\{k_y^2,k_z^2\})\Big](J_x^2-\tfrac{1}{3}J^2)+\text{c.p.}\\ &+2\Big[3\Gamma_3^2\{\{k_y k_z\}\{k_z k_x\}\}+\Gamma_2\Gamma_3\{k_x^2+k_y^2-2k_z^2,\{k_x k_y\}\}\Big]\{J_x J_y\}+\text{c.p.}\Big\}\\ &-\frac{1}{\Lambda}\frac{e\hbar}{mc}\frac{\hbar^2}{m}K\Big\{2\Gamma_3(\{k_x k_y\}H_z+\text{c.p.})(J_x J_y J_z+J_z J_y J_x)\\ &+\Big[\tfrac{9}{4}\Gamma_2(k_y^2+k_z^2-2k_x^2)H_x+\tfrac{7}{2}\Gamma_3(\{k_x k_y\}H_y+\{k_z k_x\}H_z)\Big]J_x+\text{c.p.}\\ &-\Big[\Gamma_2(k_y^2+k_z^2-2k_x^2)H_x+2\Gamma_3(\{k_x k_y\}H_y+\{k_z k_x\}H_z)\Big]J_x^3+\text{c.p.}\\ &+\Big[\Gamma_2(k_y^2-k_z^2)H_x+2\Gamma_3(\{k_x k_y\}H_y-\{k_z k_x\}H_z)\Big]V_x+\text{c.p.}\Big\}\\ &+\frac{1}{\Lambda}\left(\frac{e\hbar}{mc}\right)^2K^2[\tfrac{9}{16}H^2-\tfrac{1}{4}(\vec{\mathrm{J}}\cdot\vec{\mathrm{H}})^2] \ .\end{aligned} \tag{132}$$

It should be noted that the combinations of the spin-independent coefficients (A_2, A_3, D_2, D_3) and spin-dependent coefficients $(B_2, B_3, B_4, B_4', B_4'', E_2, E_3)$ in the first-order projections (29) and (30) are different from those appearing in the second-order projections (128), (131), and (132). [Compare Eqs. (31) and (32) with Eqs. (129).] In the absence of spin-orbit coupling, $B_4=\frac{1}{4}g_s=\frac{1}{2}$ and all other B's and E's are zero, so we may write

$$\Gamma_2=\gamma_2, \quad \Gamma_3=\gamma_3, \quad K=\kappa+1 \ , \tag{133}$$

$$D_w=D_u, \quad D'_w=D'_u \ . \tag{134}$$

As we pointed out earlier, the spin-dependent contribution to the effective-mass parameters are really quite small (i.e., of the order of q), so the approximation (133) is a rather good one. The spin-dependent contribution to the deformation potentials, however, is not generally negligible and we shall *not* make use of the assumption (134).

Each of the three types of interactions[44] $\mathcal{H}_{kk}$, $\mathcal{H}_{ke}$, and $\mathcal{H}_{ee}$ has a characteristic effect on the quantum-resonance spectrum which we shall discuss below in application to the three special cases where the stress lies along the principal crystallographic axes [001], [111], and [110].

1. $\mathcal{H}_{ee}$: Second-order strain splitting

Using the strain tensors given in Table III we obtain the second-order strain Hamiltonians [expressed in the coordinate systems defined in Table III]:

$T \,||\, [001]$:

$$\mathcal{H}_{ee}=-\frac{1}{\Lambda}\epsilon_w^2(J_3^2-\tfrac{1}{3}J^2-1) \ ; \tag{135}$$

$T \,||\, [111]$:

$$\mathcal{H}_{ee}=-\frac{1}{\Lambda}\epsilon_w'^2(J_3^2-\tfrac{1}{3}J^2-1) \ ; \tag{136}$$

$T \parallel [110]$:

$$\mathcal{H}_{ee} = -\frac{1}{\Lambda}\left[\tfrac{1}{8}(3\epsilon_w'^2 + 6\epsilon_w\epsilon_w' - \epsilon_w^2)(J_3^2 - \tfrac{1}{3}J^2) + \tfrac{1}{8}(3\epsilon_w' + \epsilon_w)(\epsilon_w' - \epsilon_w)(J_1^2 - J_2^2) - \tfrac{1}{4}(3\epsilon_w'^2 + \epsilon_w^2)\right], \tag{137}$$

where

$$\epsilon_w = \tfrac{2}{3}(s_{11} - s_{12})D_w T, \quad \epsilon_w' = \tfrac{1}{3}s_{44}D_w' T. \tag{138}$$

The splitting parts (the J terms) of $\mathcal{H}_{ee}$ in Eqs. (135)–(137) exhibit the same symmetries as the first-order strain terms [see Eqs. (76), (78), (80), and (81)], so their effect is merely to introduce a small nonlinearity in the strain splitting energies. The "non-J" terms in $\mathcal{H}_{ee}$ impart to all states in $J = \frac{3}{2}$ a uniform second-order energy shift of no consequence to our present work.

2. $\mathcal{H}_{ke}$: *Strain-dependent line shift*

The term $\mathcal{H}_{ke}$ contributes an energy shift to the Landau levels proportional to both magnetic field and strain, thus having the effect of changing the "apparent" band parameters and shifting the resonance effective mass by the order of ϵ/Λ. This effect has been considered in detail by Hasegawa[20] for classical cyclotron resonance where the shifts are uniform for all Landau levels. In the quantum case, however, where the effective masses differ for each cyclotron-resonance transition (at finite stress), the correction to each transition depends in a rather complicated fashion on the nature of the specific Landau levels involved. In the high-stress limit, however, the calculation simplifies as we can further project (128) onto the strain-split subspace $M_J = \pm\frac{1}{2}$ by the procedure described in Sec. V (only the first-order term is retained in this projection). Using the operators in the last column of Table I, we obtain from (128) the projection for $T \parallel [001]$:

$$Q_1\mathcal{H}_{ke}Q_1 = -\frac{\epsilon_w}{\Lambda}\frac{\hbar^2}{2m}4\Gamma_2(k_x^2 + k_y^2 - 2k_z^2) + \frac{\epsilon_w}{\Lambda}\frac{e\hbar}{4mc}4K(H_x\sigma_x + H_y\sigma_y + 2H_z\sigma_z). \tag{139}$$

(The projection of $\mathcal{H}_{ke}$ onto the subspace $M_J = \pm\frac{3}{2}$ vanishes.) For $T \parallel [111]$ a form identical to (139) obtains for the $M_J = \pm\frac{1}{2}$ projection with the obvious replacements: $(x, y, z) \to (1, 2, 3)$ (see Table III) for the coordinate axes, $\epsilon_w \to \epsilon_w'$ and $\Gamma_2 \to \Gamma_3$. For $T \parallel [110]$ the result is somewhat more complicated. From the foregoing we can determine the modifications to be made to the first-order projection in Eq. (122). We find that for the three principal directions of stress, the sum of the first-order projection (122) and the second-order projection (139) can again be written in the same form as (122), with $(1/m)$ and g shifted from the expressions in Table V by

$T \parallel [001]$:

$$\Delta\left(\frac{1}{m_1}\right) = \Delta\left(\frac{1}{m_2}\right) = \frac{1}{m}\frac{4\epsilon_w}{\Lambda}\gamma_2, \quad \Delta\left(\frac{1}{m_3}\right) = -\frac{1}{m}\frac{8\epsilon_w}{\Lambda}\gamma_2, \tag{140}$$

$$\Delta g_1 = \Delta g_2 = -(4\epsilon_w/\Lambda)(\kappa + 1), \quad \Delta g_3 = -(8\epsilon_w/\Lambda)(\kappa + 1); \tag{141}$$

$T \parallel [111]$:

$$\Delta\left(\frac{1}{m_1}\right) = \Delta\left(\frac{1}{m_2}\right) = \frac{1}{m}\frac{4\epsilon_w'}{\Lambda}\gamma_3, \quad \Delta\left(\frac{1}{m_3}\right) = -\frac{1}{m}\frac{8\epsilon_w'}{\Lambda}\gamma_3, \tag{142}$$

TABLE VIII. Second-order correction coefficients in the inverse effective mass m/m^* [Eq. (127)] for cyclotron resonances within the $M_J = \pm\frac{1}{2}$ band for the $\vec{H} \perp T$ configuration. The lowest-order effective masses m_1, m_2, m_3 are defined in Table V. The parameter α appearing in the coefficients A and D is defined in the second row of this table. For $T \parallel [110]$ we have made the same approximations as made in Table VI.

			$T \parallel [110]$	
	$T \parallel [001]$	$T \parallel [111]$	$\vec{H} \parallel [1\bar{1}0]$	$\vec{H} \parallel [00\bar{1}]$
m_0^*	$(m_1m_3)^{1/2}$	$(m_1m_3)^{1/2}$	$(m_2m_3)^{1/2}$	$(m_1m_3)^{1/2}$
α	$(m_1/m_3)^{1/4}$	$(m_1/m_3)^{1/4}$	$(m_2/m_3)^{1/4}$	$(m_1/m_3)^{1/4}$
A	$\frac{3}{2}\gamma_3^2 + \frac{9}{8}\alpha^4\gamma_2^2$	$\frac{1}{2}(2\gamma_2^2 + \gamma_3^2)$ $+ \frac{3}{8}\alpha^4(\gamma_2^2 + 2\gamma_3^2)$	$\frac{3}{2}\gamma_2^2 + \frac{9}{8}\alpha^4\gamma_2^2$ $+ \frac{27}{8}(\gamma_3 - \gamma_2)\gamma_2$ $- \frac{3}{8}(\beta - 1)\gamma_2^2(1 - \frac{3}{2}\alpha^4)$	$\frac{3}{2}\gamma_2^2 + \frac{9}{8}\alpha^4\gamma_2^2$ $- \frac{3}{8}(\gamma_3 - \gamma_2)\gamma_2(1 - 3\alpha^4)$ $+ \frac{3}{8}(\beta - 1)\gamma_2^2(1 - \frac{3}{2}\alpha^4)$
D	$\frac{3}{2}\alpha^2\gamma_2(\gamma_3 + \frac{1}{2}\kappa)$	$\frac{3}{2}\alpha^2(\gamma_2\gamma_3 + \frac{1}{6}\kappa\gamma_2 + \frac{1}{3}\kappa\gamma_3)$	$\frac{3}{2}\alpha^2\gamma_2(\gamma_2 + \frac{1}{2}\kappa)$ $+ \frac{3}{8}(\gamma_3 - \gamma_2)(4\alpha^2\gamma_2 - 2\alpha^{-2}\gamma_2 + \alpha^{-2}\kappa)$ $+ \frac{3}{8}(\beta - 1)\gamma_2(\alpha^2\gamma_2 + 2\alpha^{-2}\gamma_2 - \alpha^{-2}\kappa)$	$\frac{3}{2}\alpha^2\gamma_2(\gamma_2 + \frac{1}{2}\kappa)$ $+ \frac{3}{8}(\gamma_3 - \gamma_2)(2\alpha^2\gamma_2 + \alpha^2\kappa + 2\alpha^{-2}\gamma_2 - \alpha^{-2}\kappa)$ $- \frac{3}{8}(\beta - 1)\gamma_2(\alpha^2\gamma_2 + 2\alpha^2\kappa + 2\alpha^{-2}\gamma_2 - \alpha^{-2}\kappa)$

$$\Delta g_1 = \Delta g_2 = -(4\epsilon'_w/\Lambda)(\kappa+1)\,,$$
$$\Delta g_3 = -(8\epsilon'_w/\Lambda)(\kappa+1)\;; \qquad (143)$$

$T \| [110]$:

$$\Delta\left(\frac{1}{m_1}\right) = \frac{1}{m}\frac{\epsilon_w}{\Lambda}\,[3\gamma_3(\eta_2+\eta_1\beta'+\beta') - \gamma_2(3\eta_2\beta'-\eta_1+1)]\,,$$
$$\Delta\left(\frac{1}{m_2}\right) = \frac{1}{m}\frac{\epsilon_w}{\Lambda}\,2\gamma_2(3\eta_2\beta'-\eta_1+1)\,, \qquad (144)$$
$$\Delta\left(\frac{1}{m_3}\right) = -\frac{1}{m}\frac{\epsilon_w}{\Lambda}\,[3\gamma_3(\eta_2+\eta_1\beta'+\beta') + \gamma_2(3\eta_2\beta'-\eta_1+1)]\;;$$

$$\Delta g_1 = -(\epsilon_w/\Lambda)(\kappa+1)[(1-\eta_1)(3\beta'-1)+3\eta_2(\beta'+1)]\,,$$
$$\Delta g_2 = -(\epsilon_w/\Lambda)(\kappa+1)[2+\eta_1(3\beta'+1)+3\eta_2(\beta'-1)]\,,$$
$$\Delta g_3 = -(\epsilon_w/\Lambda)(\kappa+1)(3\beta'+1)(1+\tfrac{1}{2}\eta_1+\tfrac{3}{2}\eta_2)\,. \qquad (145)$$

In the above equations η_1 and η_2 are defined by Eq. (121), and β' is the spin-dependent strain-splitting anisotropy parameter, $\beta' = \epsilon'_w/\epsilon_w$; also for convenience the approximation (133) has been assumed for the band parameters. The effective-mass sum rule[20] $\sum_{i=1}(m/m_i) = 3\gamma_1$ is still obeyed for each direction of stress. The corrected effective masses given above are identical with the classical result of Hasegawa[20] if we assume $\epsilon_w = \epsilon_u$ and $\epsilon'_w = \epsilon'_u$.

3. $\mathcal{H}_{kk}$: *Magnetic-field-dependent shift*

The term $\mathcal{H}_{kk}$ is of order k^4 and hence similar in nature to the corrections (123) and (124) discussed in Sec. V. It introduces an energy shift of order $(\hbar\omega)^2/\Lambda$, where ω is the angular frequency of the resonant radiation field, and hence contributes an effective-mass correction of order $\hbar\omega/\Lambda$. Since $\hbar\omega/\Lambda$ is very small at microwave frequencies, this shift is usually negligible compared to the one in Sec. V except for those few resonance lines which admit to extremely precise measurement. For experiments in the far infrared, on the other hand, this correction may assume considerable importance. For completeness we develop below those perturbations which arise from $\mathcal{H}_{kk}$.

In the high-stress limit we can again project (132) onto the subspace $M_J = \pm\frac{1}{2}$ and obtain for $T \| [100]$:

$$Q_1\mathcal{H}_{kk}Q_1 = -\frac{1}{\Lambda}\left(\frac{\hbar^2}{m}\right)\left(-\Gamma_2^2[\tfrac{1}{2}(k_x^2+k_y^2)^2+\tfrac{9}{2}\{(k_x^2+k_y^2)k_z^2\}+2k_z^4] - \tfrac{9}{2}(\Gamma_3^2-\Gamma_2^2)\{(k_x^2+k_y^2)k_z^2\}\right)$$
$$-\frac{1}{\Lambda}\frac{e\hbar}{mc}\frac{\hbar^2}{m}K\left(\tfrac{1}{2}\Gamma_2(k_x^2+k_y^2-2k_z^2)(H_x\sigma_x+H_y\sigma_y-2H_z\sigma_z) - 3\Gamma_3[\{k_x\sigma_x+k_y\sigma_y, H_zk_z\} - \tfrac{1}{2}\{H_xk_x+H_yk_y, k_z\sigma_z\}]\right)$$
$$+\frac{1}{\Lambda}\left(\frac{e\hbar}{mc}\right)^2[(\tfrac{5}{16}K^2+\tfrac{27}{8}\Gamma_3^2)(H_x^2+H_y^2)+\tfrac{1}{2}K^2H_z^2]\,. \qquad (146)$$

The correction to the high-stress states $(n, \pm, \zeta)$, obtained by taking the expectation value of (146) in exactly the same manner as in Sec. V, is in form essentially identical to Eq. (125),

$$\hbar\frac{eH}{mc}\frac{1}{\Lambda}\,[A'(n^2+n)+B'(2n+1)\zeta^2 + C' + F'\zeta^4 \pm (D'(2n+1)+E'\zeta^2)] \qquad (147)$$

(in units of $-\hbar eH/mc$). As this energy perturbation is so small, it suffices if we use the spherical approximation for both the band parameters, $\gamma_2 = \gamma_3 = \overline{\gamma}$, [assuming, in addition, the relations (133)] and the deformation potentials, $\epsilon_u = \epsilon'_u$ to estimate it. The coefficients in Eq. (147) for $\vec{H} \| T$ now simplify and become

$$A' = -2\overline{\gamma}^2,\quad B' = -\tfrac{9}{2}\overline{\gamma}^2,$$
$$C' = -[\tfrac{1}{4}\overline{\gamma}^2+\tfrac{1}{2}(\kappa+1)^2],\quad D' = -\overline{\gamma}(\kappa+1), \qquad (148)$$
$$E' = 2\overline{\gamma}(\kappa+1),\quad F' = -2\overline{\gamma}^2\,.$$

These results based on the spherical limit are applicable for all directions of stress.[45]

We may summarize the results of this section by reiterating that the relative energies, pertinent to resonance experiments, of the Landau levels within the $M_J = \pm\frac{1}{2}$ subband *including the interactions with the spin-orbit-split-off band* can still be expressed by the form (125) with renormalized effective masses and g factors [Table V plus Eqs. (140)–(145)] and with an additional k^4 correction (147). We further note that the above-mentioned k^4 correction for the various transitions in the geometry $\vec{H} \| T$ is expressible in exactly the same form as the last term in Eq. (125) with a simple modification which consists of replacing $2x$ by $\Lambda/[\hbar(eH/mc)]$ and substituting the coefficients given in Eq. (148).

VII. CONCLUDING REMARKS

Our discussion began with the construction of the most general effective-mass Hamiltonian to order k^2 and first order in strain ϵ within the 6×6 manifold of the Γ_{25}^+ band, that is, the combined space spanning both spin-orbit-split bands, Γ_7 and Γ_8. This $k^2-\epsilon$ Hamiltonian has served as the basis for nearly all subsequent theoretical development; in particular, we have considered its projection onto each of the subspaces Γ_7 and Γ_8 and, in turn, onto the strain-split subspaces of the latter. Before we close it is of interest to examine the "lowest-order" approximation more closely and consider briefly the ways in which we can generalize the Hamiltonian to higher orders both in k, i.e., k^4, k^6, etc., and in ϵ, i.e., ϵ^2, ϵk^2, etc. Some terms of higher order for the Γ_8 band have already been considered, namely, the perturbation in Γ_8 which arises from the interaction between Γ_8 and Γ_7 (i.e. a "two-band" approximation).

First, let us consider higher-order effects in $\vec{k}$. Generally speaking, it is clear that the expectation values of the successively higher-order $\vec{k}$ terms in the Hamiltonian will diminish in magnitude by a characteristic expansion parameter $\hbar\omega/E_g$, where E_g is an appropriate energy gap between Γ_8 and other relevant perturbing bands. For microwave resonance experiments, for which $\hbar\omega \ll E_g$, the truncation of the expansion to k^2 turns out to be an excellent approximation; however, with the movement of experimental effort into the far-infrared region this assumption may no longer be satisfactory.

One way to extend the theory to orders of $\vec{k}$ higher than k^2 would be to include nearby bands into the space spanned by the $\vec{k}\cdot\vec{p}$ interaction matrix and solve the resulting Hamiltonian in this augmented space.[46] An alternative way, more in keeping with the approach developed in Sec. II A, would be to construct and solve a higher-order Hamiltonian within a single band. This procedure was first carried out for the case of a simple band by Kjeldaas and Kohn[47] who made, following the initial Luttinger-Kohn first-order canonical transformation,[2] additional transformations to remove interband momentum matrix elements to successively higher orders. An application of the Kjeldaas-Kohn technique was made to the conduction band of InSb by Wallis.[48] It is interesting to note that this band, in contrast to the Γ_8 valence band of Ge, is spherical to order k^2 and warping first appears at order k^4. (We should also mention that by neglecting the small warping part Wallis was able to obtain exact solutions to the k^4 Hamiltonian; in other words, the isotropic k^4 part could be diagonalized simultaneously with the k^2 part.)

On purely group-theoretical grounds we can construct the most general k^4 Hamiltonian for the Γ_8 band, expressible as a cubic invariant containing the J ($J=\frac{3}{2}$) operators and second and fourth powers of k. To illustrate its form we drop anisotropic terms and obtain the following *spherical* Hamiltonian for Γ_8 (up to k^4) which contains seven independent constants in addition to the usual three coefficients γ_1, $\bar{\gamma}(=\gamma_2=\gamma_3)$, and κ which appear in the k^2 Hamiltonian:

$$\begin{aligned}\mathcal{H}_k = &-\frac{\hbar^2}{m}\left((\tfrac{1}{2}\gamma_1+\tfrac{5}{4}\bar{\gamma})k^2-\bar{\gamma}(\vec{k}\cdot\vec{J})^2+\frac{e}{\hbar c}(\kappa+\tfrac{1}{2}\bar{\gamma})(\vec{H}\cdot\vec{J})\right)-\frac{\hbar^6}{m^3e^4}\Big[\delta_1 k^4+\delta_2\{k^2,(\vec{k}\cdot\vec{J})^2\}\\ &+\frac{e}{\hbar c}[\delta_3 k^2(\vec{H}\cdot\vec{J})+\delta_4\{(\vec{k}\cdot\vec{H})(\vec{k}\cdot\vec{J})\}+\delta_5\{(\vec{k}\cdot\vec{J})^2(\vec{H}\cdot\vec{J})\}]+\left(\frac{e}{\hbar c}\right)^2[\delta_6 H^2+\delta_7(\vec{H}\cdot\vec{J})^2]\Big]\,. \end{aligned} \tag{149}$$

[We should point out that the sum of Eq. (70) and $\mathcal{H}_{kk}$ in Ref. 44 is a special case of the above Hamiltonian.] The numerical coefficients $\delta_1, \ldots, \delta_7$ are to be determined by the procedures of Kjeldaas and Kohn. In cubic symmetry each of the k^4 terms in Eq. (149) splits, as seen, for example, in the cubic Hamiltonian (132).[49]

Like the Wallis case for InSb mentioned earlier, the spherical Hamiltonian (149) is exactly soluble for an arbitrary direction of magnetic field as well as finite k_H (the discussion of Appendix A 1 applies literally here) by using a Luttinger-type wave function of the form

$$\begin{aligned}\psi_{N,k_H} = &a_{N-3}(\tfrac{3}{2})u_{N-3,k_H}|\tfrac{3}{2}\rangle + a_{N-2}(\tfrac{1}{2})u_{N-2,k_H}|\tfrac{1}{2}\rangle\\ &+a_{N-1}(-\tfrac{1}{2})u_{N-1,k_H}|-\tfrac{1}{2}\rangle + a_N(-\tfrac{3}{2})u_{N,k_H}|-\tfrac{3}{2}\rangle\,.\end{aligned} \tag{150}$$

In contrast, however, to the eigensolutions for the k^2 case, the coefficients a_N in (150) are functions of the magnetic field; this field dependence can be a source of cyclotron-resonance line shifts, i.e., the apparent effective masses will depend upon the radiation frequency ω at which experiments are done. If the nonspherical parts are restored to the Hamiltonian (149), it no longer admits to solution in a finite space, and the wave function can only be represented as a series expansion similar to Eq. (111).

Next, we turn to the question of the higher-order strain terms in the Hamiltonian. We have considered the effect of deformation on the basis of the effective Hamiltonian (8), in which the deformation potential constants have been evaluated by the intraband matrix elements (23) and (24). The next lowest-order contributions beyond this approximation are the interband interaction between $\mathcal{H}_k$ [Eq. (10)] and $\mathcal{H}_\epsilon$ [Eq. (11)] and that between $\mathcal{H}_\epsilon$ and $\mathcal{H}_\epsilon$. The latter is not important for the intraband transitions we are considering. The former effect in the Γ_8 band has already been partially taken into account (in Sec. VI), and we shall here remark on the remaining contribution of this type, namely, the strain-dependent effective-mass shift caused by bands external to Γ_{25}^{+}.

All terms of order $k_\kappa k_\lambda \epsilon_{\mu\nu}$ we seek are included in Eq. (C8) which has the form of a spin Hamiltonian with undetermined coefficients. We can easily evaluate these coefficients if we adopt a two-band approximation which includes the valence band edge Γ_8^+ and the conduction band $\Gamma_7^-(=\Gamma_2^-\times\Gamma_8^+)$, the split-off band Γ_7^+ having already been taken into account earlier in Eq. (128). (Contributions from more remote bands should be much smaller and for the purposes of this discussion can be completely ignored.) The resulting spin Hamiltonian $\mathcal{H}_{ke}$ representing the contribution from Γ_7^- has the form

$$\begin{aligned}
&-\frac{\hbar^2}{m}\frac{1}{E_g}\Big(\tfrac{1}{2}(D_d-D_d')\gamma_1\epsilon_{\lambda\lambda}k^2 - D_u\gamma_2(\epsilon_{xx}k_x^2+\text{c.p.}-\tfrac{1}{3}\epsilon_{\lambda\lambda}k^2) - 2D_u'\gamma_3(\epsilon_{xy}\{k_xk_y\}+\text{c.p.})\\
&\qquad -(D_d-D_d')\gamma_2\epsilon_{\lambda\lambda}k_x^2(J_x^2-\tfrac{1}{3}J^2)+\tfrac{1}{3}D_u\gamma_1\epsilon_{xx}k^2(J_x^2-\tfrac{1}{3}J^2)+\text{c.p.}\\
&\qquad -2(D_d-D_d')\gamma_3\epsilon_{\lambda\lambda}\{k_xk_y\}\{J_xJ_y\}+\tfrac{2}{3}D_u'\gamma_1\epsilon_{xy}k^2\{J_xJ_y\}+\text{c.p.}\\
&\qquad +\frac{e\kappa}{\hbar c}\Big[(D_d-D_d')\epsilon_{\lambda\lambda}H_xJ_x-\tfrac{5}{12}D_u(2\epsilon_{xx}-\epsilon_{yy}-\epsilon_{zz})H_xJ_x+\tfrac{1}{3}D_u(2\epsilon_{xx}-\epsilon_{yy}-\epsilon_{zz})H_xJ_x^3\\
&\qquad\quad +\tfrac{4}{3}D_u'(\epsilon_{xy}H_y+\epsilon_{zx}H_z)J_x-\tfrac{2}{3}D_u'(\epsilon_{xy}H_y+\epsilon_{zx}H_z)J_x^3+\tfrac{1}{3}D_u(\epsilon_{yy}-\epsilon_{zz})H_xV_x+\tfrac{2}{3}D_u'(\epsilon_{xy}H_y-\epsilon_{zx}H_z)V_x+\text{c.p.}\\
&\qquad\quad +\tfrac{4}{3}D_u'(\epsilon_{xy}H_z+\text{c.p.})\{J_xJ_yJ_z\}\Big]\Big),
\end{aligned} \tag{151}$$

where

$$E_g = E(\Gamma_7^-) - E(\Gamma_8^+)\,,$$

and (152)

$$D_d' = \langle\beta|\mathfrak{D}_{xx}|\beta\rangle$$

is the conduction-band deformation potential. V_x and $\{J_xJ_yJ_z\}$ are defined in Eq. (130) and Table II, respectively.

With the aid of Table I we can now project the Hamiltonian (151), assuming a stress $T \parallel [001]$, onto the manifold of the strain-split states $M_J=\pm\frac{1}{2}$. When we add this projection to the projections (122) and (139) [including the approximation (133)] obtained earlier, we find the sum can be written in the form of Eq. (122) with modified effective-mass and g-tensor components given by [cf. with Eqs. (140), (141), and Table V]

$$\begin{aligned}
\frac{m}{m_1}=\frac{m}{m_2}&=(\gamma_1-\gamma_2)\left(1+\frac{\epsilon_d-\epsilon_u}{E_g}\right)+\frac{4\epsilon_w}{\Lambda}\gamma_2\,,\\
\frac{m}{m_3}&=(\gamma_1+2\gamma_2)\left(1+\frac{\epsilon_d-\epsilon_u}{E_g}\right)-\frac{8\epsilon_w}{\Lambda}\gamma_2\,,\\
g_1=g_2&=4\kappa\left(1+\frac{\epsilon_d-\epsilon_u}{E_g}\right)-\frac{4\epsilon_w}{\Lambda}(\kappa+1)\,,\\
g_3&=2\kappa\left(1+\frac{\epsilon_d-\epsilon_u}{E_g}\right)-\frac{8\epsilon_w}{\Lambda}(\kappa+1)\,,
\end{aligned} \tag{153}$$

where

$$\epsilon_d=(D_d-D_d')(s_{11}+2s_{12})T\,, \tag{154}$$

and ϵ_u and ϵ_w are defined by Eqs. (74) and (138), respectively. From the result (153) we can see that the change in the effective band gap between the interacting Γ_7^- band and the strain-split $M_J=\pm\frac{1}{2}$ subband shifts the "apparent" band parameters γ_1, γ_2, γ_3, and κ linearly with stress. The effective-mass sum rule[20] is now violated and

$$\begin{aligned}
\sum_{i=1}^{3}\frac{m}{m_i}&=3\gamma_1\left(1+\frac{\epsilon_d-\epsilon_u}{E_g}\right)\\
&=3\gamma_1+\frac{\gamma_1}{E_g}\left(\frac{dE_g}{dP}-2D_u(s_{11}-s_{12})\right)T
\end{aligned} \tag{155}$$

also changes linearly with stress. [Here P is the hydrostatic pressure and $\frac{1}{3}dE_g/dP=(D_d-D_d')\times(s_{11}+2s_{12})$]. For Ge we obtain[50]

$$\frac{\gamma_1}{E_g}\left(\frac{dE_g}{dP}-2D_u(s_{11}-s_{12})\right)\approx 5.4\times10^{-5}\ \text{cm}^2/\text{kg}\,;$$

which should be compared with the experimental result (see Paper II, Sec. IV)

$$-\sum_i\alpha_i=-(2.4\pm5.0)\times10^{-5}\ \text{cm}^2/\text{kg}\,.$$

The corresponding quantities for [111] are

$$\frac{\gamma_1}{E_g}\left(\frac{dE_g}{dP}-D_u's_{44}\right)\approx 8.8\times10^{-5}\ \text{cm}^2/\text{kg}$$

versus

$$-\sum_i\alpha_i=(4.0\pm5.0)\times10^{-5}\ \text{cm}^2/\text{kg}\,.$$

The sums of α's are consistently less than the calculated values, but in view of the large uncertainties in the experimental numbers one cannot attach much significance to this fact.

It is interesting to compare the relative magnitudes of the strain-linear effective-mass shift contributed by the Γ_7^- conduction band to that from the Γ_7^+ split-off band. For the "transverse" effective mass, $m_1=m_2$, we obtain from Eq. (153) the ratio

$$\frac{\Delta m_1(\Gamma_7^-)}{\Delta m_1(\Gamma_7^+)}=\frac{(\gamma_1-\gamma_2)(\epsilon_d-\epsilon_u)}{4\gamma_2\epsilon_w}\frac{\Lambda}{E_g}\sim0.07\,,$$

(based on the values[16] $D_w=2.3$ eV and $\gamma_2=4.24$ for

Ge, in addition to the parameters given above[50]). We note that the two effects contribute constructively, and that the Γ_7^- contribution is more than an order of magnitude smaller than that from Γ_7^+. This justifies our neglecting *interband* effects *in toto.*

ACKNOWLEDGMENTS

We have profited from numerous conversations with our colleagues. We would like to acknowledge, in particular, fruitful discussions with A. R. Hutson, E. O. Kane, J. C. Phillips, and Y. Yafet.

APPENDIX A: SYMMETRIES AND QUANTUM NUMBERS IN SOLUBLE CASES

Luttinger[3] has discussed several cases in which the secular matrix decouples to the extent that essentially exact solutions can be achieved in a finite space. It is interesting to consider these cases briefly in the context of our present analysis.

1. The "spherical" case: $\gamma_3=\gamma_2$ $(q=0)$

The magnetic Hamiltonian (29) assumes spherical symmetry [see Eq. (71)] when we set $\gamma_3=\gamma_2$ (and $q=0$) whether or not $k_H=0$. For $k_H\neq 0$ the symmetry is in essence equivalent to that of the full axial Hamiltonian D^a. The secular matrix decouples into 4×4 blocks each assigned with an axial quantum number N. Cyclotron-resonance transitions ($\vec{\mathcal{E}}\perp\vec{H}$) obey the selection rules of type M_1, i.e., $\Delta N=\pm 1$.

Next, if we set $k_H=0$, parity now becomes a good quantum number, and each 4×4 matrix further splits into two 2×2 matrices. Cyclotron resonance can only occur under the most restrictive selection rules of type M_0: $\Delta N=\pm 1$, $\Delta\pi=$ yes.

2. The trigonal case: $\vec{H}\parallel[111]$ $(k_H=0)$

Luttinger has pointed out that a remarkable simplification occurs for the case $\vec{H}\parallel[111]$ when $k_H=0$. It is then found that the infinite secular matrix factors into 4×4 blocks which can be readily solved. The reasons for this unique behavior are considerably less trivial than for the preceding case; and, in fact, until now the question has been regarded as somewhat of a mystery. Since the Hamiltonian for this particular case lacks axial symmetry, N cannot be a rigorous quantum number, so the decoupling is not an obvious group-theoretical consequence of the apparent symmetries. The crux of the matter, we find, lies in the existence of an unusual "hidden" symmetry which becomes evident when we look further into the structure of the Hamiltonian.

To reveal the nature of this symmetry, we shall demonstrate that the Hamiltonian for $\vec{H}\parallel[111]$, written here as $D_0[=D^a+D^{na}$ in Eqs. (78) and (79) with $\zeta=0]$, has the special property of being invariant under a particular kind of unitary transformation. We shall show that this invariance is responsible for the remarkable decoupling of the infinite secular matrix into analytically tractable 4×4 blocks.

Let us begin by constructing the following two operators:

$$\Lambda=-2J_3^3+\tfrac{9}{2}J_3\ , \tag{A1}$$

$$L=\Lambda+a^\dagger a+2\ , \tag{A2}$$

whose special significance within the $J=\frac{3}{2}$ manifold for the case $\vec{H}\parallel[111]$ and $k_H=k_3=0$ will become clear shortly. Using Eq. (69) we calculate commutation relations of Λ with products of the angular momentum operators,

$$[\Lambda,J_\pm^2]=\pm 2J_\pm^2\ , \tag{A3}$$

$$[\Lambda,\{J_\pm J_3\}]=\mp 2\{J_\pm J_3\}\ , \tag{A4}$$

$$[\Lambda,J_\pm^3]=0\ . \tag{A5}$$

With the help of these commutators we are able to set up a unitary transformation $e^{i\Lambda\varphi}$, where φ is any real angle, of the three types of operators $J_\pm^2$, $\{J_\pm J_3\}$, and $J_\pm^3$;

$$\begin{aligned}e^{-i\varphi\Lambda}J_\pm^2e^{i\varphi\Lambda}&=J_\pm^2+(-i\varphi)[\Lambda,J_\pm^2]\\&\quad+(-i\varphi)^2/(2!)[\Lambda,[\Lambda,J_\pm^2]]+\cdots\\&=J_\pm^2+(\mp 2i\varphi)J_\pm^2+(\mp 2i\varphi)^2/(2!)J_\pm^2+\cdots\\&=e^{\mp 2i\varphi}J_\pm^2\ ,\end{aligned} \tag{A6}$$

and similarly

$$e^{-i\varphi\Lambda}\{J_\pm J_3\}e^{i\varphi\Lambda}=e^{\pm 2i\varphi}\{J_\pm J_3\}\ , \tag{A7}$$

$$e^{-i\varphi\Lambda}J_\pm^3e^{i\varphi\Lambda}=J_\pm^3\ \text{(invariant)}\ . \tag{A8}$$

Next, we shall need analogous unitary transformations $e^{i\varphi a^\dagger a}$ which can be derived from the commutation relations (67):

$$\begin{aligned}e^{-i\varphi a^\dagger a}ae^{i\varphi a^\dagger a}&=a+(-i\varphi)[a^\dagger a,a]\\&\quad+(-i\varphi)^2/(2!)[a^\dagger a,[a^\dagger a,a]]+\cdots\\&=a+(i\varphi)a+(i\varphi)^2/(2!)a+\cdots\\&=e^{i\varphi}a\ ,\end{aligned} \tag{A9}$$

and similarly,

$$e^{-i\varphi a^\dagger a}a^\dagger e^{i\varphi a^\dagger a}=e^{-i\varphi}a^\dagger\ . \tag{A10}$$

From the foregoing we are now in position to effect a unitary transformation of the complete Hamiltonian D_0 which contains the operators $J_+^2a^2$, $J_-^2a^{\dagger 2}$, $\{J_+J_3\}a^{\dagger 2}$, $\{J_-J_3\}a^2$, J_+^3 and J_-^3. As an example, from Eqs. (A7) and (A10) we have

$$\begin{aligned}e^{-i\varphi L}\{J_+J_3\}a^{\dagger 2}e^{i\varphi L}&=e^{-i\varphi\Lambda}\{J_+J_3\}e^{i\varphi\Lambda}\\&\quad\times e^{-i\varphi a^\dagger a}a^{\dagger 2}e^{i\varphi a^\dagger a}\\&=e^{2i\varphi}\{J_+J_3\}e^{-2i\varphi}a^{\dagger 2}\\&=\{J_+J_3\}a^{\dagger 2}\ .\end{aligned} \tag{A11}$$

With this and with similar relations for the remaining operators, we finally arrive at

$$e^{-i\varphi L} D_0 e^{i\varphi L} = D_0 \,, \tag{A12}$$

proving that D_0 is invariant under a quasirotation through the angle φ. This is obviously not a rotation in real space, and its geometrical interpretation remains for the present unclear. However, in a mathematical sense the invariance under the "rotation" by φ represents a hidden symmetry embeded in the Hamiltonian for $\vec{H} \parallel [111]$ ($k_H = 0$) which is responsible for the "accidental" decoupling of the problem. This behavior is peculiar to the single case, $\vec{H} \parallel [111]$; it does not occur for any other direction of magnetic field.

Once the relation (A12) has been established it follows that the eigenstates of D_0 can be classified according to the eigenvalues of L which are simply integers, 0, 1, 2,$\cdots$ (M_J ranges from $-\frac{3}{2}$ to $+\frac{3}{2}$, and $a^\dagger a$ takes on the values 0, 1, 2,$\cdots$). From Eqs. (A1) and (A2) we find that the lowest two eigenvalues $L = 0$ and 1 each occur only once, so each is identified with a single (isolated) eigenstate, a "singlet." Likewise, $L = 2$ and 3 occur three times apiece and so give rise to "triplets." Finally, for $L \geq 4$ each eigenvalue is fourfold redundant corresponding to a "quartet" of states. Since at most four independent wave functions can belong to each value of L, we see that the secular matrix must decouple into blocks of dimension not exceeding 4×4.

From the foregoing it becomes obvious that the eigenvalues of L exactly correspond to Luttinger's quantum numbers[51] (shifted by 2). Cyclotron-resonance transitions are defined by the single selection rule $\Delta L = \pm 1$ which is, first, consistent with $\Delta K = \pm 1$ and $\Delta\pi =$ yes and, second, nearly as restrictive as the selection rule $\Delta N = \pm 1$ which holds for a *bona fide* axial symmetry.

The operator L has been constructed in an *a priori* fashion; our discussion reveals merely the identity and some of the properties of this "hidden" constant of motion.[52] Important questions remain: what is the physical significance of the rotation angle φ, and why is L conserved? Answers to these presumably will lead to a deeper understanding of the problem.

The above analysis provides as a by-product a proof of the well-known statement—the energy contour for $\vec{k} \perp [111]$ ($k_3 = 0$) is a circle—in a way which shows it to be closely related to the solubility of the quantum problem. The classical energy $E(\vec{k})$ associated with the wave vector $\vec{k}$ is obtained by solving the $\vec{k}\cdot\vec{p}$ Hamiltonian $\mathcal{H}_{\vec{k}}$, which, in the [111] representation, has the same matrix form as Eqs. (78) and (79) with $\kappa = q = 0$, $x'_u = \zeta = 0$ and with $a, a^\dagger$ reconverted to k_-, k_+ through the relation (66). From Eqs. (A6) and (A7) and from the form of the classical Hamiltonian we readily see

$$e^{-i\varphi\Lambda} \mathcal{H}_{\vec{k}} e^{i\varphi\Lambda} = \mathcal{H}_{\vec{k}'} \,, \tag{A13}$$

where $k'_\pm = e^{\pm i\varphi} k_\pm$ are the components of the transformed vector $\vec{k}'$ obtained from $\vec{k}$ by a rotation through the angle φ about the [111] axis. Since eigenvalues are invariant under unitary transformations, Eq. (A13) shows the energy to be unchanged by such a rotation; and, hence, the energy contour is a circle.

We must point out that an essential requirement for the above proofs is the fact that the Hamiltonian is expanded only to k^2. If terms of k^4 and higher are included, it can easily be shown that the conclusions regarding the Luttinger decoupling and the circular energy contours are no longer valid. (Incidentally, this breakdown caused by k^4 terms confirms the fact that the decoupling is not related in a conventional way to a rotational symmetry.)

APPENDIX B: CLASSIFICATION OF FREE-ELECTRON LANDAU STATES

In Sec. IV B we employed a scheme for identifying magnetic states of holes based on the use of two sets of canonical variables $a, a^\dagger$ and $b, b^\dagger$. It is the purpose of this appendix to elaborate a bit further on the background of this formalism.

Since Landau's original solution[53] of the electron motion in a uniform static magnetic field, considerable ambiguity has existed on the unique identification of the enormously degenerate eigenstates. In what is called the Landau gauge, one of the coordinates, say x_1, transverse to the magnetic field, does not appear in the Hamiltonian and the degeneracy is understood as connected with the choice of k_1 or of the center of the cyclotron motion. An alternative labeling scheme which reflects the axially symmetric nature of the problem was introduced by Johnson and Lippmann,[54] Dingle,[55] and Yafet, Keyes, and Adams,[56] but the classification of degenerate states was incomplete. We outline here a systematic method of identifying magnetic states which is symmetric in the sign of charge and admits to simple physical interpretation of the charged particle motion in terms of two sets of harmonic oscillators. Our method is based on the use of two sets of canonical variables first introduced by Kubo, Hasegawa, and Hashitsume[57] and discussed recently by Malkin and Man'ko,[58] and Feldman and Kahn[59] in connection with coherent states.

Apart from the translational motion along the magnetic field, the free electron (charge $e = -|e|$) in a magnetic field is described by the Hamiltonian

$$\mathcal{H}_- = \frac{\hbar^2}{2m}\left(k_1^2 + k_2^2\right) \,, \tag{B1}$$

where

$$\hbar k_1 = p_1 - \frac{\hbar}{2\lambda^2} x_2 \,,$$

$$\hbar k_2 = p_2 + \frac{\hbar}{2\lambda^2} x_1 \ . \qquad \text{(B2)}$$

In these equations $\lambda^2 = \hbar c/|e|H$ is the square of the cyclotron radius, where $\vec{H}$ is the magnetic field directed along $+x_3$. From the definition (B2) it is easy to see that the operators defined by

$$a = \frac{\lambda}{\sqrt{2}}(k_1 - ik_2) \ ,$$
$$a^\dagger = \frac{\lambda}{\sqrt{2}}(k_1 + ik_2) \qquad \text{(B3)}$$

satisfy the commutation relation (67) and the Hamiltonian transforms to

$$\mathcal{H}_- = \hbar\omega_c(a^\dagger a + \tfrac{1}{2}) \ , \qquad \text{(B4)}$$

where $\omega_c = |e|H/mc = \hbar/m\lambda^2$ is the cyclotron frequency.

The original problem involves four canonical variables (x_1, p_1, x_2, p_2), so the two operators a and $a^\dagger$ are not sufficient to describe the system completely. As for the two remaining operators, we define

$$b = \frac{\lambda}{\sqrt{2}}(k_1 + ik_2) - \frac{i}{\sqrt{2}\lambda}(x_1 + ix_2) \ ,$$
$$b^\dagger = \frac{\lambda}{\sqrt{2}}(k_1 - ik_2) + \frac{i}{\sqrt{2}\lambda}(x_1 - ix_2) \ , \qquad \text{(B5)}$$

which obey the commutation relations (85). Equations (67) and (85) confirm that $(a, a^\dagger)$ and $(b, b^\dagger)$ can act as the two independent sets of canonical variables we seek and show that the eigenvalues n_a and n_b of the operators $a^\dagger a$ and $b^\dagger b$, respectively, take on integral values 0, 1, 2, ... We therefore define the simultaneous eigenstates of $a^\dagger a$ and $b^\dagger b$ by $|n_a, n_b\rangle$ having properties listed in Eq. (86), which allow us to generate all normalized eigenstates from the ground state $|0, 0\rangle$,

$$|n_a, n_b\rangle = (n_a!\, n_b!)^{-1/2}(a^\dagger)^{n_a}(b^\dagger)^{n_b}|0, 0\rangle \ . \qquad \text{(B6)}$$

The component of angular momentum along the magnetic field $L_3 = x_1 p_2 - x_2 p_1$ is a good quantum number in the problem. This is given in terms of the operators (B3) and (B5) as

$$L_3 = \hbar(a^\dagger a - b^\dagger b) = \hbar(n_a - n_b) \ . \qquad \text{(B7)}$$

The totality of the states given by Eq. (B6) forms a complete set of orthonormal wave functions in the two variables x_1 and x_2. The orthogonality

$$\langle n_a, n_b | n_a', n_b' \rangle = \delta_{n_a n_a'} \delta_{n_b n_b'} \qquad \text{(B8)}$$

follows, since states with different n_a have different energies, and states with same n_a but different n_b have different angular-momentum components.

The foregoing discussion allows us to visualize the systematics of the electronic states in an intuitive way. Equations (B4) and (B7) suggest that the system is equivalent to an assembly of two types of harmonic oscillators. Each oscillator in the a system has frequency ω_c and angular momentum $\hbar$ along $\vec{H}$. That in the b system has frequency zero and angular momentum $-\hbar$ along $\vec{H}$. The former system corresponds to electron rotation in the direction of classical cyclotron motion and the latter in the reverse direction. The role of the operators $a, a^\dagger$ and $b, b^\dagger$ can be simply understood. In Fig. 3, a and $a^\dagger$ are vertical stepping operators while b and $b^\dagger$ are sidewise stepping operators. The energy has a fixed value in each horizontal "row" increasing in steps of $\hbar\omega_c$ from one row to the next while the angular momentum increases by $\hbar$ either by moving upward or by moving to the left.

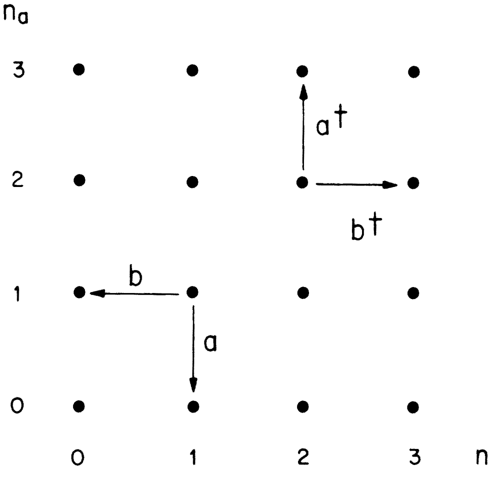

FIG. 3. Schematic classification of the eigenstates of a charged particle in a magnetic field according to the quantum numbers n_a and n_b. The arrows indicate the "transitions" between states by the designated operators.

An oscillating electric field of infinite wavelength and polarized perpendicular to the magnetic field induces a transition between the magnetic states with a transition probability proportional to the square of the matrix element of x_1 and x_2. From Eqs. (B3) and (B6) we have

$$x_1 + ix_2 = \sqrt{2}\, i\lambda(b - a^\dagger) \ ,$$
$$x_1 - ix_2 = -\sqrt{2}\, i\lambda(b^\dagger - a) \ ,$$

which, with Eq. (86), shows that the electric field induces two types of (one photon) transitions; one which changes n_b and the other n_a. In the former transition no energy is exchanged with the radiation field, while in the latter a quantum of $\hbar\omega_c$ is either absorbed or emitted. This fact justifies our considering only the change in n_a in calculating resonant absorption.

For a charge of $+|e|$, we readily see that the appropriate Hamiltonian is

$$\mathcal{H}_+ = \hbar\omega_c(b^\dagger b + \tfrac{1}{2})$$

with all definitions unchanged. We still can use Fig. 3 for this case, but now the energy increases to the right, instead of upward. The *b* oscillators now become active in absorption, and the *a* oscillators have zero frequency.

APPENDIX C: HIGHER-ORDER STRAIN EFFECTS

In this section our goal is to generalize the valence-band effective-mass Hamiltonian to the second order in strain which requires, for consistent results, that the development be carried out to an order sufficiently high to include cross terms of magnetic and first-order strain interactions as well as terms of order ϵ^2. The dynamics of an electron in the simultaneous presence of strain and magnetic field can be treated systematically by an extension of the methods of Luttinger and Kohn[2] in which one makes a cononical transformation to eliminate interband matrix elements to first order in both *k* and strain. Essentially the same results can be obtained by higher-order perturbation theory, but for the case of a degenerate band the method of canonical transformation is more transparent.

We assume that the spin-orbit interaction is already completely diagonalized at $\vec{k}=0$, and we neglect throughout the $\vec{k}$-dependent spin-orbit interaction.[60] We designate the energy of the valence band edge (Γ_8^+) by E_0 and its degenerate wave functions by i, j, i', etc. We assume inversion symmetry and designate by m, m', etc., the bands at $\vec{k}=0$ (either simple or degenerate) having positive parity other than the valence band edge and by l, l', etc., those with negative parity. The band energies at $\vec{k}=0$ are denoted by E with appropriate subscripts. Our Hamiltonian is

$$\mathcal{H}=\mathcal{H}_0+\frac{\hbar^2k^2}{2m}+\frac{\hbar}{m}\vec{k}\cdot\vec{\pi}+g_s\left(\frac{e\hbar}{mc}\right)\vec{\sigma}\cdot\vec{\mathrm{H}}+\mathcal{H}_e$$

$$=\mathcal{H}_0+\frac{\hbar^2k^2}{2m}+\mathcal{H}_k+g_s\left(\frac{e\hbar}{mc}\right)\vec{\sigma}\cdot\vec{\mathrm{H}}+\mathcal{H}_e^{(0)}+\mathcal{H}_e' , \tag{C1}$$

where we note that $\mathcal{H}_k$ is odd, and $\mathcal{H}_e^{(0)}$ and $\mathcal{H}_e'$ are even with nonvanishing intraband and interband matrix elements, respectively.

We apply a canonical transformation $T=e^S$ to (C1) and obtain[61]

$$\overline{\mathcal{H}}=e^{-S}\mathcal{H}e^S=\mathcal{H}_0+\frac{\hbar^2k^2}{2m}+\mathcal{H}_k+g_s\left(\frac{e\hbar}{mc}\right)\vec{\sigma}\cdot\vec{\mathrm{H}}+\mathcal{H}_e^{(0)}+\mathcal{H}_e'+[\mathcal{H}_0,S]+[\mathcal{H}_k,S]+[\mathcal{H}_e^{(0)},S]+[\mathcal{H}_e',S]$$

$$+\tfrac{1}{2}[[\mathcal{H}_0,S],S]+\tfrac{1}{2}[[\mathcal{H}_k,S],S]+\tfrac{1}{2}[[\mathcal{H}_e^{(0)},S],S]+\tfrac{1}{2}[[\mathcal{H}_e',S],S]+\tfrac{1}{6}[[[\mathcal{H}_0,S],S],S]+\cdots . \tag{C2}$$

Now we choose S in such a way that both the interband strain and $\vec{k}\cdot\vec{\pi}$ matrix elements vanish to first order, namely,

$$\mathcal{H}_k+\mathcal{H}_e'+[\mathcal{H}_0,S]=0 . \tag{C3}$$

When (C3) is satisfied we have

$$\tfrac{1}{2}[[\mathcal{H}_0,S],S]=-\tfrac{1}{2}[\mathcal{H}_k,S]-\tfrac{1}{2}[\mathcal{H}_e',S] ,$$

$$\tfrac{1}{6}[[[\mathcal{H}_0,S],S],S]=-\tfrac{1}{6}[[\mathcal{H}_k,S],S]-\tfrac{1}{6}[[\mathcal{H}_e',S],S] ,$$

and the transformed Hamiltonian becomes

$$\overline{\mathcal{H}}=\mathcal{H}_0+\frac{\hbar^2k^2}{2m}+g_s\left(\frac{e\hbar}{mc}\right)\vec{\sigma}\cdot\vec{\mathrm{H}}+\mathcal{H}_e^{(0)}+[\mathcal{H}_e^{(0)},S]$$

$$+\tfrac{1}{2}[\mathcal{H}_k,S]+\tfrac{1}{2}[\mathcal{H}_e',S]+\tfrac{1}{2}[[\mathcal{H}_e^{(0)},S],S]$$

$$+\tfrac{1}{3}[[\mathcal{H}_k,S],S]+\tfrac{1}{3}[[\mathcal{H}_e',S],S]+\cdots . \tag{C4}$$

From Eq. (C3) and from the inversion properties of $\mathcal{H}_k$ and $\mathcal{H}_e'$ we obtain the following matrix elements of S:

$$\begin{aligned}
&\langle i|S|l\rangle=-\langle i|\mathcal{H}_k|l\rangle/(E_0-E_l) ,\\
&\langle i|S|m\rangle=-\langle i|\mathcal{H}_e'|m\rangle/E_0-E_m) ,\\
&\langle l|S|m\rangle=-\langle l|\mathcal{H}_k|m\rangle/(E_l-E_m) ,\\
&\langle l|S|l'\rangle=-\langle l|\mathcal{H}_e'|l'\rangle/(E_l-E_{l'}) ,\\
&\langle m|S|m'\rangle=-\langle m|\mathcal{H}_e'|m'\rangle/(E_m-E_{m'}) ,\\
&\langle n|S|n\rangle=0 \text{ for } n=(i,j) \text{ or } l \text{ or } m .
\end{aligned} \tag{C5}$$

From Eq. (C4) and with the help of Eq. (C5) we obtain the following intraband matrix elements of the transformed Hamiltonians:

$$(i|\overline{\mathcal{H}}|j)=\left(E_0+\frac{\hbar^2k^2}{2m}\right)\delta_{ij}+g_s\left(\frac{e\hbar}{4mc}\right)\langle i|\vec{\sigma}|j\rangle\cdot\vec{\mathrm{H}}+\langle i|\mathcal{H}_e|j\rangle+\sum_l\frac{\langle i|\mathcal{H}_k|l\rangle\langle l|\mathcal{H}_k|j\rangle}{E_0-E_l}+\sum_m\frac{\langle i|\mathcal{H}_e|m\rangle\langle m|\mathcal{H}_e|j\rangle}{E_0-E_m}$$

$$-\frac{1}{2}\sum_l\sum_{i'}\frac{\langle i|\mathcal{H}_e|i'\rangle\langle i'|\mathcal{H}_k|l\rangle\langle l|\mathcal{H}_k|j\rangle+\langle i|\mathcal{H}_k|l\rangle\langle l|\mathcal{H}_k|i'\rangle\langle i'|\mathcal{H}_e|j\rangle}{(E_0-E_l)^2}$$

$$+\sum_{l,l'}\frac{\langle i|\mathcal{H}_k|l\rangle\langle l|\mathcal{H}_e|l'\rangle\langle l'|\mathcal{H}_k|j\rangle}{(E_0-E_l)(E_0-E_{l'})}$$

$$+\sum_{l,m}\frac{\langle i|\mathcal{H}_e|m\rangle\langle m|\mathcal{H}_k|l\rangle\langle l|\mathcal{H}_k|j\rangle+\langle i|\mathcal{H}_k|l\rangle\langle l|\mathcal{H}_k|m\rangle\langle m|\mathcal{H}_e|j\rangle}{(E_0-E_l)(E_0-E_m)}$$

$$-\frac{1}{2}\sum_{m}\sum_{i'}\frac{\langle i|\mathcal{H}_e|i'\rangle\langle i'|\mathcal{H}_e|m\rangle\langle m|\mathcal{H}_e|j\rangle+\langle i|\mathcal{H}_e|m\rangle\langle m|\mathcal{H}_e|i'\rangle\langle i'|\mathcal{H}_e|j\rangle}{(E_0-E_m)^2}\quad .$$

$$+\sum_{m,m'}\frac{\langle i|\mathcal{H}_e|m\rangle\langle m|\mathcal{H}_e|m'\rangle\langle m'|\mathcal{H}_e|j\rangle}{(E_0-E_m)(E_0-E_{m'})}\,, \tag{C6}$$

where $\mathcal{H}_e=\mathcal{H}_e^{(0)}+\mathcal{H}_e'$ (this has both interband and intraband matrix elements).

The Hamiltonian (C6) for the Γ_8 degenerate band can be expressed alternatively in the form of a spin Hamiltonian using the 16 independent J matrices. The discussion here proceeds in the reverse logical order to the one in Sec. II. The sum of the first, second, and fourth terms gives the familiar $\vec{k}\cdot\vec{\pi}$ Hamiltonian in the absence of strain, Eq. (29); and the third term gives the intraband strain interaction, Eq. (30). The fifth term is a second-order strain interaction which can be written as a spin Hamiltonian in the form

$$F_1(\epsilon_{\lambda\lambda})^2+F_2(\epsilon_{xy}^2+\text{c.p.})+F_3[\epsilon_{xx}^2+\text{c.p.}-\tfrac{1}{3}(\epsilon_{\lambda\lambda})^2]$$
$$+[F_4\epsilon_{\lambda\lambda}\epsilon_{xx}+F_5\epsilon_{yz}^2+F_6(\epsilon_{xx}^2+2\epsilon_{yy}\epsilon_{zz})](J_x^2-\tfrac{1}{3}J^2)+\text{c.p.}$$
$$+[F_7\epsilon_{yz}\epsilon_{zx}+F_8(\epsilon_{xx}+\epsilon_{yy}-2\epsilon_{zz})\epsilon_{xy}]\{J_xJ_y\}+\text{c.p.}\,, \tag{C7}$$

where the coefficients $F_1,\ldots,F_8$ can be determined by comparing appropriate matrix elements with Eq. (C6). Equation (C7) represents a generalization of $\mathcal{H}_{ee}$ in Eq. (131), the latter being the single contribution from $E_0-E_m=\Lambda$. (The coefficients F_1 and F_4 accidentally vanish in this case.)

We next consider the sixth through eighth terms of Eq. (C6) together. The sixth term accounts for the change of band parameters with strain caused by the dilatational shift as well as uniaxial splitting of the degenerate band edge. (The summation over i' extends over all members of the degenerate set including i and j.) The $l=l'$ part of the seventh term is responsible for the change of band parameters resulting from a dilatational strain shift and uniaxial strain splitting (in case of a degenerate band, e.g., for Γ_8^-) of the intermediate odd-parity states. The $E_0-E_m=\Lambda$ part in the eighth term is the strain-linear coupling, Eq. (128), discussed in Sec. VII.

The sum of the sixth through eighth terms in Eq. (C6) can again be expressed in the form of a spin Hamiltonian. Group theory shows that there are in all 21 independent coefficients in the Hamiltonian of order $k_\kappa k_\lambda\epsilon_{\mu\nu}$. The 21 independent invariants each having a coefficient $C_1,\ldots,C_{21}$ are listed below (the representations at the left refer to the J operators in the invariants):

Γ_1: (1) $\epsilon_{\lambda\lambda}k^2$,
(2) $\epsilon_{xy}\{k_xk_y\}+\text{c.p.}$,
(3) $\epsilon_{xx}k_x^2+\text{c.p.}-\frac{1}{3}\epsilon_{\lambda\lambda}k^2$,
Γ_{12}: (4) $\epsilon_{\lambda\lambda}k_x^2(J_x^2-\frac{1}{3}J^2)+\text{c.p.}$,
(5) $\epsilon_{xx}k^2(J_x^2-\frac{1}{3}J^2)+\text{c.p.}$,
(6) $\epsilon_{yz}\{k_yk_z\}(J_x^2-\frac{1}{3}J^2)+\text{c.p.}$,
(7) $(\epsilon_{xx}k_x^2+\epsilon_{yy}k_z^2+\epsilon_{zz}k_y^2)(J_x^2-\frac{1}{3}J^2)+\text{c.p.}$;
Γ_{25}: (8) $\epsilon_{\lambda\lambda}\{k_xk_y\}\{J_xJ_y\}+\text{c.p.}$,
(9) $\epsilon_{xy}k^2\{J_xJ_y\}+\text{c.p.}$,
(10) $(\epsilon_{yz}\{k_zk_x\}+\epsilon_{zx}\{k_yk_z\})\{J_xJ_y\}+\text{c.p.}$,
(11) $(\epsilon_{xx}+\epsilon_{yy}-2\epsilon_{zz})\{k_xk_y\}\{J_xJ_y\}+\text{c.p.}$,
(12) $\epsilon_{xy}(k_x^2+k_y^2-2k_z^2)\{J_xJ_y\}+\text{c.p.}$, (C8)
(13) $(\epsilon_{yy}-\epsilon_{zz})H_xV_x+\text{c.p.}$,
(14) $(\epsilon_{xy}H_y-\epsilon_{zx}H_z)V_x+\text{c.p.}$;
Γ_2: (15) $(\epsilon_{xy}H_z+\text{c.p.})\{J_xJ_yJ_z\}$;
Γ_{15}: (16) $\epsilon_{\lambda\lambda}(H_xJ_x+\text{c.p.})$,
(17) $\epsilon_{\lambda\lambda}(H_xJ_x^3+\text{c.p.})$,
(18) $(\epsilon_{yy}+\epsilon_{zz}-2\epsilon_{xx})H_xJ_x+\text{c.p.}$,
(19) $(\epsilon_{xy}H_y+\epsilon_{zx}H_z)J_x+\text{c.p.}$,
(20) $(\epsilon_{yy}+\epsilon_{zz}-2\epsilon_{xx})H_xJ_x^3+\text{c.p.}$,
(21) $(\epsilon_{xy}H_y+\epsilon_{zx}H_z)J_x^3+\text{c.p.}$;

where V_x and $\{J_xJ_yJ_z\}$ are defined in Eq. (130) and Table II, respectively. Equation (128) represents a special case of the general Hamiltonian and contains all but seven of the 21 coefficients, C_1, C_4, C_5, C_8, C_9, C_{16}, and C_{17}, which have accidentally vanished. The corresponding invariants contain either $\epsilon_{\lambda\lambda}$ or k^2 or both and therefore do not appear in the Γ_7-Γ_8 interaction. Some of the invariants (C8) admit to simple physical interpretation. Term (8), for example, can be interpreted in a straightforward way as the strain-dependent change of the k^2-band parameter γ_3; but this simple assignment is not always possible for other invariants. The coefficients C_1 through C_{21} can be determined in exactly the same way as in Sec. II by comparing the spin Hamiltonian with Eq. (C6) term by term.

The last two terms in Eq. (C6) give third-order strain energies expressible as a spin Hamiltonian of order $\epsilon_{\theta\iota}\epsilon_{\kappa\lambda}\epsilon_{\mu\nu}$, which we shall not write out explicitly.

In passing it is worthwhile to point out that exactly the same mathematical procedure would be followed if we were to replace $\mathcal{H}_e$ by $\mathcal{H}_{so}$, both of which have identical inversion properties. The source of the q term, Eq. (38), that we picked up then would correspond to the seventh term in Eq. (C6) if we set $l=l'$.

It is possible, although we have not done so, to split each coefficient, $C_1, \ldots, C_{21}$, into components representing contributions from bands of each symmetry classification. In this regard we note that the eighth term of Eq. (C6) includes intermediate states of even parity, so this sum, therefore, extends over positive as well as negative parity bands.

It is interesting to ask oneself how many independent coefficients are required if we make a *spherical* approximation? The answer to this is given by group theory and the result is quite simple. For the second-order strain Hamiltonian the spherical counterpart to Eq. (C7) contains but four independent coefficients, namely, the coefficients of the four terms in the expression $\mathcal{H}_{ee}$ given in Ref. 44. The same is true for $\mathcal{H}_{ke}$; the 21 independent coefficients in Eq. (C8) reduce to eight. The remark made in Sec. VII on the solvability of $\mathcal{H}_{kk}$ for the spherical case still applies: the spherical Hamiltonian including the second-order strain and strain-magnetic terms can be solved in a finite space for any direction of uniaxial stress collinear with magnetic field and for any value of k_H using a wave function of the form (150).

---

*Present address: Osaka University, Toyonaka, Japan, where part of this work was completed.

[1] Deviations in Landau level spacing which often occur due to band nonparabolicity can be considered classically as an anharmonic effect.

[2] J. M. Luttinger and W. Kohn, Phys. Rev. 97, 869 (1955).

[3] J. M. Luttinger, Phys. Rev. 102, 1030 (1956).

[4] R. C. Fletcher, W. A. Yager, and F. R. Merritt, Phys. Rev. 100, 747 (1955).

[5] G. Dresselhaus, A. F. Kip, and C. Kittel, Phys. Rev. 98, 368 (1955), hereafter referred to as DKK.

[6] R. N. Dexter, H. J. Zeiger, and B. Lax, Phys. Rev. 104, 637 (1956).

[7] J. C. Hensel, *Proceedings of the International Conference on the Physics of Semiconductors, Exeter*, 1962 (The Institute of Physics and Physical Society, London, 1962), p. 281; W. Mercouroff, Phys. Status Solidi 2, 282 (1962); K. J. Button and B. Lax, Bull. Am. Phys. Soc. 14, 432 (1969).

[8] J. J. Stickler, H. J. Zeiger, and G. S. Heller, Phys. Rev. 127, 1077 (1962).

[9] R. R. Goodman, Phys. Rev. 122, 397 (1961).

[10] The possibility of anomalous k_H effects occurring was first pointed out by R. F. Wallis and H. J. Bowlden [Phys. Rev. 118, 456 (1960)] who considered only the spherical case ($\gamma_3=\gamma_2$). Also see V. Evtuhov, Phys. Rev. 125, 1869 (1962); and E. Kaczmarek, Phys. Rev. 132, 1929 (1963).

[11] M. Okazaki, J. Phys. Soc. Japan 17, 1865 (1962).

[12] J. C. Hensel and G. Feher, Phys. Rev. 129, 1041 (1963).

[13] J. C. Hensel, Solid State Commun. 4, 231 (1966).

[14] E. Otsuka, K. Murase and H. Fujiyasu, Phys. Letters 21, 284 (1966).

[15] A brief outline of this work has been presented at the Tenth International Conference on the Physics of Semiconductors, J. C. Hensel and K. Suzuki, *Proceedings of the Tenth International Conference on the Physics of Semiconductors, Cambridge*, 1970, edited by S. P. Keller, J. C. Hensel, and F. Stern, CONF-700801 (U. S. AEC Division of Technical Information, Springfield, Va., 1970), p. 541.

[16] J. C. Hensel and K. Suzuki, following paper, Phys. Rev. B 9, 4219 (1974). A preliminary account of some of this work was first given in Ref. 13.

[17] J. C. Hensel and K. Suzuki (to be published). A preliminary account of this work has been given earlier: J. C. Hensel, Phys. Rev. Lett. 21, 983 (1968) and J. C. Hensel and K. Suzuki, Phys. Rev. Lett. 22, 838 (1969).

[18] J. C. Hensel and K. Suzuki (to be published). A synopsis of the spectroscopy of unstressed Ge has been presented earlier, J. C. Hensel and K. Suzuki, *Proceedings of the 3rd Materials Research Symposium, "Electronic Density of States," Gaithersburg, Maryland*, 1969 (National Bureau of Standards, Special Publication 323, Washington, D. C., 1971, L. H. Bennett, ed.) p. 431. See also Ref. 15.

[19] We use the notation of Ref. 5 for the representations of O_h and their basis functions.

[20] H. Hasegawa, Phys. Rev. 129, 1029 (1963).

[21] The "conventional" strain components are defined by $e_{xx}=\epsilon_{xx}$, $e_{xy}=2\epsilon_{xy}$, etc.

[22] M. Cardona and F. H. Pollak, Phys. Rev. 142, 430 (1965).

[23] G. D. Whitfield, Phys. Rev. 121, 720 (1961).

[24] (a) G. E. Pikus and G. L. Bir, Fiz. Tverd. Tela 1, 1642 (1959). [Sov. Phys.-Solid State 1, 1502 (1959)]; (b) G. L. Bir and G. E. Pikus, *Simmetriya i deformatsionnye effekty v poluprovodnikakh* (Symmetry and Deformation Effects in Semiconductors) (Nauka, Moscow, 1972).

[25] W. H. Kleiner and L. M. Roth, Phys. Rev. Lett. 2, 334 (1959).

[26] Other notations commonly used are DKK (Ref. 5): $A=-\gamma_1$, $B=-2\gamma_2$, $C^2=12(\gamma_3^2-\gamma_2^2)$, and $L=-\gamma_1-1-4\gamma_2$, $M=-\gamma_1-1+2\gamma_2$, $N=-6\gamma_3$; Pikus-Bir (Ref. 24): $a=+D_d$, $b=-\frac{2}{3}D_u$, $d=-(2/\sqrt{3})D_u'$. The definition of a in Ref. 24(a) differs in sign from that in Ref. 24(b). This ambiguity in sign crops up elsewhere in the literature. The sign given here conforms with the definition in Ref. 24(b).

[27] If we work in the double group representations with the exact $\vec{k}=0$ eigenstates of the electron Hamiltonian including spin-orbit interaction, the contributions in question appear in second order rather than third order.

[28] L. R. Saravia and D. Brust, Phys. Rev. 176, 915 (1968); F. Herman, R. L. Kortum, C. D. Kuglin, J. P. VanDyke, and S. Skillman, in *Methods in Computational Physics*, edited by B. Alder and S. Fernbach (Academic, New York, 1968), p. 193; and G. G.

Wepfer, T. C. Collins and R. N. Euwema, Phys. Rev. B4, 1296 (1971). Experimental values of Δ_{15} are given in Paper III and also by J. E. Fischer, in Ref. 15, p. 427; and T. M. Donovan, J. E. Fischer, J. Matsuzaki, and W. E. Spicer, Phys. Rev. B3, 4292 (1971).

[29] C. R. Pidgeon and S. H. Groves, Phys. Rev. 186, 824 (1969).

[30] P. J. Melz and I. B. Ortenburger, Phys. Rev. B3, 3257 (1971).

[31] The transition probability, Eq. (50), appears to be formally identical to that for a simple band. However, it should be pointed out that the transition operator $\vec{\mathcal{E}}\cdot\vec{v}$ [see Eq. (48)] is now a 4×4 matrix operator for the degenerate $J=3/2$ valence band edge of Ge.

[32] The real electric field is $\mathrm{Re}(\vec{\mathcal{E}}e^{i\omega t})$, so that $|\vec{\mathcal{E}}| = \mathcal{E}_l$ for a linear polarization $\mathcal{E}_x=\mathcal{E}_l\cos\omega t$, $\mathcal{E}_y=\mathcal{E}_z=0$, and $|\vec{\mathcal{E}}|=\sqrt{2}\,\mathcal{E}_c$ for a circular polarization $\mathcal{E}_x=\mathcal{E}_c\cos\omega t$, $\mathcal{E}_y=\mathcal{E}_c\sin\omega t$.

[33] It should be noted that $\vec{\mathcal{E}}$ and $\vec{e}$ are, in general, complex quantities, and $\vec{e}\cdot\vec{u}$ is not a hermitian operator. Consequently, $|F_{st}|^2$ is different from $|F_{ts}|^2$. This difference is responsible for the polarization properties which distinguish hole resonances from electron resonances for simple bands.

[34] Okazaki (Ref. 11), by neglecting the partition function $Z(\eta)$ entirely, obtained an $H^{3/2}$ factor in the coefficient-one power of H coming from the matrix element squared and $H^{1/2}$ appearing from the transformation of integration variables from k_H to ζ. The latter should cancel since the same transformation would ordinarily also be made in the denominator $Z(\eta)$. Stickler, Zeiger, and Heller (Ref. 8) arrive at a correct result although their discussion is not completely clear. In their expression they insert an extra *ad hoc* factor of H ascribed to a "density of Landau levels" which could be misinterpreted as the extra degeneracy of the Landau levels associated with the "hidden" degree of freedom from k_y (which corresponds to the center of cyclotron motion). This factor too appears in $Z(\eta)$ and, hence, should cancel. The results of Goodman (Ref. 9) are essentially correct although the magnetic field dependence is not readily evident unless suitable transformations are first made.

[35] The split into axial and nonaxial parts is to some extent arbitrary, since the axial part is a special case of a nonaxial part. We have made the split in such a way that the nonaxial part contains no part of axial symmetry. In other words, the nonaxial part never connects states of the same N where N is the axial quantum number defined in Eq. (93).

[36] Some selection rules in the absence of strain have been given in a different form by H. Kamimura, Phys. Rev. 129, 614 (1963).

[37] This transformation is equivalent to using a different gauge for the microwave fields in the interaction Hamiltonian (47). The relations (106) and (107) have a particular advantage since a and $a^\dagger$ are simple nonmatrix operators.

[38] A similar approach was taken in the exciton problem by K. Suzuki and E. Hanamura, J. Phys. Chem. Solids 30, 749 (1969).

[39] Equation (112) gives isotropic splitting for $\beta=-1$ also. However, the splitting is not "uniaxial" except for T along the particular directions [001] and [111] since the right-hand side of Eq. (114) does not otherwise vanish.

[40] See Ref. 16.

[41] For compression, $\epsilon<0$, and the band "edge" consists of the $M_J=\pm\frac{1}{2}$ Kramers pair.

[42] In terms of the angle η defined by Eq. (121), the four stressed Bloch eigenstates for $T \parallel [110]$ are: energy $=+\epsilon$, $\cos(\frac{1}{2}\eta-\frac{1}{6}\pi)\,|\frac{3}{2}\rangle+\sin(\frac{1}{2}\eta-\frac{1}{6}\pi)\,|-\frac{1}{2}\rangle$ and its time-reversed conjugate state; energy $=-\epsilon$, $-\sin(\frac{1}{2}\eta-\frac{1}{6}\pi)\,|\frac{3}{2}\rangle+\cos(\frac{1}{2}\eta-\frac{1}{6}\pi)\,|-\frac{1}{2}\rangle$ and its time-reversed conjugate state. Here $|M_J\rangle$ is the Bloch state with angular momentum M_J along the stress direction.

[43] We have dropped from Eq. (125) an unimportant term $(1/2x)F\zeta^4$ which should be included if this expression were to be completely general up to ζ^4.

[44] When $\Gamma_2=\Gamma_3$ and $D_w=D'_w$, all three second-order Hamiltonians reduce to spherical invariants listed as follows:

$$H_{ke}=-\frac{1}{\Lambda}\frac{\hbar^2}{m}D_w\Gamma_2\Big[4\epsilon_{\lambda\nu}\{k_\mu k_\nu\}\{J_\lambda J_\mu\}-\tfrac{4}{3}\epsilon_{\lambda\lambda}\{k_\mu k_\nu\}\{J_\mu J_\nu\}$$

$$-\tfrac{4}{3}\epsilon_{\lambda\mu}k_\nu k_\nu J_\lambda J_\mu-7\epsilon_{\lambda\mu}\{k_\lambda k_\mu\}+4\epsilon_{\lambda\lambda}k_\mu k_\mu\Big]$$

$$-\frac{1}{\Lambda}\frac{e\hbar}{mc}KD_w\Big[\tfrac{4}{3}\epsilon_{\lambda\mu}H_\nu\{J_\lambda J_\mu J_\nu\}-\tfrac{20}{9}\epsilon_{\lambda\mu}H_\lambda J_\mu-\tfrac{7}{9}\epsilon_{\lambda\lambda}H_\mu J_\mu\Big],$$

$$H_{ee}=-\frac{1}{\Lambda}D_w^2\Big[\tfrac{4}{3}\epsilon_{\lambda\nu}\epsilon_{\mu\nu}J_\lambda J_\mu-\tfrac{8}{9}\epsilon_{\lambda\lambda}\epsilon_{\mu\nu}J_\mu J_\nu$$

$$-\tfrac{7}{3}\epsilon_{\lambda\mu}\epsilon_{\lambda\mu}+\tfrac{4}{3}\epsilon_{\lambda\lambda}\epsilon_{\mu\mu}\Big],$$

$$H_{kk}=\frac{1}{\Lambda}\left(\frac{\hbar^2}{m}\right)^2\Gamma_2^2\left(\tfrac{9}{4}k^4-\{k^2,(\vec{k}\cdot\vec{J})^2\}\right)+\frac{1}{\Lambda}\left(\frac{\hbar^2}{m}\right)$$

$$\times\left(\frac{e\hbar}{mc}\right)K\Gamma_2\Big[\tfrac{3}{2}k^2(\vec{H}\cdot\vec{J})+3\{(\vec{k}\cdot\vec{J})(\vec{k}\cdot\vec{H})\}-2\{(\vec{k}\cdot\vec{J})^2,(\vec{H}\cdot\vec{J})\}\Big]$$

$$+\frac{1}{\Lambda}\left(\frac{e\hbar}{mc}\right)^2\left(\tfrac{1}{4}K^2[\tfrac{9}{4}H^2-(\vec{J}\cdot\vec{H})^2]+\tfrac{9}{4}\Gamma_2^2[(\vec{J}\cdot\vec{H})^2-\tfrac{1}{4}H^2]\right),$$

where the "triple" symmetric product $\{J_\lambda J_\mu J_\nu\}$ is defined in Table II.

[45] The exact forms for the corrections to the $(0,-\frac{1}{2})\to(1,-\frac{1}{2})$ transitions in two special cases, $\vec{H}\parallel T\parallel[001]$ and [111], are given in Paper II, Eqs. (19) and(20).

[46] C. R. Pidgeon and R. N. Brown, Phys. Rev. 146, 575 (1966).

[47] T. Kjeldaas, Jr. and W. Kohn, Phys. Rev. 105, 806 (1957).

[48] R. F. Wallis, J. Phys. Chem. Solids 4, 101 (1958).

[49] The general selection rules discussed in Sec. IV are unchanged in the presence of k^4 terms.

[50] This estimate is based on the following values of the parameters: $dE_g/dP=12\times10^{-6}$ eV/kg cm^{-2} [W. Paul and D. M. Warschauer, *Solids Under Pressure* (McGraw-Hill, New York, 1963), p. 226]; $D_u=3.32$ eV and $\gamma_1=13.38$ (J. C. Hensel and K. Suzuki, Paper II); $s_{11}=9.37\times10^{-7}$ cm^2/kg and $s_{12}=-2.57\times10^{-7}$ cm^2/kg [H. J. McSkimin, J. Appl. Phys. 24, 988 (1953)]; and $E_g\sim1$ eV.

[51] The constant 2 in Eq. (A2) is added for convenience so the quantum number assigned to the lowest level in the Luttinger energy level scheme is $L=0$ rather than -2 as quoted in the original paper (Ref. 3).

[52] Our present case is in some ways analogous with the Kepler problem where there also appears a hidden constant of motion, the Runge vector. Consideration of the conservation of this vector plus angular momentum

led W. Pauli [Z. Phys. 36, 336 (1926)] to an elegant solution of the Kepler problem. The full significance of this constant of motion and its relationship to the "accidental" degeneracy of the hydrogen atom was later pointed out by V. Fock, Z. Phys. 98, 145 (1935).

[53] L. D. Landau, Z. Phys. 64, 629 (1930).

[54] M. H. Johnson and B. A. Lippmann, Phys. Rev. 76, 828 (1949).

[55] R. B. Dingle, Proc. R. Soc. A211, 500 (1952).

[56] Y. Yafet, R. W. Keyes, and E. N. Adams, J. Phys. Chem. Solids 1, 137 (1956).

[57] R. Kubo, H. Hasegawa, and N. Hashitsume, Phys. Rev. Lett. 1, 279 (1958). See also, R. Kubo, S. J. Miyake, and N. Hashitsume, Solid State Phys. 17, 269 (1965).

[58] I. A. Malkin and V. I. Man'ko, Zh. Eksp. Teor. Fiz. 55, 1014 (1968) [Sov. Phys.-JETP 28, 527 (1969)].

[59] A. Feldman and A. H. Kahn, Phys. Rev. B1, 4584 (1970).

[60] See the discussion of E. O. Kane, J. Phys. Chem. Solids 1, 82 (1956).

[61] We neglect interband matrix elements of $\vec{\sigma}\cdot\vec{H}$.